Evidence of Anisotropic Mechanical Properties of Fibroblast Membranes

by

Russell M. Basch

S.B., Massachusetts Institute of Technology, 1986

Submitted in Partial Fulfillment of the
Requirements for the Degree of
Master of Science

at the

Massachusetts Institute of Technology
February 1988

Signature of Author _____
Department of Electrical Engineering and Computer Science
February 1988

Certified by _____
Thesis Supervisor

Accepted by _____
Chair, Department Committee

Evidence of Anisotropic Mechanical Properties of Fibroblast Membranes

by

Russell M. Basch

Submitted to the Department of Electrical Engineering and Computer Science in partial fulfillment of the requirements for the Degree of Master of Science, February 1988

Abstract

The recent quantification of frequency and amplitude dependence of the fibroblast protein biosynthetic response to low frequency sinusoidal electric fields has focused more interest toward searching for a mechanism. One conceivable mechanism involves the redistribution of cell surface receptors. This mechanism requires anisotropy of the mechanical properties of the membrane.

New experimental methods were established and initial studies were performed to quantify the diffusion coefficient and the "effective" electrophoretic mobility of MHC antigen receptors as a function of direction in the membrane. A directional dependence would lead to a net displacement even in a pure sinusoidal field and may activate a cellular response.

Fluorescence recovery after photobleaching (FRAP) techniques under isothermal conditions in the presence of an electric field were used to detect the relative contribution of diffusion and "effective" electrophoresis to the kinetics of fluorescence recovery. The diffusion coefficient measured was $1.4 \pm 0.70 \times 10^{-9}$ cm^2/sec, and the "effective" electrophoretic mobility measured was $7.5 \pm 2.9 \times 10^{-7}$ cm^2/V·sec. Pretreating the cells with neuraminidase significantly reduced ($p < 0.02$) the "effective" electrophoretic mobility to $3.1 \pm 0.26 \times 10^{-7}$ cm^2/V·sec. This confirmed our hypothesis that MHC proteins move in the prescence of an electric field due to viscous forces created by electroosmotic flow.

The fluorescence near one pole on the major axis of the cell changed in the presence of an electric field due to protein redistribution. Removal of the field allowed the proteins to diffuse back to uniform distribution. The diffusion coefficients in the two directions along the major axis on the same cell proved to be different ($p < 0.10$). To our knowledge, this work is the first to present uniaxial anisotropy of the resistance to movement of cell surface receptors.

Thesis Supervisor: Dr. Raphael C. Lee

Title: Karl Van Tassel Assistant Professor of Electrical Engineering and Bioengineering

Acknowledgements

Certainly this thesis would not rightfully be put to rest without acknowledging those who did their part helping me to finish. To the following people I owe gratitudes:

Dr. Raphael Lee for introducing me to the world of bioengineering. His support and guidance were instrumental in bringing this work to a successful completion. His patience was admired, his friendliness appreciated, and his excitability contagious.

Dr. David Golan for the use of his laboratory, for his suggestions, and for his pleasant disposition.

Dr. Eliot Frank for his analytical answers, his mechanical answers, his computer answers, his latex answers, etc., anytime!

Dr. Alan Stolpen for his interest in the project and for donating his invaluable FITC-W6/32 antibody.

Patrick Yacono for all his help, patience, and ability with the FRAP equipment.

My colleagues, who added input in different capacities, John Kenny, David Huang, Caroline Wang, David Askey, Achal Aggarwal, Diane Gaylor, Bob Sah, Dr. Doug Ramos, Karen Adler (when she's here), Paul Grimshaw, and Linda Bragman.

My family for always being supportive and understanding. It's a great comfort to have such a caring family.

Finally, I would like to thank my fiancé, Ingrid, for all of the support and encouragement she has given me. Her love, caring, and understanding have been inspiring. To her, as a small appreciation for all that she has meant, and all that she will mean to me, I dedicate this thesis.

This research was supported by The Office of Naval Research, Grant N0014-85-K-0153, and the Searle Scholars Program of the Chicago Community Trust. Their assistance is gratefully acknowledged.

Russell M. Basch
29 Feb. 1988

Contents

List of Figures

List of Tables

Chapter I

Background and Motivation

1.1 Overview

The fundamental objective of this thesis project was to test the proposition that the resistance to movement of cell surface glycoproteins is anisotropic and argue that this anisotropy may allow cells to detect electric fields.

In this first chapter the background information necessary to motivate this study is presented. The first section examines some of the effects that low-frequency electric fields have on biological systems. The following section then presents possible mechanisms for these effects. In particular, one possible mechanism that occurs because the membrane is fluid and contains fixed charges on its surface is described in detail. A review of relevant cell surface receptor convection and diffusion measurements is given below. This is followed by a brief review of the biology of class I major histocompatibility complex (MHC) proteins and the motivation for studying them. Past evidence for anisotropic mechanical properties of cell membranes is then presented. Finally, the scope the thesis is defined.

1.2 Cellular Responses to Low-Frequency, Weak Electric Fields

The current densities and frequencies of endogenous fields found in mammalian living systems span a wide range. Current densities range from $5\mu a/cm^2$ in fractured mouse metatarsals [Borgens, 1984] to $1ma/cm^2$ near the surface of nerve fibers [Aidley, 1978], while frequencies range from almost dc to $\sim$ 10kHz due to streaming potentials generated by mechanical deformation of bone and soft connective tissue [Frank, 1987] and action potentials in excitable membranes. The exact physiologic parameter that these electric fields effect is unknown, Studies are currently being conducted that begin to characterize the effects of these low-frequency,

weak electric fields on cellular responses.

In a physiologic context, a low-frequency electric field can be practically defined as having a frequency below which extracellular currents are severely limited from the cell's interior. McLeod [1986] analytically showed that for a spherical cell in a physiologic conducting media, frequencies below 700 kHz will increasingly exclude extracellular currents from the interior of the cell. A weak electric field is considered to have a field intensity that changes the indigenous transmembrane potential (-30 to -90mV) by no more than 1%. Therefore, a field intensity of 250mV/cm across a cell that is 10μm long would be considered the threshold of a weak electric field.

Over the past twenty years, many experiments have produced evidence that cells respond to imposed electric fields. However, many variations in these studies, including cell type, frequency, field strength, and procedure make it difficult to formulate basic concepts. Presented here is a sampling of some of the literature categorized to show the wide range of effects over the wide range of cell types, frequency, and current densities.

Response to electric fields has been demonstrated with different cell types. Brevet et al. [1976] exposed embryonic chick breast muscle cells to pulsed fields on the order of 250mV/cm for forty-eight hours and showed an increase in the pyrophosphate extracted protein. In 1983, Kloss and Cartensen detected an alteration in the heart rate of isolated frog hearts. Gray [1986] and McLeod [1986] showed changes to calf epiphysial cartilage and bovine fibroblast biosynthesis respectively. Changes occurred over a range of field strengths (0.1 - 100μa/cm^2) and frequencies (0.1 - 100Hz).

Other effects have been shown throughout the physiologic frequency domain. Brighton et al. [1976] cultured rat costochondrial junction in media in a petri dish between capacitor plates and reported significant increases in ^{45}Ca, ^{35}S-sulfate, and ^{3}H-thymidine in response to dc fields in the surrounding air of magnitude up to 3,000V/cm. Capacitively coupled dc fields, however, will not induce local electric

fields at the site of the tissue of interest. The cell probably sensed an increased surface charge. Rodan et al. [1978] later showed that pulsed fields enhanced DNA synthesis in chick chondrocytes in suspension within the frequency spectrum 5-500Hz; this effect, however, was phenotype specific, for no response was demonstrated in chick embryo fibroblasts. In 1982, Lee et al. showed that fourteen-day-old chick chondrocytes on elastin membranes exposed to a 60 Hz. sinusoidal field incorporated greater amounts of ^{35}S-sulfate than the cells not exposed to the field. McLeod et al. [1987] showed that the threshold required to produce a decrease in the protein synthesis rate in bovine fibroblasts proved to be frequency dependent with peak sensitivity occurring between 1 and 10 Hz.

Current densities also varied between the studies. Assailly et al. [1981] reported an enhanced calcium intake in embryonic chick tibia exposed to 27μs current pulses of current density 1-3μa/cm^2. In 1982, Brighton et al. showed that a 60 Hz, 37μa/cm^2 current increased effect of serum variation in the bovine chondrocytes. Serum enhanced ^{3}H-amino acid intake and depressed ^{35}S-Sulfate uptake. The electric current amplified this response. McLeod et al. [1987] showed effects for fields as low as .3μa/cm^2.

Further studies have indicated that cell orientation with respect to the direction of the current may determine the sensitivity of the cells. McLeod [1986] found that cells oriented parallel to the current are more sensitive to the current than cells oriented perpendicular to the current. Norton et al. [1977] showed enhanced cAMP accumulation in tibiae oriented exposed to a 10^{-5} second pulsed field of 5 Hz and 600 V/cm. Cells parallel to the field were more sensitive.

Where this section focused on the effects of interactions between electric fields and cells, the next sections consider possible indirect and direct mechanisms for these interactions.

1.3 Indirect Mechanisms for Interaction

Several indirect mechanisms for the interaction of an external electric field about cells have been shown. Current flow (especially dc and low-frequency) can generate pH changes by electrolysis at the electrodes. Electrode reaction products can also be generated at the cathode due to a metal oxidation process specific to the electrode metal. MacGinitie [1988] showed that these products alter the biosynthesis in calf cartilage.

Joule heating also occurs in an external field. A rise in temperature can alter the cell's metabolic rate, which has been shown to produce artificial changes in biosynthesis that are not due to a direct field effect [Schlesinger, 1982].

1.4 Direct Mechanisms for Interaction

At the cellular level, endogenous and applied electric fields may directly effect the mechanical and chemical properties of the cell by altering the intracellular mechanisms, the transmembrane ion transport, or the membrane receptor distribution. These mechanisms are described in the following subsections.

1.4.1 Alteration of Intracellular Mechanisms

In 1981, Poo calculated the solution for the intracellular electric field in the low-frequency limit. He showed that for a cell resembling a sphere, in a dc field, the intracellular field was four orders of magnitudes less than the external field. When he applied an extracellular field of strength 1 V/cm to frog muscle cells of radius 10μm, he found that the resultant intracellular field was less than 0.1 mV/cm. It is generally believed that this small intracellular field is unlikely to produce significant intracellular effects. A more likely site of interaction is the membrane.

Electric fields may effect the membrane mechanisms in two apparent ways:

by altering the transmembrane ion transport or by altering the membrane receptor distribution.

1.4.2 Alteration of Transmembrane Ion Transport

Monovalent and divalent ions are transported across the cell membrane by several processes. These processes may be modulated chemically or by mechanical or electrical stresses. Although this study examines a possible mechanism of electrical modulations, it is closely coupled to the other two processes. An applied extracellular electric field may change the transmembrane potential, causing a mechanical change by opening (or closing) voltage gated channels or by changing the radius of the pores within the membrane. An electric field may also affect the chemical processes by altering the ion concentration gradients across the cell's membrane.

Voltage Gated Channels

In the membrane are proteins that form transmembrane conducting aqueous channels that allow for transmembrane ion transport. The proteins in these channels may behave like gates with sensors capable of opening and closing the channels. These modulated gates may respond to a change in the membrane potential; thus, these protein channels are called voltage gated channels (VGC). Hille [1984] reviewed this subject and pointed out that the change from the equilibrium ratio of open to closed gates in VGC's is given by $e^{\Delta V/V_T}$, where V_T is the thermal voltage equal to 25mV at 25°C. For a field strength of 3 mV/m, shown to have an effect on the biosynthesis of protein in fibroblasts [McLeod, 1987], across a cell length of $100\mu m$, the equilibrium state of the gates changes $e^{.3\mu V/25mV} - 1 = 0.001\%$. This change should not account for any modulation in cellular function. Even for the upper limit of physiologic field intensities (creating a transmembrane potential 250μV), the equilibrium state of the gates changes only $\sim$1%. Although this change

is small, it may account for some of the differences in cellular function.

Electrodiffusion

Concentration gradients of ionic species (sodium, potassium, calcium, chloride, etc.) exist across cell membranes. The gradients are created by active ion pumps in the membrane. They use ATP to drive the transport against concentration gradients. An indigenous field is created due to the charge separation caused by the gradient in charge. The magnitude of the field is $\sim$75 mV/5nm = 15 $\times$ 10^6 V/m where 75mV is the maximum potential difference due to the charge separation and 5nm is the approximate length of the membrane. Unless an amplification mechanism exists, an applied field of physiologic strength should have no effect on the ion transport due to electrodiffusion.

Electroporation

Fields may also effect the transport of ions through aqueous pores that transiently exist between phospholipid molecules in the bilayer. The radius of these pores are proportional to electrical polarization stresses created by the membrane electric field. Gradients in polarization arise because the permittivity of water is thirty-forty times that of the fatty acids in the hydrophobic portion of the lipid bilayer. But, as in the case above, the large differences between the existing transmembrane fields and the applied fields make it unlikely that the pore size is significantly modulated by physiologic field strengths.

1.4.3 Alteration of Membrane Receptor Distribution

Embedded in the cell membrane and extending into the extracellular matrix are glycoprotein receptors. These receptors have binding sites with a highly specific affinity for a particular signaling substance (a ligand). When the ligand binds to the receptor, the receptor-ligand complex initiates a sequence of reactions that leads to

specific cellular responses.

The possible mechanism of altering the membrane receptor distribution with an electric field involves the mechanical movement of membrane proteins that may alter the receptor-ligand binding kinetics.

The membrane and membrane proteins have a fixed negative charge that arises from the attached sialic acid residues and the charged carbohydrate chains. In the presence of an electric field, electrophoretic and viscous drag forces act on the proteins moving them, in the plane of the cell surface, toward one of the field's poles.

Using the expression for the "effective" electrophoretic mobility developed in chapter II, the expected distance traveled by a concanavalin A receptor, with an "effective" electrophoretic mobility of $\sim 2 \times 10^{-7}$ cm^2/V-sec, in one-half period in a field of strength 1 V/m and 1 Hz is less than one angstrom. Although this distance is negligible compared with Brownian motion, if the membrane has anisotropic properties, rectification of the protein movement may occur. A net migration of the proteins would cause a change in the density of the receptors. Altering the density may change the probability of a receptor binding to a ligand or may cause clustering of receptors.

Many receptor-ligand interactions behave according to simple second order chemical reaction kinetics:

$$R + L \underset{k_b}{\overset{k_f}{\rightleftharpoons}} RL. \tag{1.1}$$

This equation states that the receptors, R, and ligands, L, form receptor-ligand complexes, RL, at a forward rate constant k_f. The backward rate constant is k_b. In equilibrium equation 1.1 can be expressed by

$$k_f[R][L] = k_b[RL], \tag{1.2}$$

which gives

$$\frac{[R][L]}{[RL]} = \frac{k_b}{k_f} = K, \tag{1.3}$$

where K is the dissociation constant.

If the ligand concentration, [L] , is constant, then the concentration of the bound receptors, [RL], becomes

$$[RL] = A \times [R], \tag{1.4}$$

where A is a constant equal to [L]/K.

If migration within the plane of the cell surface changes the concentration of the receptors, then according to equation 1.4 the concentration of receptor-ligand complexes also changes. A change in the concentration of the receptor-ligand pairs may promote patching, coated pits, or capping which may cause an increase in the endocytosis-exocytosis rate or a modulation of ligand-controlled cellular processes. Also, the clustering of receptors at one pole of the cell might act similarly to receptor-ligand pairs that have capped at one side of the cell.

1.5 Electrophoresis of Cell Membrane Receptors

Jaffe [1977] was the first to point out that an electric field parallel to the surface of the cell should redistribute charged macromolecules that freely moving laterally in the plasma membrane. This "lateral electrophoresis" in cell membranes could be a mechanism underlying the effects of electric fields in developing systems.

Experimentally, it has been demonstrated that within four hours an extracellular electric field of 4 V/cm redistributes concanavalin A (con A) receptors in the plasma membranes of living *Xenopus* muscle cells [Poo and Robinson, 1977]. The movement appeared to have reached a steady state. The next year, Poo et al. [1978] showed that a uniform field of 10 V/cm applied across the surface of *Xenopus* muscle cells for ten minutes results in an accumulation of con A receptors at the

cathode pole of the cell. Relaxation occurs after removal of the field and results in complete recovery in thirty minutes. Additionally, Poo et al. found the threshold of the field required to induce a detectable accumulation across a 20μm wide cell is between 1-1.5 V/cm which corresponds to a voltage difference of 2-3mV. Recently, Guigni et al. [1987] showed that a field of 15 V/cm for thirty minutes at 23°C induced a redistribution of unoccupied epidermal growth factor (EGF) receptors such that the concentration of receptors at the cathode facing pole approximately triples.

Poo et al. [1978, 1979] made measurements of the electrophoretic mobility of con A receptors by applying a 10 V/cm field for ten minutes, reversing the polarity, and measuring the time it takes for the proteins to travel the length of the cell. The values for the electrophoretic mobility were found to be 2×10^{-9}m/sec per V/cm and 1.9×10^{-9}m/sec per V/cm on *Xenopus* muscle cells and myoblasts respectively.

According to experiments by McLauglin and Poo [1981], con A receptors that normally accumulate on the cathode side of embryonic muscle cells in an applied field could be induced to accumulate at the anode side by adding positive charges to the surface of the cells or pre-incubating the cells in neuraminidase [Poo et al. 1979], a treatment that removes the negatively charged sialic acid residues on the cell surface [Eylar et al., 1962]. On the other hand, adding more negative charge in the form of lipid monosialogangliosides (G_M1) enhances the convective transport causing an accumulation of con A receptors at the cathode side of the cell.

In modeling the protein kinetics, McLauglin and Poo accounted for the forces acting on the proteins: an electrophoretic force and a viscous drag force created by the electroosmotic flow of the counter-ions near the cell surface. They developed an expression for the "effective" electrophoretic mobility of the cell surface proteins, by equating these forces. Chapter'II further investigates this theory.

1.6 Diffusivity of Cell Surface Glycoproteins

In an attempt to measure the diffusivities of cell surface glycoproteins two techniques were employed: fluorescence recovery after photobleaching (FRAP) techniques and by monitoring the relaxation of the proteins after the termination of an electric field. Background of these two methods is reviewed below.

1.6.1 Diffusivity Measurements using FRAP techniques

A FRAP experiment consists of irreversibly photolysing the fluorescently labeled molecules in a region of the cell surface and monitoring the recovery of the fluorescence which is due to the movement of the bleached and unbleached fluorophores. Experiments using FRAP began in 1974 to measure the lateral mobility of rhodopsin in amphibian retinal disk membranes ($D \sim 5 \times 10^{-9}$ cm^2/s) [Poo and Cone, 1974; Liebmann and Entine, 1974]. Since that time, FRAP has been used more generally to make quantitative measurements of macroscopic lateral mobilities of fluorescently labeled molecules. A small sampling of the work done since 1974 is given below to show the diversity of cell types and glycoproteins studied as well as the wide range of diffusion coefficients reported.

Jacobson et al. [1976] studied the fluorescence recovery kinetics of succinyl-fluorescein Con A in glycerol-saline solutions ($D \sim 4 \times 10^{-9}$ cm^2/s), and bound to the surface of mouse fibroblasts ($D \sim 7 \times 10^{-11}$ cm^2/s). Studies were undertaken to investigate the diffusion of Con A receptors on rat myoblasts ($D \sim 10^{-11}$ cm^2/s) [Schlessinger et al., 1976], the diffusion of lipid probes, dil ($D \sim 9 \times 10^{-9}$ cm^2/s), and other labeled proteins ($D \sim 2 \times 10^{-10}$ cm^2/s) on L-6 myoblast membranes [Schlessinger et al., 1977], and the diffusion of fluorescent derivatives of insulin and EGF bound to 3T3 mouse fibroblasts ($D \sim 4 \times 10^{-10}$ cm^2/s) at 25°C [Schlessinger et al., 1978]. Eldridge et al. [1980] compared the diffusion coefficients of dil ($D \sim 9 \times 10^{-9}$ cm^2/s), the diffusion coefficients of a fluorescent ganglioside derivative, G_M1 ($D \sim 5 \times 10^{-9}$ cm^2/s), and the diffusion coefficient of tetramethyl-rhodamine

labeled succinylated con A ($D \sim 4 \times 10^{-10}$ cm^2/s) on normal and transformed cultured mouse fibroblasts; the variations on the different cell types, however, were not significant. More recently, Livneh et al. [1986] showed that deletions in the cytoplasmic kinase domain of the EGF receptors in monkey COS cells do not affect their lateral diffusion coefficient ($D \sim 1.5 \times 10^{-10}$ cm^2/s).

1.6.2 Diffusivity Measurements by Monitoring Post-field Relaxation

The monitoring of the recovery of the proteins' uniform distribution after removal of an electric field has also been used to quantitatively solve for a diffusion coefficient. Poo et al. [1978] measured the asymmetry of the labeled proteins on *Xenopus* muscle cells at various times in the relaxation process and found that the characteristic 1/e time for the relaxation of asymmetry induced by a 10 V/cm field for ten minutes ranged from fifteen to twenty-five minutes. This characteristic 1/e time corresponds to a diffusion coefficient of $4 - 7 \times 10^{-10}$ cm^2/sec. On *Xenopus* myoblasts, Poo et al. [1979] found a diffusion coefficient of 5.1×10^{-9} cm^2/sec. Justification for diffusion coefficients that are lower than the ones reported in section 1.6.1 comes from the receptors being complexed with the ligands after relaxation. Therefore, the diffusion coefficients measured only the receptor diffusivity and not the diffusivity of the larger receptor-ligand complex.

1.7 Major Histocompatibility Complex Antigens

According to Bjorkman et al. [1987], class I major histocompatibility complex (MHC) antigens comprise a family of polymorphic transmembrane cell surface glycoproteins present in nearly all nucleated cells. The MHC contains three loci, HLA-A,B,C in man and H-2K,D,L in mouse, which have a large number of alleles. MHC antigens are the targets of antibodies and cytotoxic T lymphocytes during rejection of foreign transplants. The movement of these receptors was investigated in order to compare the results with documented results of anisotropic behavior of

MHC antigens on human dermal fibroblasts [Stolpen et al., 1987].

The lateral diffusion of the MHC antigens has been studied extensively in fibroblasts and lymphocytes. By measuring the lateral diffusion of H-2 antigens on mouse fibroblasts, Edidin and Wei [1982] found that the diffusion coefficient varied more than twentyfold from cell to cell, though they varied no more than twofold at different points on the same cell. The average diffusion coefficient was $\sim 1.6 \times 10^{-9}$ cm^2/s. Petty et al. [1980] showed that HLA antigens have a dispersed distribution and have diffusion coefficients between $\sim 10^{-9}$ and 10^{-10} cm^2/s in peripheral blood leukocytes. For HLA antigens on VA-2 human cells, Su et al. [1984] found a diffusion rate of $\sim 3 \times 10^{-10}$ cm^2/s. Further, this rate could be changed by incubating the cells in different medias and at different pH levels. Wier and Edidin [1986] studied the effects of cell density on the lateral mobility of MHC antigens in fibroblasts. They found a decrease in both the fractional recovery and the diffusion coefficient in more confluent cultures. (Other articles investigating the lateral diffusion of MHC antigens on different cell types include: Henis and Gutman, [1983], Damjanovich et al., [1983], and Beirer et al., [1987]).

1.8 Evidence for Anisotropic Mechanical Properties

Finally, the background literature of the evidence for anisotropic mechanical properties needs to be reviewed. In 1979, Smith et al. demonstrated that succinyl Con A receptors diffuse anisotropically on murine fibroblasts with the most rapid diffusion in the direction parallel to the underlying actin stress fibers. They used a technique of photobleaching in a two-dimensional periodic pattern and, using Fourier analysis, determined the diffusion coefficients [Smith and McConnell, 1978]. Rabinowitz [1982] showed that charged surface molecules redistribute in an ac field and accumulate on the surface perpendicular to the field. In contrast, Kapitza et al.[1985], using a "video-FRAP" technique, observed that Con A receptor diffusion on human foreskin fibroblasts is independent of direction. Recently, Stolpen et

al. [1987], using a new technique called "line FPR," observed that human dermal fibroblasts, but not human vascular endothelial cells, exhibit anisotropic diffusion of class I MHC proteins. "Line FPR" uses a highly eccentric elliptical beam to photobleach and measure the sample. The lateral diffusion is measured in the direction of the minor axis of the beam.

1.9 Organization

In the following chapters, theory, procedures, and results of the study will be discussed. Chapter II models the glycoproteins in an electric field and develops an expression for the "effective" electrophoretic mobility. This expression is then used in chapter III to model the kinetics of the protein movement and the recovery of the fluorescence after photobleaching. Chapter IV discusses the apparatus used and the experimental protocols developed to measure the "effective" electrophoretic mobility discussed in chapter two. Chapter V presents the results of the experiments and chapter VI discusses the significance of these findings and offers ideas for the continuation of this investigation.

Chapter II

Theory of Electrophoresis and Electroosmosis of Cell Surface Receptors

2.1 The Plasma Membrane

The plasma membrane is the outer cell boundary separating the intracellular from extracellular space. Its structure is primarily that of a phospholipid bilayer containing abundant proteins. At physiologic temperatures the lipid bilayer is primarily a highly viscous fluid. It is characterized by a viscosity of approximately one poise, which is approximately one thousand times that of water. However, the lipid bilayer is not isotropic. Rather, the microdomains exist in the bilayer containing phospholipids condensed in a liquid crystal or gel state. The phospholipid molecules in the gel microdomain are less mobile and the measured viscosity is at least ten thousand times greater than water. In fibroblasts, microdomains have characteristic dimensions in the range of one to two microns.

Other microdomains of altered mechanical properties are centered around integral proteins, usually macromolecules, which span the bilayer several times, displacing fifty to one hundred phospholipid molecules [Hoppe et al., 1983] and adding structural stability to the surrounding bilayer. Integral proteins in the membrane are stabilized in that position by a hydrophobic section of the protein consisting of apolar amino acids. The apolar region is attached to the central hydrophobic section of the bilayer by strong hydrophobic interactions. In general, integral proteins tend to increase the viscosity of the bilayer.

In the fluid state, macromolecules are free to move laterally in the plane of the plasma membranes. At 37°C, phospholipid molecules have been found to undergo ten million position exchanges per second with adjacent like molecules. The measured lateral diffusivity of phospholipids is in the range of 10^{-8} cm^2/sec.

Proteins have lower diffusivities in the range of 10^{-9} to 10^{-11} cm^2/sec.

Many of the proteins in the bilayer are glycosylated. The oligosaccharide moiety of these glycoproteins contains fifty to one hundred disaccharide groups on a linear chain extending into the extracellular space. These oligosaccharide chains have many ionized side groups which give the glycoprotein a fixed negative charge. Glycoproteins frequently function as receptors for hormones or for other ligands.

The next section models the membrane more simply and describes the forces acting on it in the presense of an electric field. This model is used for the theoretical calculations in this chapter and in chapter III.

2.2 Modeling and Equating Forces

For this analysis of the effects of external electric fields on the cell surface receptor movement, the membrane is a poorly conducting, viscous fluid with a fixed negative surface charge due in part by the sialic acid side-chains on the membrane glycolipids. This charge, located close to the phospholipid heads, causes the mobile positive counter ions to accumulate near the surface of the membrane forming an electrical double layer. Helmholz modeled this charged interface as a parallel-plate capacitor. The Debye length describes the characteristic length of the potential drop between the charged surface and the mobile ions. Figure 2.1 is a diagram of the planar Helmholtz capacitor model for an electrical double layer. The Debye length is expressed by parameter, δ. In an electric field, the counter ions (positive in for a cell membrane) flow at a velocity v_z in the direction of the field (this flow is also called the electroosmotic flow). The zeta potential, ζ, is defined as the electrical potential in the slipping plane between the fixed and flowing liquid in the Helmholz capacitor model.

These experiments use cells that are plated to coverslips. Since these cells are much longer and wider than they are high, and the electric field tangential to the cell's surface is only in the $\hat{z}$ direction, the movement of the proteins within

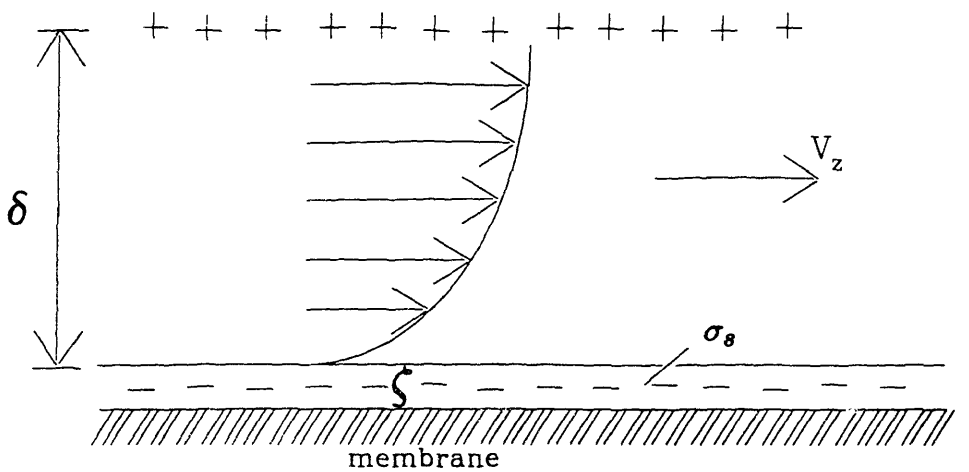

Figure 2.1: The Helmholtz capacitor model for the electrical double layer is shown

the membrane is modeled one-dimensionally. The glycoproteins are represented as a pair of tethered spheres (figure 2.2), one, within the membrane of radius a_1, and one, extracellular of radius a_2. The viscosity of the extracellular media is given by η and the viscosity of the membrane is given by η_m.

In an imposed electric field, an electrophoretic force acts on the charged proteins. The positively charged counter ions create an electroosmotic flow toward the cathode side. The inertial force density of the protein is much less than the viscous force due to the flow. This assumption allows for a low Reynold's number evaluation of the viscous flow, resulting in a Stoke's drag force on the protein [Melcher, 1981]. Viscous forces act to retard protein movement. In the steady state, the electrophoretic force, F_{el}, on the extracellular sphere is equal to the Stoke's drag on this sphere, F_{s1}, plus the Stoke's drag on the sphere in the bilayer, F_{s2}. The forces in this system are given:

$$F_{s1} = -6\pi\eta a_2(U_z + v_z) \tag{2.1}$$

$$F_{s2} = -6\pi\eta_m a_1 U_z \tag{2.2}$$

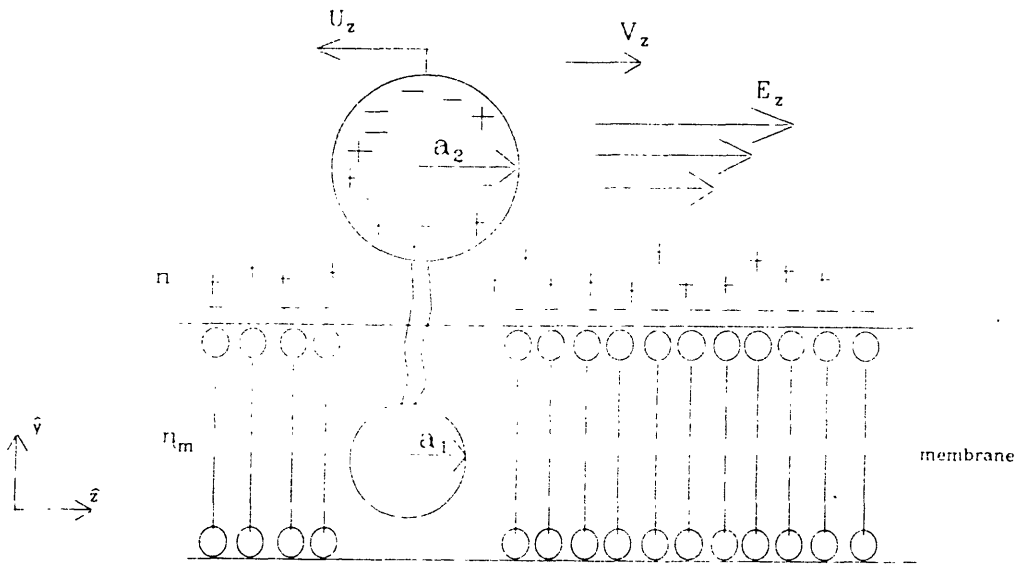

Figure 2.2: The glycoprotein receptors are modeled as a pair of tethered spheres in the membrane.

$$F_{el} = 6\pi\eta a_2 U_z' \tag{2.3}$$

where v_z is the velocity of the cell surface electroosmotic fluid flow, U_z' is the electrophoretic velocity of an untethered particle in an electric field with no fluid flow ($v_z = 0$), and U_z is the "effective" electrophoretic velocity of the glycoprotein. The next section the solution for the U_z and v_z will be found, and then the fact that in the steady state all the forces sum to zero can be used to calculate the "effective" electrophoretic velocity in terms of the physical properties of the cell surface, the cell membrane, the extracellular fluid, and the applied electrical field, E_z. The following analysis uses approaches found in Levich [1962], Melcher [1981], and McLauglin and Poo [1981] to solve for the "effective" electrophoretic velocity.

2.2.1 Calculation of Electroosmotic Velocity

Although the double layer of the electrolyte surrounding a cell is thin ($\sim$ 1nm), an electric field exerts a force density $\rho_f E_z$ on the fluid, and a shear flow results (figure 2.3). Balancing the electrical and viscous shear forces on the cell

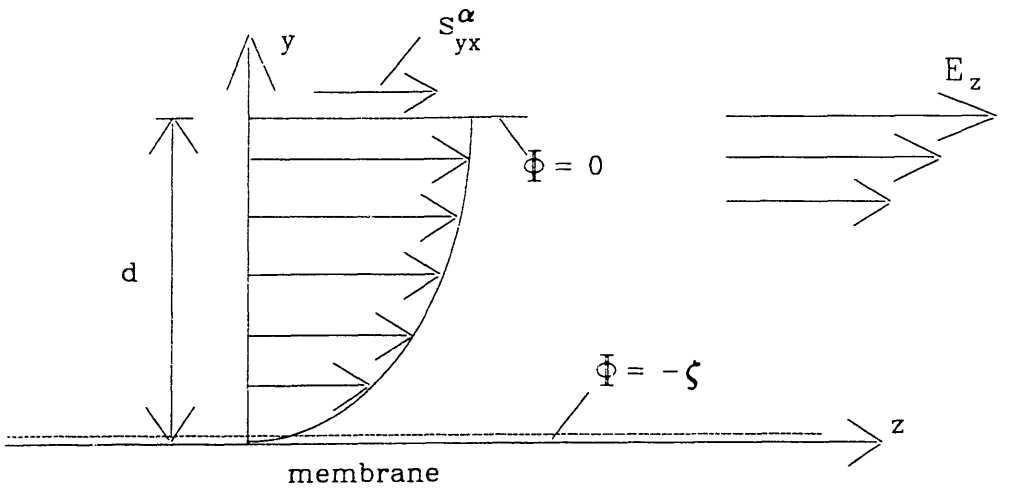

Figure 2.3: An applied electric field results in a fluid flow due to electroosmosis.

surface gives

$$\eta \frac{\partial^2 v_z}{\partial y^2} = -\frac{\partial T_{zy}}{\partial y} \tag{2.4}$$

where T_{zy}, the electrical stress at the surface of the cell in the tangential direction, is equal to $\rho_f E_z$. Integrating once from $y = 0$ to $y = \delta$ gives

$$\eta \frac{\partial v_z}{\partial y} = -T_{zy} + S^{\alpha}_{zy} \tag{2.5}$$

where the constant of integration, S^{α}_{zy}, is the shear viscous stress at a distance, d, from the slip plane, where the fluid maintains a velocity $v^{\alpha}_z \hat{z}$. The electrical shear stress falls to zero at $y = \delta$.

Substituting

$$T_{zy} = \epsilon E_z E_y \tag{2.6}$$

and

$$E_y = -\frac{d\Phi}{dy} \tag{2.7}$$

into equation 2.5 and integrating from 0 to y, noting that E_y and S^{α}_{zy} are constants,

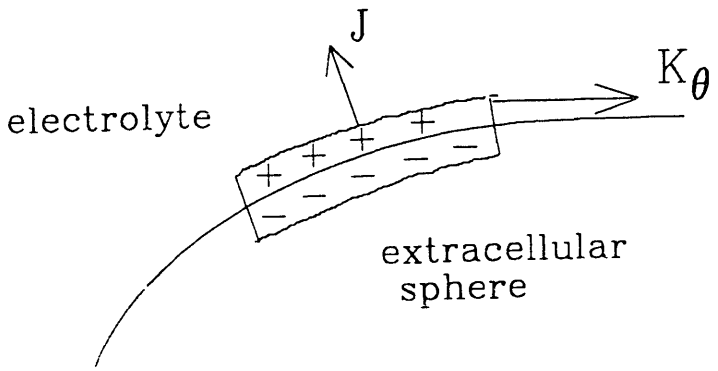

Figure 2.4: Surface control volume of the extracellular sphere in the glycoprotein model. The protein has a fixed negative charge.

yields

$$\eta v_z = \int_0^y \epsilon E_z \frac{d\Phi}{dy} dy + \int_0^y S^{\alpha}_{zy} dy \tag{2.8}$$

$$\eta v_z = \epsilon E_z [\Phi(y) - \Phi(0)] + y S^{\alpha}_{zy}. \tag{2.9}$$

The potential at the slip plane is $-\zeta_1$, while that at y=d is zero. The stress term on the large scale compared to the debye length can be ignored. The fluid flow velocity due to electroosmosis, therefore, is given by

$$v_z = \frac{\epsilon \zeta_1}{\eta} E_z. \tag{2.10}$$

2.2.2 Calculation of the Electrophoretic Velocity of a Spherical Protein in an Electrolyte

The extracellular protein is assumed to be spherical and insulating with a smooth charged surface. The electrophoretic velocity of the extracellular protein is calculated without concern for either the electroosmotic effects or the tethered part of the glycoprotein in the membrane. The extracellular protein is modeled as a charged sphere with radius a_2 which is much larger than the thickness of the double layer. The electric field is assumed uniform in the $\hat{z}$ direction. The conservation of charge in a surface control volume shown in figure 2.4 is given by

$$\hat{n} \cdot (J_1 - J_2) + \nabla \cdot K = 0 \tag{2.11}$$

where J_1 is the current density $J_1 = \sigma E$; $J_2 = 0$, K is the surface current density given by

$$K = \int_0^\infty \rho_f(r) v_\theta(r,\theta) dr. \tag{2.12}$$

$v_\theta(r,\theta)$ is the velocity of the counter ions around the charged particle.

Using the Helmholz double layer model,

$$\rho_f(r) = -\rho_0(r - (R+d))\sigma_m \tag{2.13}$$

and

$$\sigma_m = \left(\frac{\epsilon}{\delta}\right)\zeta_2 \tag{2.14}$$

where σ_m is the surface charge of the protein.

Solving for K consists of first finding an expression for $v_\theta(r,\theta)$, analogously to solving for equation 2.10, and substituting it and equation 2.13 into equation 2.12. As Melcher [1981] shows

$$K = \sigma_s E_\theta, \tag{2.15}$$

where

$$\sigma_s = \frac{\rho_0 \zeta_2^2 \epsilon \delta}{n V_T}, \tag{2.16}$$

and $V_T = KT/q$ is the thermal voltage.

Substitution of equation 2.15 into equation 2.11 gives another expression for the continuity of charge

$$\sigma E_\theta + \frac{1}{r \sin\theta} \frac{\partial}{\partial \theta}(\sigma_s E_\theta \sin\theta) = 0. \tag{2.17}$$

The form of the solution of the potential outside the double layer where where charge density is zero ($\rho = 0$) is a superposition of a constant field at infinity and a

dipole centered at r=0:

$$\Phi = -E_0 r\cos\theta + A\frac{\cos\theta}{r^2}. \tag{2.18}$$

Solving equation 2.18 for E_θ gives a solution for A:

$$A = \frac{E_0 a_2^3}{2}\frac{[\sigma - \frac{2\sigma_s}{a_2}]}{[\sigma + \frac{\sigma_s}{a_2}]}. \tag{2.19}$$

So at $r = a_2$,

$$E_\theta = \frac{3E_0\sigma}{2(\sigma + \frac{\sigma_s}{a_2})}\sin\theta. \tag{2.20}$$

The slip velocity for a spherical protein with a zeta potential, ζ_2, follows directly from equation 2.10:

$$v_\theta = \frac{\epsilon\zeta_2}{\eta}E_\theta = \tilde{v}_\theta\sin\theta. \tag{2.21}$$

Now substituting equation 2.20 into equation 2.21 results in

$$\tilde{v}_\theta = -\frac{3\epsilon\zeta_2}{2\eta}\frac{E_0}{1 + \frac{\sigma_s}{\sigma a_2}}. \tag{2.22}$$

Knowing that the forces on the sphere must vanish, the velocity, U', of the free particle can be found. The force in the $\hat{z}$ direction is given by

$$f_z = \int_0^\pi [\tilde{S}_{rr}\cos\theta - \tilde{S}_{\theta r}\sin\theta]2\pi a_2^2\sin\theta d\theta \tag{2.23}$$

which simplifies to

$$f_z = \frac{8}{3}\pi a_2^2(\tilde{S}_{rr} - \tilde{S}_{\theta r}). \tag{2.24}$$

The stress-velocity relations are given by

$$\begin{pmatrix} \tilde{S}_{rr} \\ \tilde{S}_{\theta r} \end{pmatrix} = \frac{-\eta}{2a_2}\begin{pmatrix} 9 & 3 \\ 6 & 6 \end{pmatrix}\begin{pmatrix} -\frac{U_z'}{2} \\ \tilde{v}_\theta + U_z' \end{pmatrix} \tag{2.25}$$

so the skip velocity can be related to the uniform velocity of the particle:

$$U_z' = \frac{2}{3}\tilde{v}_\theta. \tag{2.26}$$

The final relationship between the electrophoretic velocity, U_z', and the applied field, E_0, can now be defined:

$$U_z' = \left(\frac{\frac{\epsilon\zeta_2}{\eta}}{1+\frac{\sigma_s}{\sigma a_2}}\right) E_0. \tag{2.27}$$

In the case of most proteins $|\frac{\sigma_s}{\sigma a_2}| \ll 1$; therefore,

$$U_z' = \frac{\epsilon\zeta_2}{\eta} E_0. \tag{2.28}$$

2.2.3 Calculation of the "Effective" Electrophoretic Velocity

To arrive at the expression for the "effective" electrophoretic velocity, it is assumed that the glycoprotein movement on the cell's surface is in the steady state. The forces given by equations 2.1, 2.2, and 2.3 must, therefore, sum to zero. That is

$$F_{s1} + F_{s2} + F_{el} = 0. \tag{2.29}$$

Substituting equations 2.1, 2.2, 2.3, 2.10, and 2.28 into equation 2.29 gives

$$U_z = \frac{a_2(\epsilon\zeta_1 - \epsilon\zeta_2)}{a_1\eta + a_2\eta_m} E_z. \tag{2.30}$$

The "effective" electrophoretic mobility, μ, is given as

$$\mu = \frac{U_z}{E_z} = \frac{a_2\epsilon(\zeta_1 - \zeta_2)}{a_1\eta + a_2\eta_m}. \tag{2.31}$$

Equation 2.31 shows that the movement (velocity and direction) of the macromolecules in the cell's surface depends on both the charge on the protein and the

charge on the cell membrane. McLaughlin and Poo demonstrated that negatively charged particles accumulate at the positive pole of the cell when $\zeta_1 < \zeta_2$ and at the negative pole of the cell when $\zeta_1 > \zeta_2$. They altered the surface charge on the cell and made it more negatively charged by adding lipid monosialogangliosides (G_{M1}) or less negatively charged by adding neuraminidase which removes the sialic acid residues from the cell surface, and monitored the direction of the movement of Concanavalin A receptors in an applied electric field. It is this "effective" electrophoretic mobility, μ, that is used in the theory in the next chapter and is measured experimentally as a function of direction to determine if it has anisotropic behavior.

2.3 Direction of the "Effective" Electrophoretic Mobility of MHC Receptors

Determining the charge of the MHC receptor will give an indication of the dominant force acting on the protein in an electric field. Although the major histocompatibility complex is polymorphic, the amino acid sequences of HLA-B7 and HLA-A2, two major alleles of the MHC [Krangel et al. 1980], indicate a net charge of only -7 and +3 coulombs respectively. From these, it is hypothesized that the MHC is basically uncharged. The "effective" electrophoretic velocity, therefore, is driven mainly by the electroosmotic movement of the ions counter, so the proteins are expected to accumulate at the negative pole of the cell.

Chapter III

The Theoretical Fluorescence Recovery Curves and Protein Distribution in the Presence of an Electric Field

3.1 Overview

This chapter explains the theoretical background for the two approaches used in this thesis to solve for the diffusion coefficient and the "effective" electrophoretic mobility. The first approach uses fluorescence recovery after photobleaching (FRAP) techniques. The fluorescence recovery curve is governed by the diffusion and the convection of the fluorescent proteins in an applied electric field after an intense laser pulse bleaches a small Gaussian area on the cell. The pure diffusion curve and the pure flow curve are found by taking the limit as $E \rightarrow 0$ and $D \rightarrow 0$ respectively. The "effective" electrophoretic mobility is found as a function of direction in the membrane by changing the polarity of the field.

In the second approach, the fluorophores are not bleached. The fluorescence is monitored at one point on the cell. With the application of an electric field, initially uniform concentrations of charged macromolecules become nonuniform by accumulating at one side of the cell. Changing the polarity of the field changes the side of the cell that the macromolecules aggregate. Removal of the field allows the diffusion of the proteins to uniform fluorescence. Depending on the side of the cell that the proteins have accumulated, the diffusion coefficient can be determined as a function of direction.

3.2 The Theoretical Fluorescence Recovery Curves in the Prescence of an Electric Field

In this section, the governing equations for the theoretical fluorescence recovery curves are derived. The approach follows that published by Axelrod et al.

[1976] and Elson and Magde [1974]; however, all intermediate steps are included here.

3.2.1 The Convection-Diffusion Equation

The continuity law describing the movement of the fluorophores attached to the proteins within the membrane states that the total time rate of change of the concentration, $c(r,t)$, of the fluorophores, plus the velocity, $\bar{v}$, of the membrane flow dotted with the gradient of the concentration is equal to the negative divergence of the flux, Γ:

$$\frac{\partial c(r,t)}{\partial t} + \bar{v} \cdot \nabla c(r,t) = -\nabla \cdot \Gamma. \tag{3.1}$$

As justified by Axelrod et al., the velocity of the membrane flow is inconsequential in the time frame of the FRAP experiments and is therefore, ignored:

$$\frac{\partial c(r,t)}{\partial t} = -\nabla \cdot \Gamma. \tag{3.2}$$

The flux seen by our system is given by

$$\Gamma = \mu\, c(r,t)\; E - D\; \nabla c(r,t), \tag{3.3}$$

where μ is the "effective" electrophoretic mobility of the ligand-receptor complex discussed in the last section, and D is the diffusion coefficient.

Combining equations 3.2 and 3.3 gives the convection-diffusion differential equation:

$$\frac{\partial c(r,t)}{\partial t} = D\nabla^2 c(r,t) - \mu\nabla \cdot c(r,t)E. \tag{3.4}$$

To remain consistent with the last chapter, the cell is assumed flat in the y-z plane, and the electric field is constant in the $\hat{z}$ direction; therefore, equation 3.4

can now be simplified:

$$\frac{\partial c(r,t)}{\partial t} = D\nabla^2 c(r,t) - U_z \frac{\partial c(r,t)}{\partial z} \tag{3.5}$$

where U_z is, again, the electrophoretic velocity, equal to $\mu \cdot E_z$, of a protein in a cell membrane. A solution to the above equation is found in the next two sections. First, the initial conditions and a definition of the fluorescence needs to be presented.

3.2.2 Initial Conditions and Definition of Fluorescence

The concentration at two different times is needed to solve equation 3.5. The initial condition at time, $t = 0$, is defined by the concentration of the fluorophores immediately after an intense laser beam bleaches a small Gaussian spot on an evenly stained cell. The concentration at very long times is defined as the concentration at $t \rightarrow \infty$.

To find the concentration at $t = 0$, the bleaching kinetics of the fluorophores is modeled as an irreversible first order reaction with a rate constant $\alpha I(r)$. The concentration $c(r,t)$ of the unbleached fluorophores immediately after the bleach at position r and time t can be found from the following equation:

$$\frac{\partial c(r,t)}{\partial t} = -\alpha I(r) c(r,t), \tag{3.6}$$

where $I(r)$ is the Gaussian intensity profile of the laser beam given by

$$I(r) = \left(\frac{2P_0}{\pi w^2}\right) \exp\left(\frac{-2r^2}{w^2}\right), \tag{3.7}$$

where P_0 is the laser power at the sample and w is the radius of the Gaussian beam defined as the half width at the e^{-1} height as shown in figure fig:oneoe.

The concentration of the fluorophores immediately after photobleaching ($t = 0$) can now be found by solving equation 3.6 for a bleaching time, T, which

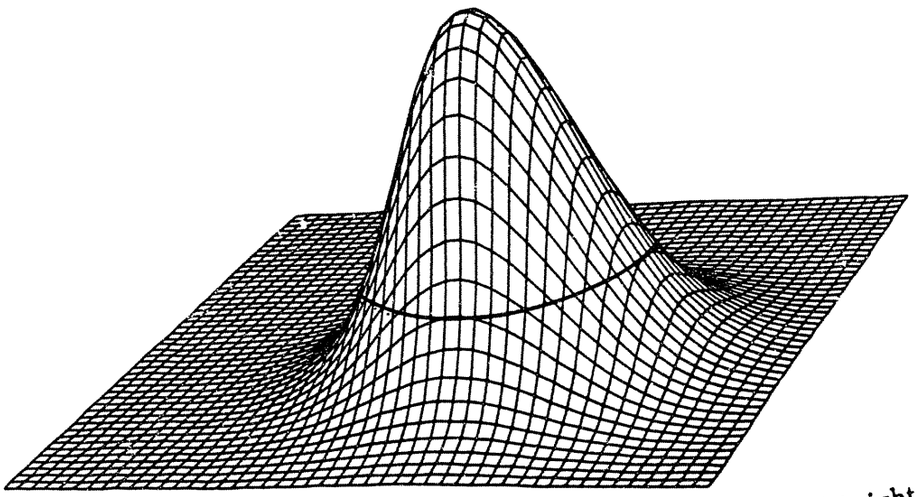

Figure 3.1: An illustration of a Gaussian beam is shown with the e^{-1} height marked. The radius of the beam, w, is defined at this height.

must be short compared to the characteristic time of recovery. This gives

$$c(r,0) = c_0 e^{-\alpha T I(r)} \tag{3.8}$$

where c_0 is the initial concentration of the fluorophore.

It is useful to define a bleach parameter K which is defined as the "amount" of bleach related to the time period T:

$$K = \alpha T I(0) = \frac{2\alpha T P_0}{\pi w^2}. \tag{3.9}$$

The second condition on the concentration is that it returns to c_0 at $t \to \infty$. Although enough information is now known to solve for the concentration in equation 3.5, it is the fluorescence recovery that is being modeled. Therefore, the fluorescence, F(t), excited by a low intensity monitoring beam in the bleached spot,

is defined for $t \geq 0$ by

$$F(t) = \frac{q}{A}\int_0^{2\pi}\int_0^{\infty} I(r)c(r,t)rdrd\theta. \tag{3.10}$$

The parameter q is the product of the quantum efficiencies of the light absorption, emission, and detection. A is the attenuation factor of the beam during observation of the recovery.

The bleaching parameter, K, can now also be related to the percentage of the bleach by

$$\frac{F(0)}{F(-)} = \frac{K^{-1}}{1-e^{-K}}, \tag{3.11}$$

where F(0) is the fluorescence intensity immediately following bleaching, and F(-) is the prebleach fluorescence.

All the information to solve equation 3.10 for the fluorescence as a function of time is now known. The next section presents one approach to the solution with plots of its characteristic curves.

3.2.3 Calculation of Fluorescence Recovery Equation

To solve equation 3.10, an expression for the concentration profile must first be found. One way to solve equation 3.5 is to take its Fourier transform

$$\tilde{c}(\kappa,t) = \frac{1}{2\pi}\int_0^{2\pi}\int_0^{\infty} e^{-i\kappa\cdot r}c(r,t)rdrd\theta, \tag{3.12}$$

which leads to

$$\frac{\partial\tilde{c}(\kappa,t)}{\partial t} = -[\kappa^2 D - i\kappa_z U_z]\tilde{c}(\kappa,t), \tag{3.13}$$

where

$$\kappa^2 = \kappa_y^2 + \kappa_z^2. \tag{3.14}$$

The solution to the first-order equation is simply

$$\tilde{c}(\kappa,t) = \tilde{c}(\kappa,0)e^{-(\kappa^2 D - iU_x\kappa_x)t} \tag{3.15}$$

with

$$\tilde{c}(\kappa,0) = \frac{1}{2\pi}\int_0^{2\pi}\int_0^{\infty} e^{i\kappa\cdot r'}c(r',0)r'dr'd\theta', \tag{3.16}$$

and $c(r',0)$ as defined in equation 3.8.

Substituting the inverse Fourier transform

$$c(r,t) = \frac{1}{2\pi}\int_{-\infty}^{\infty}\int_{-\infty}^{\infty} e^{i\kappa\cdot r}\tilde{c}(\kappa,t)d\kappa_y d\kappa_z, \tag{3.17}$$

and equations 3.15, and 3.16 into equation 3.10, an expression for the observed fluorescence recovery can be written:

$$F(t) = \frac{qc_0}{4\pi^2 A}\int_{-\infty}^{\infty}\int_{-\infty}^{\infty} d\kappa_y d\kappa_z e^{-[\kappa^2 D - iU_x\kappa_x]t}\cdot\int_0^{2\pi}\int_0^{\infty} r dr d\theta I(r)e^{i\kappa\cdot r}\cdot$$
$$\cdot\int_0^{2\pi}\int_0^{\infty} r'dr'd\theta' e^{[i\kappa\cdot r' - \alpha I(r')T]}. \tag{3.18}$$

The last two pairs of integrations can be solved independently and multiplied to the first integrand. Then the final integration can be performed. The solution begins by integrating the third double integral (essentially $\tilde{c}(\kappa,0)$):

$$A = \int_0^{2\pi}\int_0^{\infty} r'dr'd\theta' e^{i\kappa\cdot r'}e^{-\alpha I(r')T}. \tag{3.19}$$

Substituting the expression for I(r') (equation 3.7) and K (equation 3.9) into equation 3.19 gives

$$A = \int_0^{2\pi}\int_0^{\infty} r'dr'd\theta' e^{i\kappa\cdot r'}e^{-K\exp\left(\frac{-2r'}{w^2}\right)}. \tag{3.20}$$

Expanding the exponential into a Taylor series,

$$e^{-K\exp\left(\frac{-2r'}{w^2}\right)} = \sum_{n=0}^{\infty} \frac{(-K)^n}{n!} e^{-\frac{2n}{w^2}r'}, \tag{3.21}$$

and changing to the y'-z' coordinate system yields

$$A = \sum_{n=0}^{\infty} \frac{(-K)^n}{n!} \int_{-\infty}^{\infty}\int_{-\infty}^{\infty} dy'dz' e^{(i\kappa_y y' + i\kappa_x z')} e^{-\frac{2n}{w^2}(y'^2 + z'^2)}. \tag{3.22}$$

Thus, by separating variables, equation 3.22 becomes,

$$A = \sum_{n=0}^{\infty} \frac{(-K)^n}{n!} \int_{-\infty}^{\infty} dy' e^{-(\frac{2n}{w^2}y'^2 - i\kappa_y y')} \int_{-\infty}^{\infty} dz' e^{-(\frac{2n}{w^2}z'^2 - i\kappa_x z')}. \tag{3.23}$$

The y' and z' integrals are independent and can be separately solved. In solving for the y' integral,

$$A_{y'} = \int_{-\infty}^{\infty} dy' e^{-(\frac{2n}{w^2}y'^2 - i\kappa_y y')}. \tag{3.24}$$

The above integral can be solved by completing the square:

$$A_{y'} = \int_{-\infty}^{\infty} dy' e^{-(\frac{2n}{w^2}y'^2 - i\kappa_y y' - \frac{\kappa_y^2 w^2}{8n})} \cdot e^{-\frac{\kappa_y^2 w^2}{8n}}$$

$$A_{y'} = \int_{-\infty}^{\infty} dy' e^{-(\frac{\sqrt{2n}}{w}y' - \frac{i\kappa_y w}{2\sqrt{2n}})^2} \cdot e^{-\frac{\kappa_y^2 w^2}{8n}}. \tag{3.25}$$

These equations can be simplified by making the following substitutions:

$$\chi = \left(\frac{\sqrt{2n}}{w}y' - \frac{i\kappa_y w}{2\sqrt{2n}}\right) \tag{3.26}$$

and

$$dy' = \frac{w}{\sqrt{2n}} d\chi. \tag{3.27}$$

Because

$$\int_{-\infty}^{\infty} e^{-a^2\chi^2} d\chi = \frac{\sqrt{\pi}}{a} \quad a > 0 \tag{3.28}$$

equation 3.25 gives the following value for $A_{y'}$:

$$A_{y'} = \frac{w}{\sqrt{2n}}\sqrt{\pi}e^{-\frac{\kappa_y w^2}{8n}}. \tag{3.29}$$

Solving similarly for the z' integral results in

$$A = \sum_{n=0}^{\infty} \frac{(-K)^n}{n!}\frac{w^2\pi}{2n}e^{-\frac{w^2}{8n}(\kappa_y^2+\kappa_z^2)}. \tag{3.30}$$

The second pair of integrals in equation 3.18 is now considered:

$$B = \int_0^{2\pi}\int_0^{\infty} r dr d\theta I(r)e^{i\kappa\cdot r}. \tag{3.31}$$

Substituting equation 3.7 into equation 3.31 and changing to the y-z coordinate system yields

$$B = \frac{2P_0}{\pi w^2}\int_{-\infty}^{\infty}\int_{-\infty}^{\infty} dydze^{(i\kappa_y y + i\kappa_z z)}e^{-\frac{2}{w^2}(y^2+z^2)}. \tag{3.32}$$

Solving equation 3.32 can be done analogously to that used to solve equation 3.22. The result is

$$B = P_0 e^{-\frac{w^2}{8}(\kappa_y^2+\kappa_z^2)}. \tag{3.33}$$

Combining equations 3.18, 3.19, 3.30, 3.31, and 3.33, the fluorescence can now be defined:

$$F(t) = \sum_{n=0}^{\infty}\frac{(-K)^n}{n!}\frac{qc_0P_0w^2}{8An\pi}\int_{-\infty}^{\infty}\int_{-\infty}^{\infty} d\kappa_y d\kappa_z e^{-(\kappa_y^2+\kappa_z^2)Dt}e^{iU_z\kappa_z t}e^{-\frac{w^2}{8}(\kappa_y^2+\kappa_z^2)(1+\frac{1}{n})}. \tag{3.34}$$

Again, separating the two integrals,

$$F(t) = \sum_{n=0}^{\infty}\frac{(-K)^n}{n!}\frac{qc_0P_0w^2}{8An\pi}\int_{-\infty}^{\infty} d\kappa_y e^{-\left[\frac{w^2}{8}\left(1+\frac{1}{n}\right)+Dt\right]\kappa_y^2}\int_{-\infty}^{\infty} d\kappa_z e^{-\left\{\left[\frac{w^2}{8}\left(1+\frac{1}{n}\right)+D\tilde{t}\right]\kappa_z^2 - iU_z t\kappa_z\right\}}. \tag{3.35}$$

Since the κ_y integration is already in the form of equation 3.28, equation 3.35

becomes

$$F(t) = \sum_{n=0}^{\infty} \frac{(-K)^n}{n!} \frac{qc_0P_0w^2}{8An\pi} \frac{\sqrt{\pi}}{\sqrt{\frac{w^2}{8}\left(1+\frac{1}{n}\right)+Dt}} \int_{-\infty}^{\infty} d\kappa_z e^{-\left\{\left[\frac{w^2}{8}\left(1+\frac{1}{n}\right)+Dt\right]\kappa_z^2 - iU_z t\kappa_z\right\}}. \tag{3.36}$$

The κ_z integration can be carried out by again completing the square:

$$F(t) = \sum_{n=0}^{\infty} \frac{(-K)^n}{n!} \frac{qc_0P_0w^2}{8An\sqrt{\pi\frac{w^2}{8}\left(1+\frac{1}{n}\right)+Dt}} \cdot$$

$$\cdot \int_{-\infty}^{\infty} d\kappa_z e^{-\left\{\sqrt{\frac{w^2}{8}\left(1+\frac{1}{n}\right)+Dt}\kappa_z - \frac{iU_z t}{2\sqrt{\frac{w^2}{8}\left(1+\frac{1}{n}\right)+Dt}}\right\}^2} e^{-U_z^2t^2/4\left[\frac{w^2}{8}\left(1+\frac{1}{n}\right)+Dt\right]}. \tag{3.37}$$

The following substitution is made for convenience:

$$F(t) = \sum_{n=0}^{\infty} \frac{(-K)^n}{n!} \frac{qc_0P_0w^2}{8An\left[\frac{w^2}{8}\left(1+\frac{1}{n}\right)+Dt\right]} \exp\left\{-U_z^2t^2/4\left[\frac{w^2}{8}\left(1+\frac{1}{n}\right)+Dt\right]\right\}. \tag{3.38}$$

Making the following substitution:

$$\frac{w^2}{8}\left(1+\frac{1}{n}\right)+Dt = \frac{8n}{w^2}\left[\frac{1}{1+n(1+\frac{2t}{\tau_D})}\right] \tag{3.39}$$

where

$$\tau_D = \frac{w^2}{4D}. \tag{3.40}$$

Equation 3.38 can now be written

$$F(t) = \frac{qc_0P_0}{A} \sum_{n=0}^{\infty} \frac{(-K)^n}{n!} \frac{\exp\left[-2n\left(\frac{t}{\tau_F}\right)^2 / \left(1+n(1+\frac{2t}{\tau_D})\right)\right]}{1+n(1+\frac{2t}{\tau_D})}, \tag{3.41}$$

where

$$\tau_F = \frac{w}{U_z} = \frac{w}{\mu E_z}. \tag{3.42}$$

By making the assumption that $F(\infty) = qc_0P_0/A$, the fluorescence recovery equation can be put in its final form:

$$F(t) = F(\infty) \sum_{n=0}^{\infty} \frac{(-K)^n}{n!} \frac{\exp\left[-2n\left(\frac{t}{\tau_F}\right)^2 / \left(1 + n(1 + \frac{2t}{\tau_D})\right)\right]}{1 + n(1 + \frac{2t}{\tau_D})}. \tag{3.43}$$

This four parameter model for the recovery is used as the fitting function for the data generated with an electric field. Two other fitting functions, one diffusion dominated and the other flow dominated, can be derived by taking different limits of equation 3.43.

Characteristic curves for different ratios of τ_D to τ_F are plotted in figure 3.2. For convenience, the curves are displayed in a fractional form, $f(t)$, defined as

$$f(t) = \frac{F(t) - F(0)}{F(\infty) - F(0)}. \tag{3.44}$$

3.2.4 Limits to the Fluorescence Recovery Curve

Diffusion Dominated Recovery

With no applied electric field, or a very small "effective" electrophoretic mobility ($U_z \rightarrow 0$), the time constant, τ_F, given in equation 3.42 becomes very large. Taking the limit of equation 3.43 as $\tau_F \rightarrow \infty$ gives

$$F(t) = F(\infty) \sum_{n=0}^{\infty} \frac{(-K)^n}{n!} \left[1 + n(1 + \frac{2t}{\tau_D})\right]^{-1}. \tag{3.45}$$

Figure 3.2 shows a characteristic plot of diffusion dominated recovery.

Flow Dominated Recovery

If the flow term is dominant in equation 3.5 ($D \rightarrow 0$), then, from equation 3.40, $\tau_D \rightarrow \infty$. Substitution of this limit in equation 3.43 yields

$$F(t) = F(\infty) \sum_{n=0}^{\infty} \frac{(-K)^n}{(n+1)!} \exp\left\{\left[\frac{-2n}{(n+1)}\right]\left(\frac{t}{\tau_F}\right)^2\right\}. \tag{3.46}$$

In figure 3.2, a characteristic plot of flow dominated recovery is also given.

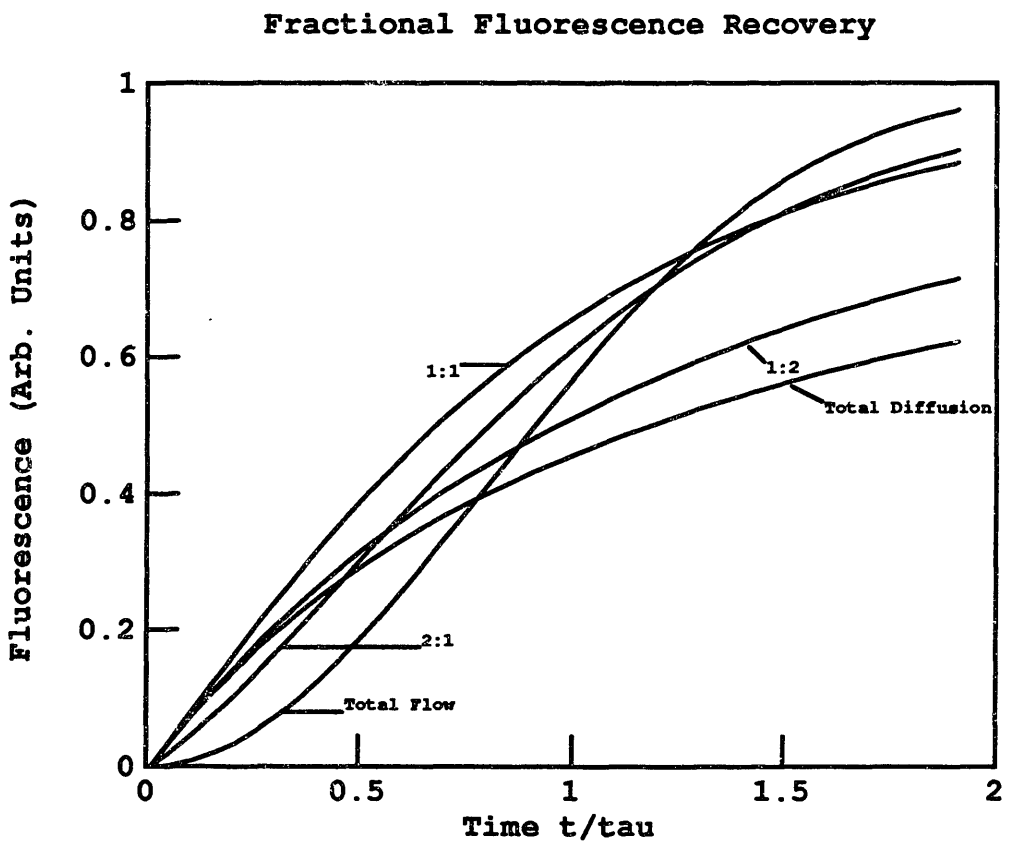

Figure 3.2: Characteristic fractional fluorescence recovery curves with $K = 2.0$ and $F(\infty) = 1$ for different ratios of $\tau_D : \tau_F$.

3.3 Theoretical Protein Distribution in the Presence of an Electric Field

This section solves for the fluorescence profile of the stained proteins throughout the length of the cell for all time in the presence of a dc electric field in the $\hat{z}$ direction.

3.3.1 Modeling

The cell surface is assumed to be rectangular with length, l, oriented in the $\hat{z}$ direction, so in the applied electric field the concentration will vary only in this direction. The fluorescence is monitored at only one point on the cell by a constant intensity beam as used for the monitoring in section 3.2.

Again, equation 3.10 gives the fluorescence. Assumably, the laser beam width is much smaller than the length of the cell, so the spatial concentration profile changes little within the laser radius and is assumed constant within the monitoring beam. With these assumptions, equation 3.10 can be rewritten:

$$F(t) = \frac{q}{A}\left(\frac{2P_0}{\pi w^2}\right)\int_0^{2\pi}\int_0^{\infty} c(z,t)e^{-\frac{2r^2}{w^2}} r dr d\theta = \frac{qP_0}{A}c(z,t). \tag{3.47}$$

The above equation indicates that the fluorescence profile can be found by solving for the concentration profile.

The concentration profile can be found by solving the convection-diffusion equation (equation 3.4) in the $\hat{z}$ direction:

$$\frac{\partial c(z,t)}{\partial t} = D\frac{\partial^2 c(z,t)}{\partial z^2} - \mu E_z \frac{\partial c(z,t)}{\partial z}, \tag{3.48}$$

where the concentration is a superposition of a homogeneous solution, $c_h(z,t)$, and a particular solution, $c_p(z)$:

$$c(z,t) = c_h(z,t) + c_p(z). \tag{3.49}$$

A particular solution is found by calculating the concentration profile at $t \rightarrow \infty$. The homogeneous solution is found by making use of the boundary values, and the complete solution is found by making use of the initial concentration profile. Because the concentration of the fluorophore is conserved, the flux at the boundaries must be zero, or

$$\Gamma(z=0) = \mu E c(z=0,t) - D\frac{\partial c(z=0,t)}{\partial z} = 0. \tag{3.50}$$

$$\Gamma(z=l) = \mu E c(z=l,t) - D\frac{\partial c(z=l,t)}{\partial z} = 0. \tag{3.51}$$

These boundary conditions are satisfied by finding the correct eigenfunctions for the homogeneous concentration profile.

The initial conditions assume the uniformity of the concentration profile throughout the cell:

$$c(z,t=0) = c_0, \tag{3.52}$$

when a constant electric field,

$$E = E_0 U_{-1}(t), \tag{3.53}$$

is turned on at $t = 0^+$.

Sections 3.3.2 to 3.3.4 solve for a solution to equation 3.48 by first finding a particular solution and then satisfying both boundary conditions with the homogeneous solution. Section 3.3.4 combines the solutions from section 3.3.2 and 3.3.3 and uses the initial conditions given here to solve for the complete solution.

3.3.2 Finding a Particular Solution

A particular solution, $c_p(z)$, to equation 3.48 can be found when the fluorophores are in a steady state; that is, when the flux is zero everywhere within the

boundaries:

$$\Gamma(z) = \mu E c_p(z) - D\frac{\partial c_p(z)}{\partial z} = 0. \tag{3.54}$$

Solving for $c_p(z)$ yields,

$$c_p(z) = c' e^{\frac{\mu E}{D} z} \tag{3.55}$$

where c' can be found by using the fact that concentration is conserved, or

$$\int_0^l c_p(z) dz = c_0 l, \tag{3.56}$$

and c_0 is defined in equation 3.52.

The following equation now gives a particular solution:

$$c_p(z) = \frac{\mu E c_0 l}{D(e^{\frac{\mu E}{D} l} - 1)} e^{\frac{\mu E}{D} z} \tag{3.57}$$

3.3.3 Satisfying Boundary Conditions

This section is concerned with finding the eigenvalues and eigenfunctions for the homogeneous solution to equation 3.48. Because the variables are separable, the homogeneous solution is in the form

$$c_h(z,t) = \left(A e^{z\lambda^+} + B e^{z\lambda^-}\right) e^{-t/\tau}, \tag{3.58}$$

where λ^+ and λ^- can be found by substituting $c_h(z,t) = A' e^{\lambda z} e^{-t/\tau}$ into equation 3.48, yielding

$$\frac{1}{\tau} = -\mu E \lambda + D\lambda^2, \tag{3.59}$$

and by solving for the roots of the quadratic expression

$$\lambda^{\pm} = \frac{\mu E}{2D} \pm \sqrt{\left(\frac{\mu E}{2D}\right)^2 - \frac{1}{D\tau}}. \tag{3.60}$$

Substituting equation 3.58 into equations 3.50 and 3.51 gives

$$\Gamma(z) = \mu E \left(A e^{z\lambda^+} + B e^{z\lambda^-} \right) - D \left(A\lambda^+ e^{z\lambda^+} + B\lambda^- e^{z\lambda^-} \right). \tag{3.61}$$

Substituting the boundary conditions that the flux must be zero at $z = 0$ and $z = l$ into equation 3.61 and arranging the two resulting equations into a matrix form gives

$$\begin{pmatrix} -\mu E + D\lambda^+ & -\mu E + D\lambda^- \\ -\mu E e^{l\lambda^+} + D\lambda^+ e^{l\lambda^+} & -\mu E e^{l\lambda^-} + D\lambda^- e^{l\lambda^-} \end{pmatrix} \begin{pmatrix} A \\ B \end{pmatrix} = \begin{pmatrix} 0 \\ 0 \end{pmatrix}. \tag{3.62}$$

For a nontrivial solution to equation 3.62 to exist, the determinant of the coefficients must vanish. The eigenvalues are the values for λ^+ and λ^- which make the following equality true:

$$(-\mu E + D\lambda^+)(-\mu E e^{l\lambda^-} + D\lambda^- e^{l\lambda^-}) - (-\mu E + D\lambda^-)(-\mu E e^{l\lambda^+} + D\lambda^+ e^{l\lambda^+}) = 0. \tag{3.63}$$

Regrouping terms yields

$$(-\frac{\mu E}{D} + \lambda^-)(-\frac{\mu E}{D} + \lambda^+)(e^{l\lambda^-} - e^{l\lambda^+}) = 0. \tag{3.64}$$

The first two expressions give the trivial solution that $\lambda^+ = \lambda^- = \frac{\mu E}{D}$. The third expression also gives the trivial solution, $\lambda^+ = \lambda^-$, unless the expression under the quadratic equation 3.60 is a negative number. If the expression were negative, then the roots could be separated into their real and imaginary parts:

$$\lambda_R^{\pm} = \lambda_R = \frac{\mu E}{2D} \tag{3.65}$$

and

$$i\lambda_i^{\pm} = \pm i \sqrt{\frac{1}{D\tau} - \left(\frac{\mu E}{2D}\right)^2}. \tag{3.66}$$

In this case, the third zero of equation 3.64 can be rewritten as

$$e^{-il\lambda_i^-} - e^{il\lambda_i^+} = 0 \tag{3.67}$$

or

$$\sin(l\lambda_i) = 0. \tag{3.68}$$

From the above expression, the eigenvalues of the equation 3.58 must be

$$\lambda_i = \frac{n\pi}{l}, \tag{3.69}$$

where n is an integer. Making use of the identities

$$e^{i\lambda_i} = \cos\lambda_i + i\sin\lambda_i \tag{3.70}$$

and

$$e^{-i\lambda_i} = \cos\lambda_i - i\sin\lambda_i, \tag{3.71}$$

equation 3.58 can be rewritten, using modal expressions, as

$$c_h(z,t) = e^{\frac{\mu E}{2D}z} \cdot \sum_{n=0}^{\infty}(A_n \sin\frac{n\pi}{l}z + B_n \cos\frac{n\pi}{l}z)e^{-t/\tau_n}. \tag{3.72}$$

The above equation indicates that the eigenfunctions of equation 3.48 are $\sin\frac{n\pi}{l}$ and $\cos\frac{n\pi}{l}$.

Substitution of the eigenvalues, $n\pi/l$, into equation 3.66 yields the expression for the modal time constant, τ_n:

$$\tau_n = \frac{l^2}{D\pi^2}\left(n^2 + \left(\frac{\mu El}{2D\pi}\right)^2\right)^{-1}. \tag{3.73}$$

The solution to equation 3.48 now needs only to satisfy the initial condition to be complete.

3.3.4 Satisfying the Initial Condition

Combining the homogeneous (equation 3.72) and the particular (equation 3.57) solutions, the expression for the concentration profile is now written

$$c(z,t) = e^{\frac{\mu E}{2D}z} \cdot \sum_{n=0}^{\infty} (A_n \sin \frac{n\pi}{l} z + B_n \cos \frac{n\pi}{l} z) e^{-t/\tau_n} + c' e^{\frac{\mu E}{D}z}, \tag{3.74}$$

where τ_n is given in equation 3.73 and c' is the same as in equation 3.55.

Substituting the initial condition that, at $t = 0$, $c(z,0) = c_0$ and multiplying both sides by $e^{-\frac{\mu E}{2D}z}$, equation 3.74 becomes

$$c_0 e^{-\frac{\mu E}{2D}z} - c' e^{\frac{\mu E}{2D}z} = \sum_{n=0}^{\infty} A_n \sin \frac{n\pi}{l} z + B_n \cos \frac{n\pi}{l} z. \tag{3.75}$$

The Fourier coefficients, A_n and B_n, are found by multiplying both sides of the above equation by $\sin \frac{m\pi}{l} z$ and $\cos \frac{m\pi}{l} z$ respectively and integrating from $z = 0$ to $z = l$. Making use of the orthogonality of sines and cosines,

$$\int_0^l \sin \frac{n\pi}{l} z \sin \frac{m\pi}{l} z = \begin{cases} \frac{l}{2} & \text{if } m = n \\ 0 & \text{if } m \neq n \end{cases} \tag{3.76}$$

$$\int_0^l \cos \frac{n\pi}{l} z \cos \frac{m\pi}{l} z = \begin{cases} \frac{l}{2} & \text{if } m = n \\ 0 & \text{if } m \neq n \end{cases} \tag{3.77}$$

$$\int_0^l \sin \frac{n\pi}{l} z \cos \frac{m\pi}{l} z = 0, \tag{3.78}$$

expressions for A_n and B_n can be written as

$$A_n = \frac{2}{l} \int_0^l (c_0 e^{-\frac{\mu E}{2D}z} \sin \frac{n\pi}{l} z - c' e^{\frac{\mu E}{2D}z} \sin \frac{n\pi}{l} z) \tag{3.79}$$

and

$$B_n = \frac{2}{l} \int_0^l (c_0 e^{-\frac{\mu E}{2D}z} \cos \frac{n\pi}{l} z - c' e^{\frac{\mu E}{2D}z} \cos \frac{n\pi}{l} z). \tag{3.80}$$

Solutions to the integrals are

$$A_n = \frac{2\left(\frac{n\pi}{l}\right)}{l\left(\left(\frac{\mu E}{2D}\right)^2 + \left(\frac{n\pi}{l}\right)^2\right)}\left[-c_0\left((-1)^n e^{-\frac{\mu E}{2D}l} - 1\right) + c'\left((-1)^n e^{\frac{\mu E}{2D}l} - 1\right)\right] \quad (3.81)$$

and

$$B_n = \frac{2\left(\frac{\mu E}{2D}\right)}{l\left(\left(\frac{\mu E}{2D}\right)^2 + \left(\frac{n\pi}{l}\right)^2\right)}\left[-c_0\left((-1)^n e^{-\frac{\mu E}{2D}l} - 1\right) - c'\left((-1)^n e^{\frac{\mu E}{2D}l} - 1\right)\right]. \quad (3.82)$$

Thus, the expression for the concentration profile for all time throughout the length of the cell, given a step input of the electric field, is now known. Simplifications are made to this model in the next section by assuming that the laser beam monitors only a small point on the cell, and the field is applied for a short time compared to the characteristic time constant.

3.3.5 Linearization of the Concentration Profile

The concentration profile relevant to the experiments in this thesis is simplified from the one given in equation 3.74 by assuming that the concentration is only slightly perturbed by the electric field about one small monitoring point on the cell.

By substituting the value for the position of the monitoring beam into equation 3.74, the concentration profile at that point on the cell can be written as

$$c(t) = (c_0 - c_p)e^{-t/\tau} + c_p \quad (3.83)$$

where τ is the first harmonic of τ_n given in equation 3.73, and c_p is the final concentration at that point given by equation 3.57.

The fluorescence is directly proportional to the concentration, as shown by

equation 3.47, so the fluorescence profile at any point can be written as

$$F(t) = (F_0 - F_\infty)e^{-t/\tau} + F_\infty \tag{3.84}$$

where F_0 is the uniform fluorescence at $t = 0$ and F_∞ is the fluorescence at steady state.

In these experiment, the electric field applied only long enough to see a small change (~10-20%) in fluorescence at the monitoring spot. The duration of the applied field is assumed to be much smaller than τ, so the exponential term in equation 3.84 can be linearized:

$$F(t) = (F_0 - F_\infty)(1 - \frac{t}{\tau}) + F_\infty. \tag{3.85}$$

The above equation states that the slope of the fluorescence (the time derivative) is equal to

$$\frac{\partial F}{\partial t} = \frac{F_0 - F_\infty}{\tau}. \tag{3.86}$$

Assuming the null hypothesis that the diffusion coefficient and the "effective" electrophoretic mobility are independent of direction, then the time constant τ should also be independent of direction. The ratio, therefore, of the slopes of the fluorescence with a positive field (defined in chapter IV), m_+, and with a negative field, m_-, should be equal to the absolute value of the ratio of the differences in final and initial fluorescence (or concentration) with the field in each polarity (noted by the + or − sign).

$$\frac{m_+}{m_-} = \left|\frac{F_0 - F_\infty^+}{F_0 - F_\infty^-}\right| = \left|\frac{1 - \frac{F_\infty^+}{F_0}}{1 - \frac{F_\infty^-}{F_0}}\right| = \left|\frac{1 - \frac{c_\infty^+}{c_0}}{1 - \frac{c_\infty^-}{c_0}}\right|. \tag{3.87}$$

The ratios c_∞^+/c_i and c_∞^-/c_i can be found at $t = 0$ and $t \gg \tau$ from the theoretical concentration profile (equation 3.74) by substituting in the diffusion coefficient and the "effective" electrophoretic mobility found in the FRAP experiments, the cell length, l, the beam position, z, and the field intensity, E. (Refer to section 3.4 for

limitations to this model.)

If it can be shown that the ratios in equation 3.87 are significantly different, then the time constants (equation 3.73) would have to be different; therefore, there would have to be some dependence on direction of either the diffusion coefficient or the "effective" electrophoretic mobility. The dependence on the direction of the diffusion coefficient alone, however, can be found by monitoring the fluorescence back to uniform concentration after the field has been removed.

3.3.6 Back Diffusion

Assumably, after the field has been turned off, the concentration of the proteins diffuse back to their original concentration, c_0. The diffusion equation governing this process is given by

$$\frac{\partial c(z,t)}{\partial t} = D\frac{\partial^2 c(z,t)}{\partial z^2}. \tag{3.88}$$

The approach to the solution is the same as taken for equation 3.48. With no electric field, there are no real roots of λ, given by the equation 3.65 The boundary conditions that the flux must be zero at $z = 0$ and $z = l$ are the same as in section 3.3.3, so the eigenvalues are again $\frac{n\pi}{l}$. Since the time constant is

$$\tau_n = \frac{1}{D}\left(\frac{l}{n\pi}\right)^2, \tag{3.89}$$

and the concentration as $t \to \infty$ is c_0, the form of the solution is

$$c(z,t) = \sum_{n=0}^{\infty}(A_n \sin\frac{n\pi}{l}z + B_n \cos\frac{n\pi}{l}z)e^{-t/\tau_n} + c_0. \tag{3.90}$$

The profile of the proteins immediately after the field is removed becomes the initial condition ($t = 0$) for the back diffusion problem. This initial condition is used to solve for the coefficients A_n and B_n. The values of A_n and B_n are not

needed for this thesis because the concentration profile can, again, be simplified by monitoring one small spot on the cell.

With the fluorescence directly proportional to the concentration, the fluorescence profile at any point can be written as

$$F(t) = \left(F_i - F'_\infty\right) e^{-t/\tau} + F'_\infty, \tag{3.91}$$

where F_i is the initial fluorescence and $F'_\infty = F_0$ is the final condition that the fluorescence is uniform.

$$\tau = \frac{l^2}{D\pi^2} \tag{3.92}$$

is the first harmonic of τ_n. Equation 3.92 relates the time constant to the diffusion coefficient and the length of the cell.

The approximate length of the cells was 55μm; however, the precise length of each cell was hard to determine for they had irregular shapes. The fact that this thesis is mainly concerned with determining if the mechanical properties are dependent on direction and not actual values, together with the fact that an error in the estimation of the cell length effects the diffusion coefficient as the square of the error was motivation to consider only the ratios of the diffusion coefficients. The ratio is given as

$$\frac{D_+}{D_-} = \frac{\tau_-}{\tau_+} \tag{3.93}$$

where D_+ and τ_+ correspond to the post-field recovery kinetics after an increase in the protein concentration, and D_- and τ_- correspond to the recovery kinetics after a decrease in concentration. The average of the ratios is compared to one to determine if the diffusion coefficients are different in the two directions along the major axis of the cell.

3.4 Limitations of the Theoretical Models

The models in sections 3.2 and 3.3 were formulated with assumptions, so their limitations must be considered. The model for the fluorescence recovery after photobleaching assumes an infinite pool of fluorophores in all directions, so in an electric field, the proteins will flow through the bleached spot. If, however, the proteins accumulate or decrease at the measuring spot, in the time frame of the FRAP experiment, the data will not be accurately modeled. An accumulation of the proteins at the measuring point will create an abnormally high fractional recovery. Conversely, if the fluorescence decreases, an abnormally low fractional recovery would be noticed.

The FRAP experiments without an electric field will give an average of the percentage of mobile fluorophores. It is assumed that this fractional recovery does not change in the presence of an electric field unless the protein concentration increases or decreases. The data collected in chapter V was examined and runs in which the last data point was more than a standard deviation from the expected last point (found from the fractional recovery) were discarded, for they could not be accurately fit.

Limitations of the theory of the fluorescence redistribution in the prescence of an electric field also exist. As explained in section 3.3.5, the ratio of the slopes must be compared to the ratio of the differences of the concentration at $t \rightarrow \infty$ and $t = 0$ in a positive and negative field, or

$$\frac{m_+}{m_-} = \left| \frac{1 - \frac{c_\infty^+}{c_0}}{1 - \frac{c_\infty^-}{c_0}} \right|. \tag{3.94}$$

The value of c_∞ is defined by c_p in equation 3.57.

The model for c_∞ was incorrect, however, for it did not account for the steric interactions among the proteins. The concentration profile solved for in section 3.3 is only valid if the particles are assumed infinitely small. For example, a fibroblast is

assumed to be $55\mu m$ long with the monitoring beam placed at $45\mu m$ along its major axis. The field strength is either 10 V/cm or -10 V/cm. Substituting these values and the values of D ($D \sim 1.4 \times 10^{-9}\text{cm}^2/\text{sec}$) and $\mu = (\mu \sim 7.6 \times 10^{-7}\text{cm}^2/\text{V}\cdot\text{sec})$, calculated from the FRAP experiments, into equation 3.57, the two values for c_∞ are found. For a 10 V/cm field, $c_\infty = 1.3 \times 10^{-1} c_0$, and for a -10 V/cm, $c_\infty = 7.3 \times 10^{-10} c_0$. A drop in fluorescence in a positive field, however, was not detected.

Because the experimental process was modeled incorrectly, no conclusions can be made about the possible differences in the ratios. The back diffusion model, on the other hand, does not depend on c_∞, so the values for the diffusion time constants and their ratios could be found and compared.

Chapter IV

Experimental Methods and Apparatus

4.1 Cell Culture

In conducting the experiments for this thesis, human dermal fibroblast cells were used. These cells were chosen because they exhibit a biosynthetic response to ac electric fields and because they contain sufficient class I MHC protein binding sites for the W6/32 fluorescinated antibody to achieve an adequate signal when excited by the laser of the FRAP system. These cells readily attach to glass and plastic culture vessels. When plated, they are about $50\mu m$ long and have unequal principal axes. The size allows a small Gaussian spot, approximately $4\mu m$ in radius, to be bleached on the cell without significantly depleting the pool of mobile fluorophores; the shape allows for defined parallel and perpendicular directions with respect to the applied field. Cell passage includes trypsinization which can cause cell mutation and irregular cell growth. Therefore, to model *in vivo* cells most accurately, only low passage ($<$ P5) cells were used.

The human dermal fibroblast (HDF) primary culture was obtained through collaganase digestion of dissected foreskin samples. First, all fat and blood vessels were removed from the foreskin tissue. It was then washed twice in sterile phosphated buffer solution (PBS) without calcium and magnesium. To remove the endothelial cells, the tissue was placed in 50ml centrifuge tube with 20ml of hydrated 10X trypsin solution and 0.025% EDTA and incubated for fifteen minutes. The tissue was then cut up into small pieces and placed in sterile DMEM with 0.4% collaganase, 2X penicillin (10,000 units/ml), and 2X streptomycin (10,000 mcg/ml). It was then incubated and agitated for several hours. When most of the tissue was digested, as much liquid as possible was removed and spun down. The supernatant was saved and put back into the chunks for further digestion. Following that, the cells were resuspended in DMEM and centrifugally washed twice more to remove all

collaganase, and seeded in flasks at a density of $\approx 10^6$ cells/25cm^2. Several hours later, the chunks that were further digesting were treated similarly to isolate and wash the cells.

After the cells had grown to 80% confluency they were passed (P1) and cultured in monolayer again to 80% confluency. The cells were then passed and frozen using preservation media containing 50% calf serum, 45% DMEM, and 5%DMSO. In each vial, one ml of preservation media containing one million cells was frozen. One vial was thawed and plated in a T75 culture dish and allowed to grow to 80% confluency. Approximately 72 hours prior to each experiment, the cells were passed into 15mm petri dishes containing a sterile 24 x 35mm microscope coverslip. Six ml of DMEM with 10% calf serum and 200 units/ml of recombinant human γ interferon (IFN-γ) [HG-IFN, Genzyme, Cambridge, MA] was added to each dish along with approximately 250,000 cells. The IFN-γ increases the expression of class I MHC antigens [Stolpen et al., 1987]. After staining, the fluorescence of the antibody directed against the receptor was enhanced. The IFN-γ was stored frozen at -100°C in aliquots containing 10μl or 10,000 units. On the day of the experiment, the coverslips were placed in a sterile specimen cup (Fisher Scientific) for transport with 5ml of DMEM (buffered for air with 10mM HEPES) and 10% calf serum, and 200 units/ml IFN-γ.

4.2 Cell Preparation

In preparing the cell for the experiments, cell surface class I MHC proteins were labeled with an IgG_{2a} antibody (W6/32) directed against a monomorphic determinant of HLA-A,B,C [Barnstable et al., 1978]. The antibody was conjugated with fluorescein isothiocyanate [Stolpen et al., submitted]. Preparation began by gently washing the cells on the coverslips two to three times in PBS with calcium and magnesium at room temperature. For the experiments which removed the sialic acid residues from the membrane, the cells were first incubated at 37°C in

0.1 unit/ml neuraminadase [NEAU, Worthington Biochemical, Freehold, NJ] at pH 6.6 in PBS with calcium and magnesium for one hour. The coverslips were then placed on ice in a staining chamber containing 1.4ml of DMEM and 100μl of the fluorescinated antibody. A 26 X 36.5mm well in a piece of polysulfone served as a staining chamber. These dimensions were chosen because the volume of the antibody was originally frozen in an aliquot to be added to a 35mm petri dish, the same area as the staining chamber.

After one hour, the coverslip was washed twice in PBS without calcium and magnesium to remove most of the bound calcium on the cell membrane and the unbound antibody. The coverslip was then mounted cell side down on the exposure chamber, which was filled with PBS without calcium and magnesium.

4.3 Experimental Apparatus

The exposure chamber that was used to apply an electric field to the cells on a coverslip was machined from a block of polysulfone, an autoclavable electrical insulator. Design considerations for the chamber consisted of preventing Joule heating, electrode residues, and hydrolysis. (Figures 4.1 and 4.2 show a photograph of the chamber mounted on the microscope stage and a drawing of the chamber that illustrates its features.

To prevent Joule heating by extracellular currents, the coverslip was mounted, with a small amount of silicon grease to prevent leakage, only 250μm above an optically polished sapphire window [Adolf Meller, Providence, RI] that was over a second chamber that contained circulating cooled nitrogen. Sandwiched between a thin coverslip and the sapphire window was a foil type-T copper-constantan thermocouple [20102-1, Rdf Corp., Hudson, NH]. Sapphire was chosen because of its high thermal conductivity, as well as, for its optical transparence since it forms part of the microscope illumination pathway. The foil type thermocouple was used because it is only 5μm thick. For type T thermocouples temperatures can range

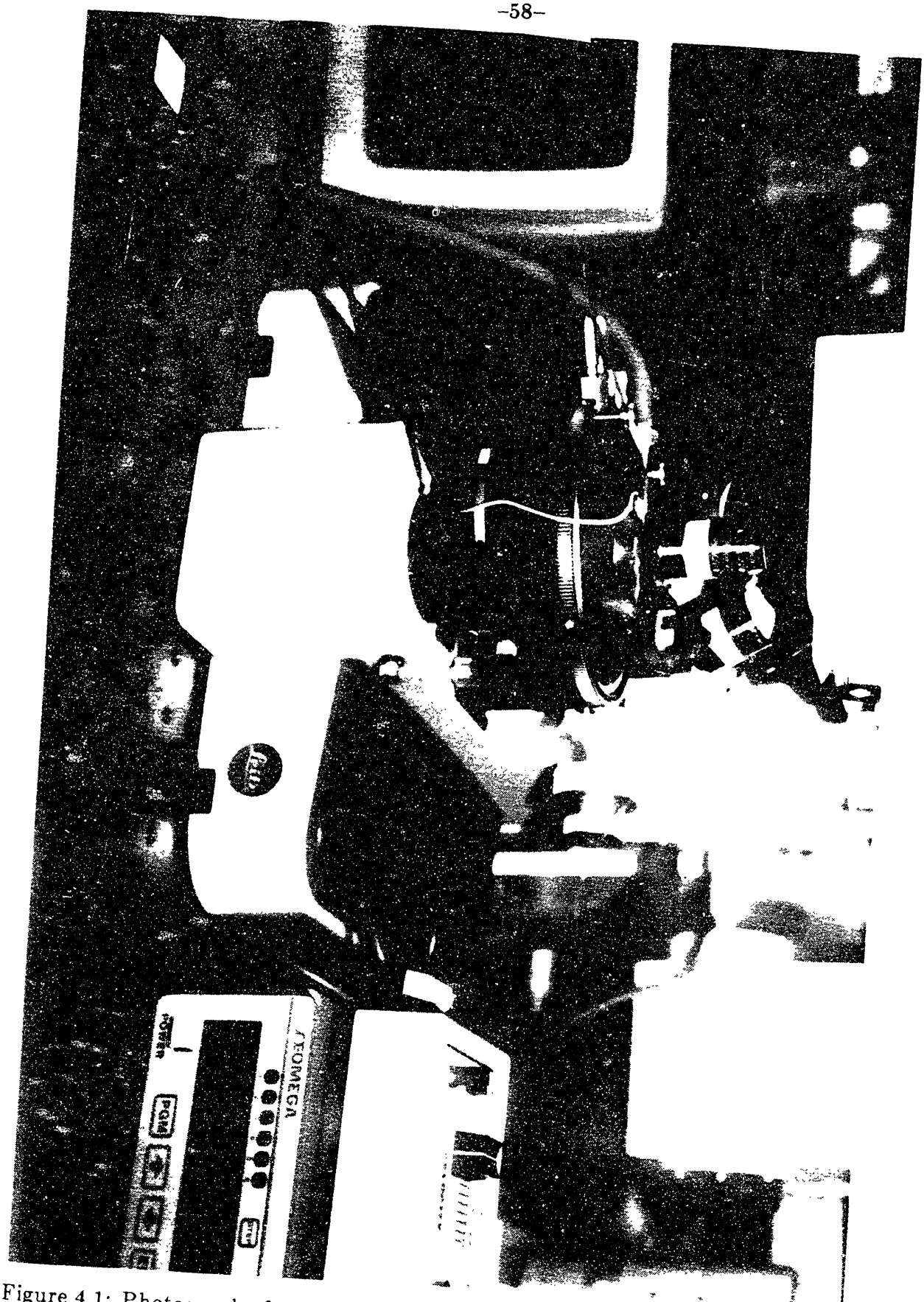

Figure 4.1: Photograph of exposure chamber on the stage of the microscope. Thermometer is also shown in the figure.

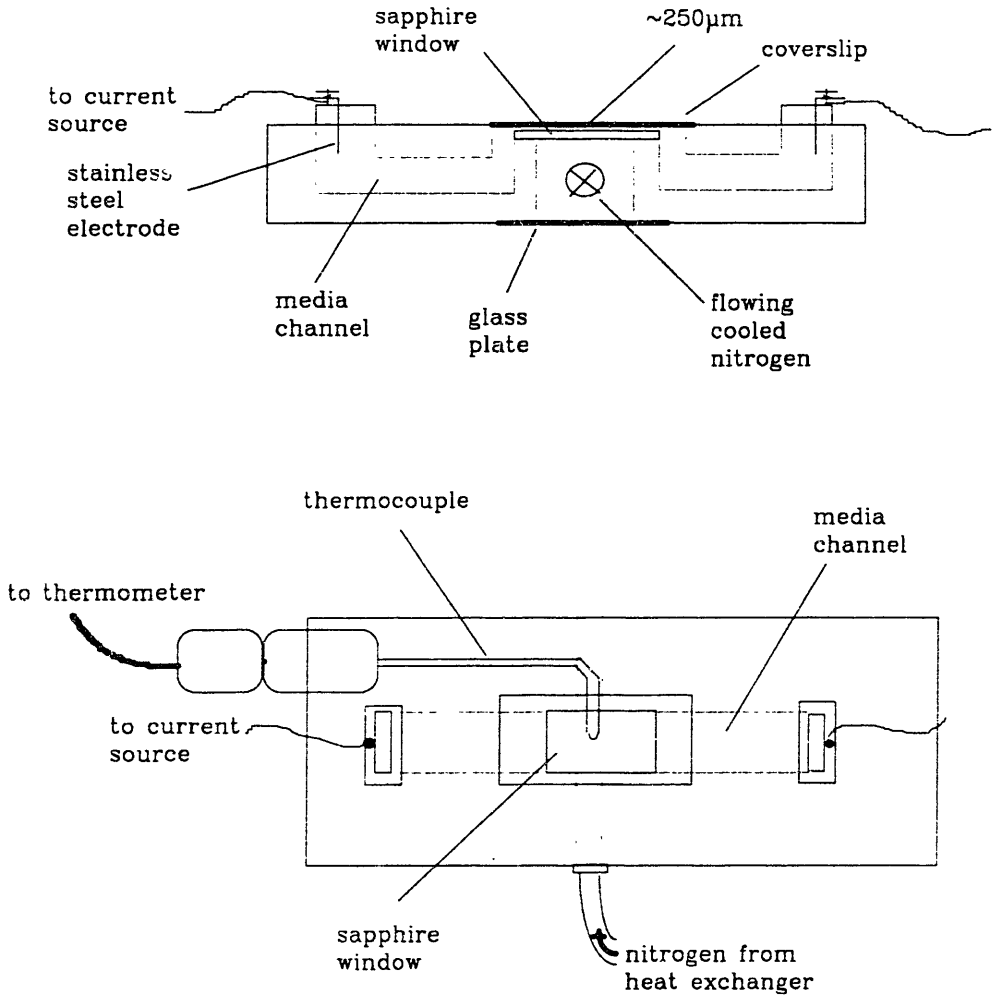

Figure 4.2: Drawing of exposure chamber illustrating its features.

from −150° to 400°C. The assembly of the sandwiched thermocouple began by using RTV silicon glue [G.E. Corp., Waterford, NY] to affix the coverslip on the chamber's posts. Then, the thermocouple was placed on the coverslip and a small drop of highly viscous, virtually transparent epoxy [Epo-tex, Epoxy Technology, Inc., Billerica, MA] was applied in the middle of the coverslip. Next, the sapphire window was placed on top taking care not to trap air bubbles in the glue. To insure a thin, even coat of epoxy, a weight was placed on top of the window. Finally, the leads of the thermocouple were attached to a connector [SMP-T-MF, Omega Engineering, Inc., Stamford, CT] that led to a thermometer [DP86-T, Omega Engineering, Inc.].

To prevent the formation of undesirable electro-chemical by-products at the electrodes, the field exposure area of the chamber was separated by media bridges. The cross-sectional area of the media bridges is more than two orders of magnitude greater than the area of the field exposure surface. The resistance, R, of a conductive substance with conductivity, σ, length, L, and cross-sectional area, A, is equal to

$$R = \frac{L}{\sigma A}. \tag{4.1}$$

Therefore, the resistance of and the power drop across the exposure area is much greater than that of the media bridges.

With most of the power drop across the exposure area, and not the electrodes, the temperature rise of the media should be limited to this area. Assuming no heat conduction between the air and the media, The media temperature rise per unit time is given by

$$\frac{\Delta T}{t} = \frac{E^2 \sigma}{\rho \theta} \tag{4.2}$$

where σ is the conductivity of the media (8×10^{-3} mhos/m), ρ is the density of the media (1 g/cm^3), and θ is the specific heat of the media (4.13 Joules/gm °C). For an electric field strength, E, of 10 V/cm, a temperature rise of 0.19°C/sec is expected. Experiments showed an initial rise of approximately 0.1°C/sec and a

maximum change of 4-5°C above room temperature. The differences are probably due to conduction between the thin coverslip and the air. A flow of nitrogen under the sapphire plate cooled through a heat exchanger in ice water countered this temperature rise. The heat exchanger was made from copper tubing molded into a coil. A hand-controlled valve regulated the flow of nitrogen to keep the media at room temperature.

By applying a known voltage across the electrodes and measuring the current, the exact resistance of the exposure area was calculated. The exact height of the exposure area was found to be ~250μm by using the length (1.83cm), the width (1.93cm), the value for the resistance (3.9 kΩ), and equation 4.1. The needed current source [BOP 36-5, Kepco] output for this cross sectional area (48.3 $\times 10^{-3}$ cm^2) can be calculated using

$$I = \sigma A E. \tag{4.3}$$

A field strength of 10 V/cm across this area requires a current of 4.75mA.

Human dermal fibroblasts plated on a coverslip may get as large as 100μm long. In order keep the transmembrane potential ($V = \int E \cdot dl$) of the cell under 100mV, the magnitude of the field strength was not increased over 10V/cm.

4.4 Fluorescence Recovery After Photobleaching

4.4.1 Equipment

The objective of the fluorescence recovery after photobleaching (FRAP) setup was to provide two magnitudes of laser light pulses focused on the cells. The more intense pulse bleached the fluorophores on the cell surface, and the attenuated pulse excited the fluorophores so that the kinetics of the recovery could be measured.

Experiments were run at Dr. David Golan's laboratory at Harvard Medical School. The standard FRAP setup is described in detail in his publication [Golan

et al., 1986] and shown in figures 4.3 and 4.4:

> A 4 Watt argon ion laser (164-08; Spectra-Physics Inc, Mountain View, CA), tuned to 488nm was used as the excitation source for a fluorescence microscope (Leitz Orthoplan) equipped for incident-light (Ploem) illumination. The beam was focused to a waist at the secondary image plane of the microscope by a weak planoconvex lens and to another waist at the specimen by a phase fluorescence objective (Leitz). An interferometer (Ealing Corp., S. Natick, MA) placed in excitation path was used to split the beam into measuring and bleaching paths [Golan et al., 1984]. The interferometer mirrors were fitted with remote-control linear actuators (Newport Corp., Fountain Valley, CA) to allow precise alignment of bleaching and measuring beams at the sample plane. ...The optical apparatus was mounted on a 4' × 6' research quality vibration isolation table (Newport Corp.).
>
> Emitted light was collected by the objective, filtered by the dichroic mirror (Leitz TK510) and suppression filter (Leitz K510), and directed through a series of lenses, beamsplitters, and mirrors (Leitz MPV-3) to an extended S-20 photomultiplier tube (9558QA; Thorn EMI Gencom Inc., Fairfield, NJ) in a thermoelectrically cooled housing (TE-104RF; Products for Research, Inc., Danvers, MA) driven by a stabilized high-voltage power supply (HVS-1; Princeton Applied Research [PAR], Princeton, NJ). An adjustable field diaphragm placed in the image plane was used to discriminate out-of-plane fluorescence. The photocurrent was fed into a series of single-photon pulses. The pulses were counted within specified time intervals by a photon counter (PAR 1109), and the number of counts per interval stored in a computer (PDP 11/23; Digital Equipment Corp., Marlboro, MA). ...The computer was used to direct the sequence of opening and closing shutters for bleaching and

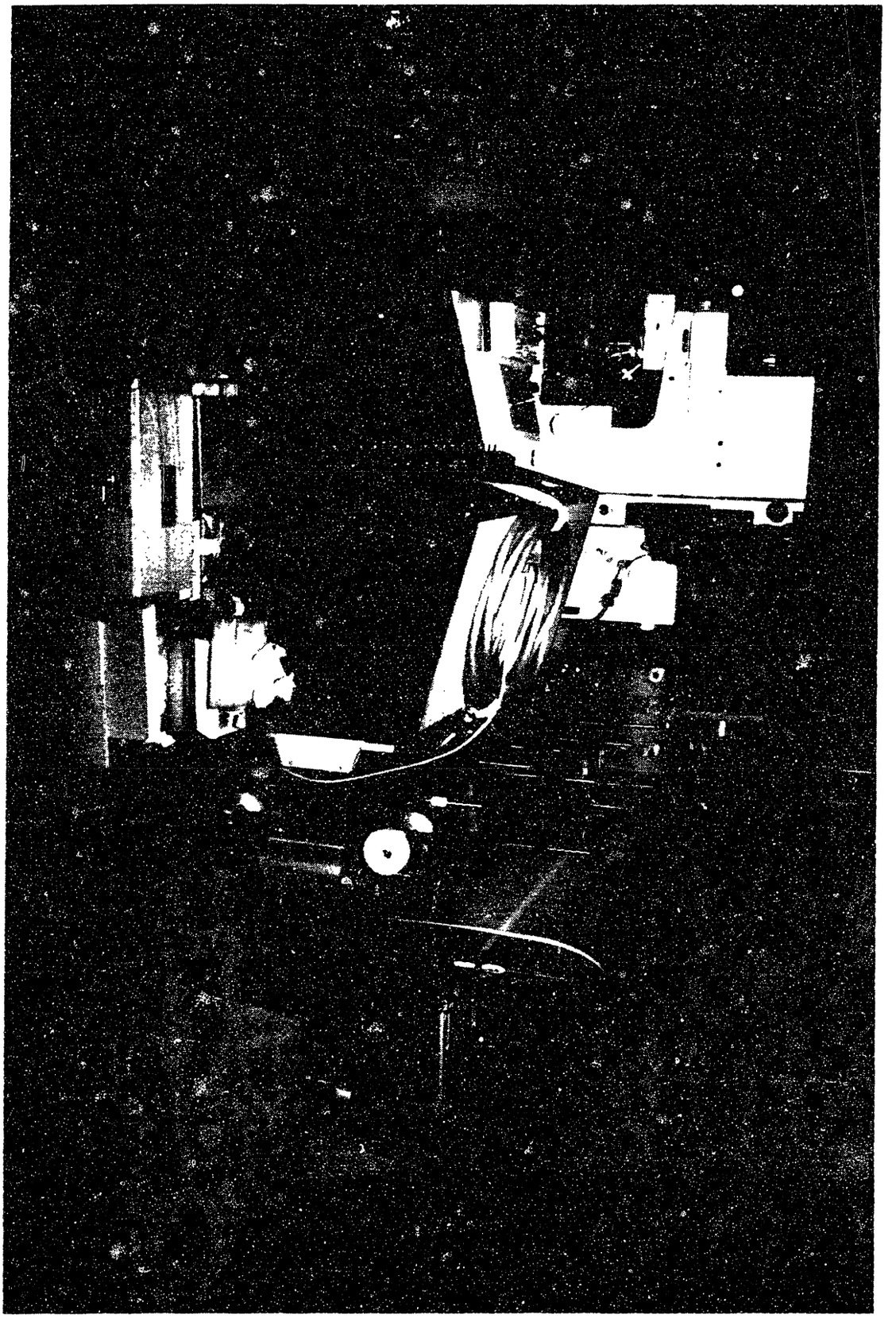

Figure 4.3: Photograph of FRAP setup.

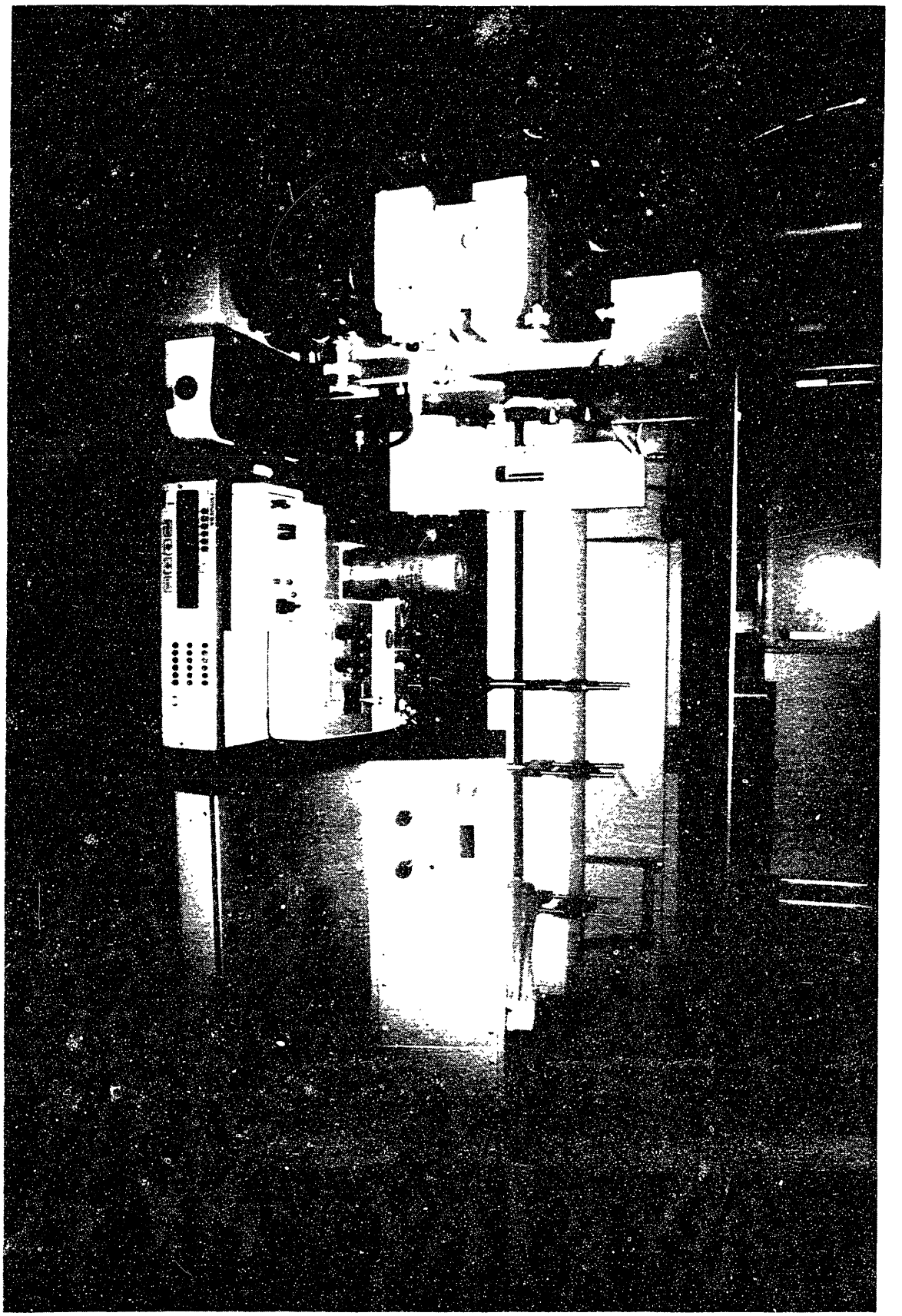

Figure 4.4: Photograph of FRAP setup.

measuring pulses, to gate the photon counter in step with the shutters, and to collect data.

A concern of the FRAP experiments was the ability to detect flow in the system. To aid detection, the time constant for flow, given in equation 3.42, was increased optically by maximizing the beam radius, w. This system used the 25X objective and a 500mm lens to focus to a waist at the secondary image plane. With these optics, a 4μm Gaussian beam radius was achieved.

In the experiments monitoring protein accumulation, the beam size was reduced so the assumption that the concentration does not change over the radius of the beam could be made. In this case the 63X objective and 350mm lens were used to achieve a beam radius of $\sim$1.3μm.

A two-dimensional scan of the emission diaphragm was used to gather intensities, a best fit routine was used to determine the Gaussian beam radius at the sample plane [Stolpen et al., submitted]. A plot of the intensity of the beam in two-dimensional space, along with the best fit Gaussian curve is shown in figure 4.5.

4.4.2 Measurement Protocol

The highest fluorescence and most consistent counts were obtained when the measuring beam was focused to its smallest diameter. Focusing needed to be done quickly ($<$ 1 sec) to insure no bleaching of the fluorophores. Measurements were first made of the background. These counts were later subtracted from the experimental data. Generally, FRAP was done on an area close to, but not on, the nucleus of the cell. For experiments with an applied field, the cells were oriented parallel to the field. For the experiments which monitored the fluorescence redistribution in an applied electric field, the measuring beam was focused at a point at the edge of the cell on the leading edge side. The measuring was done near the edge to maximize the difference in fluorescence. The leading edge side was arbitrarily

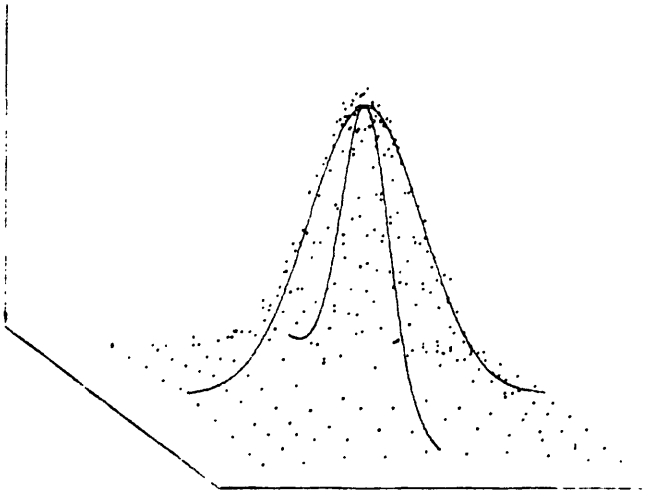

Figure 4.5: This figure shows the data collected during a two dimensional scan with the microscope's emission diaphragm and the best fit Gaussian curve.

chosen, but was always used for consistency sake. The leading edge side of the cell is defined as the side of the cell which leads its movement on a substrate [Albrecht-Buehler, 1968]. The movement of the membrane also defines the leading edge. The membrane movement has been shown to circulate from the leading edge to the trailing edge where it pitches off and forms a vesicle. This vesicle travels back to the leading edge through the intracellular matrix and reforms with the membrane through exocytosis. Figure 4.7 shows the orientation of the cell in the electric field, the direction of membrane flow, and the measuring points for the different experiments. The leading and trailing edges of the cell under the 25X objective were indistinguishable due to problems with the phase of the microscope, so a measuring point was chosen for the FRAP experiments only in relation to the nucleus.

For the FRAP experiments, several initial data points were collected to establish a pre-bleach fluorescence, F(-). The bleaching shutter was then opened briefly, producing a gradient in the fluorophore concentration. The photobleaching power at the sample was $\sim 100\mu W$, and the measuring beam intensity was $\sim 0.2\mu W$. Typically, the measuring time was 150ms. The bleaching time was set

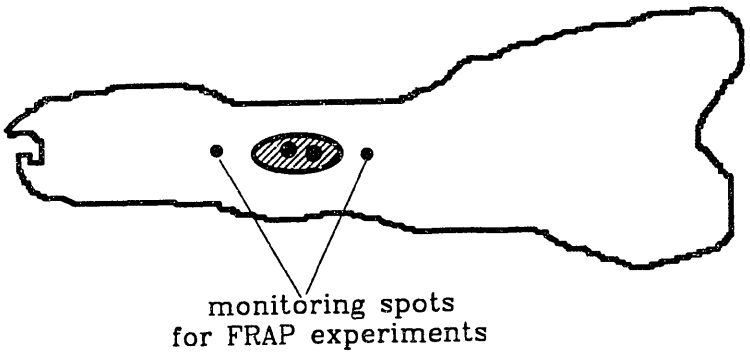

Figure 4.6: Illustration of a cell and typical monitoring points for a FRAP experiment are indicated.

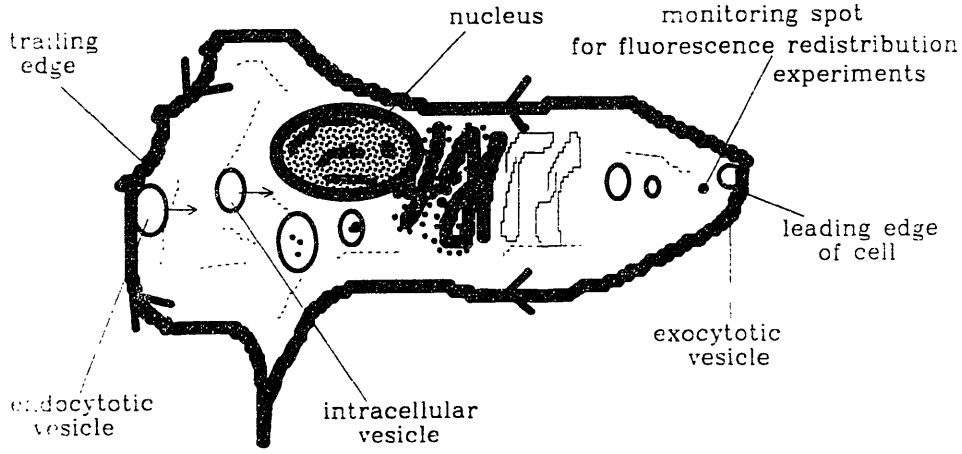

Figure 4.7: Illustration of a cell and a monitoring point for a typical experiment which monitors the fluorescence redistribution is shown. Cell orientation and direction of membrane flow are also given.

	Number of Measurements	Seconds Between Measurements
Pre-bleach:	3	6
Post-bleach:	2	3
	2	6
	2	12
	2	24
	2	50
	3	75
Total:	13	412

Table 4.1: A Measurement schedule for a typical FRAP experiment is given.

long enough to bleach 50-70% of the initial fluorescence intensity, but it was short compared to the observed characteristic times of transport. Bleaching time was generally 150ms. The measurement schedule was set up so more points were gathered during the initial rise than during the asymptotic approach. Table 4.1 gives a typical FRAP measurement schedule.

The experiments which monitored the fluorescence change required no bleaching. Several points were collected prior to the onset of the field. The field was then applied, and the fluorescence monitored. Upon significant change in the intensity (10-20%), the field was turned off and the recovery of the fluorophores was monitored. When the fluorescence reached the initial concentration, the field was applied again, this time with the opposite polarity. Again, the field was removed after a 10-20% change (this time with the opposite slope) and the recovery monitored. Measuring times were set every twelve seconds and the experiment was stopped after the second post-field recovery.

Data from both experiments was collected and stored in a Digital PDP 11/23. It was later transferred to an IBM-AT where the data analysis took place.

4.4.3 Data Analysis

FRAP data was fit to the theory using Marquardt's non-linear least squares algorithm described in detail in Bevington's book [1969]. Data describing recovery governed only by diffusion was fit to equation 3.45, while data collected with an applied electric field was fit to equation 3.43.

Using this fitting routine, initial guesses for each of the parameters must be supplied. By averaging the prebleach points, an initial guess for F(-) was found. An initial guess for F(∞) was found by multiplying the average of the last three data points by 1.1. K was initially set to 2.0, and τ_D and τ_F to the time when approximately one-half of the fluorescence had recovered. The curve fit was evaluated to within 0.01% error. The infinite series was carried out until the series varied by less than one thousandths of a percent. For $k = 2$, the series truncates in less than ten terms.

With the best fit value of K, F(0) can be calculated using equation 3.11. The fractional recovery was then calculated using

$$\text{Fractional Recovery} = \frac{F(\infty) - F(0)}{F(-) - F(0)}. \tag{4.4}$$

The diffusion coefficient was found using the best fit parameter for τ_D and equation 3.40, while the "effective" electrophoretic mobility was found using the best fit parameter for τ_F and equation 3.42.

For the experiments monitoring the fluorescence accumulation at one point, data analysis consisted of fitting two sets of data. The data points collected with the field applied were fit to a straight line, as justified in section 3.3.5, so a measure of the "effective" electrophoretic mobility could be found. The points collected after termination of the field were fit to an exponential, so a time constant could be found. With this, a diffusion coefficient was found using equation 3.92.

Finally, the output of the data analysis routines set up files to plot the data

points and the best fit curves. These files could then be sent to the printer for hardcopy output.

Chapter V

Results

This chapter presents the data obtained from the FRAP experiments and the experiments that monitored the fluorescence change in the presence of an electric field. The data which satisfied the limitations of the theoretical curves were fit, and the values for the diffusion coefficient and "effective" electrophoretic mobility were found. The processes that did not satisfy the limitations were reexamined and an indication of which theoretical assumptions needed modification is given.

5.1 Control Studies

An assumption in the model of the FRAP experiments was that the laser beam does not bleach the fluorophores during fluorescence measurement. Figure 5.1 shows the fluorescence measured every twelve seconds. The measuring beam was placed at a point approximately where a FRAP experiment would be run, as shown in figure 4.7. The results in figure 5.1 substantiate the assumptions that the measuring beam does not bleach the fluorophores. In the time frame of a FRAP experiment, the fluorescence did not change due to membrane flow or possible receptor aggregation. Similar results were found at different points on the cell.

The first FRAP experiments performed were used to determine the diffusion coefficient of the MHC antigens in the absence of an applied field. Figure 5.2 displays typical data collected and the corresponding best fit curve. Results of these FRAP experiments is summarized in table 5.1. The table gives the diffusion coefficients, the fractional recoveries, and the least-squares error, χ^2, for each of the runs as well as the average and standard deviations of all the runs. The average diffusion coefficient ($D \sim 1.15 \pm .18 \times 10^{-9}$ cm^2/sec) compares favorably with the one found by Stolpen et al. [1987] ($D \sim 1.2 \pm 0.3 \times 10^{-9}$ cm^2/sec). The average fractional recovery found in both is greater than 87%.

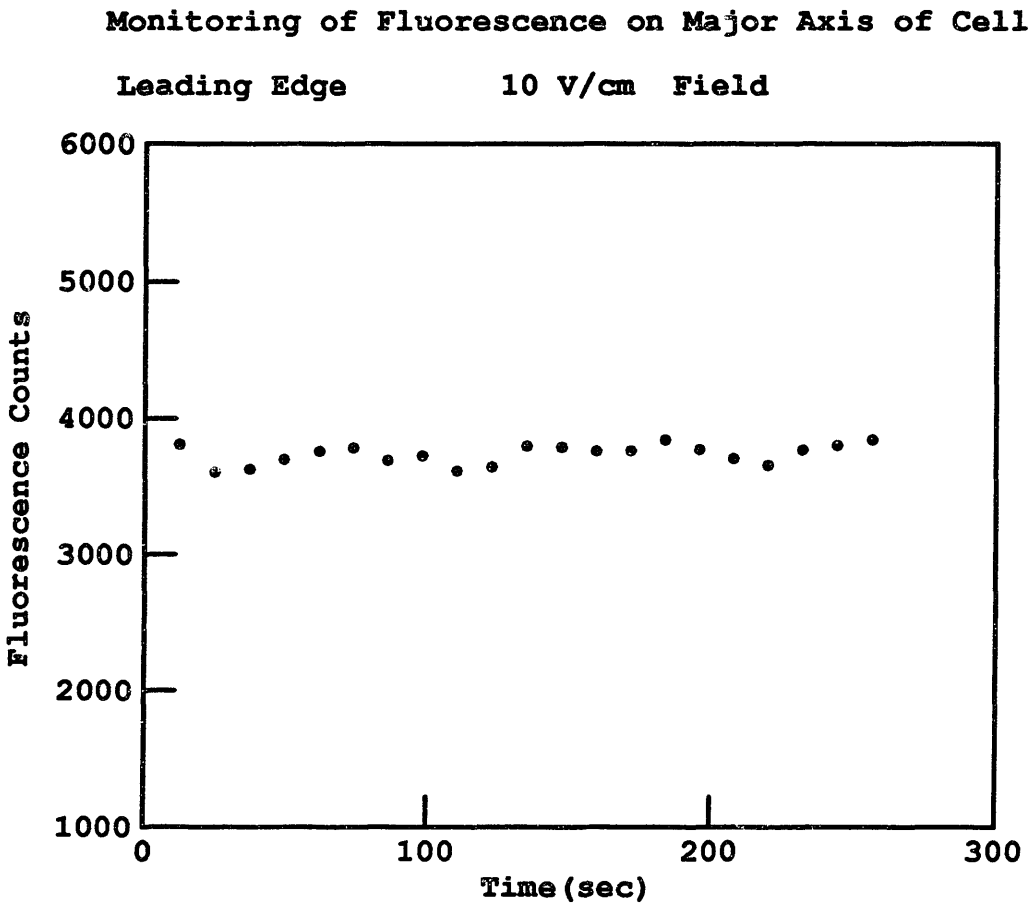

Figure 5.1: Fluorescence measured without a bleaching pulse or an applied electric field is plotted as a function of time. Plot shows that the measuring beam does not bleach the fluorophores nor does the fluorescence change, in the time frame of a FRAP experiment, due to membrane flow or possible receptor aggregation. Measuring points are taken every 12 seconds.

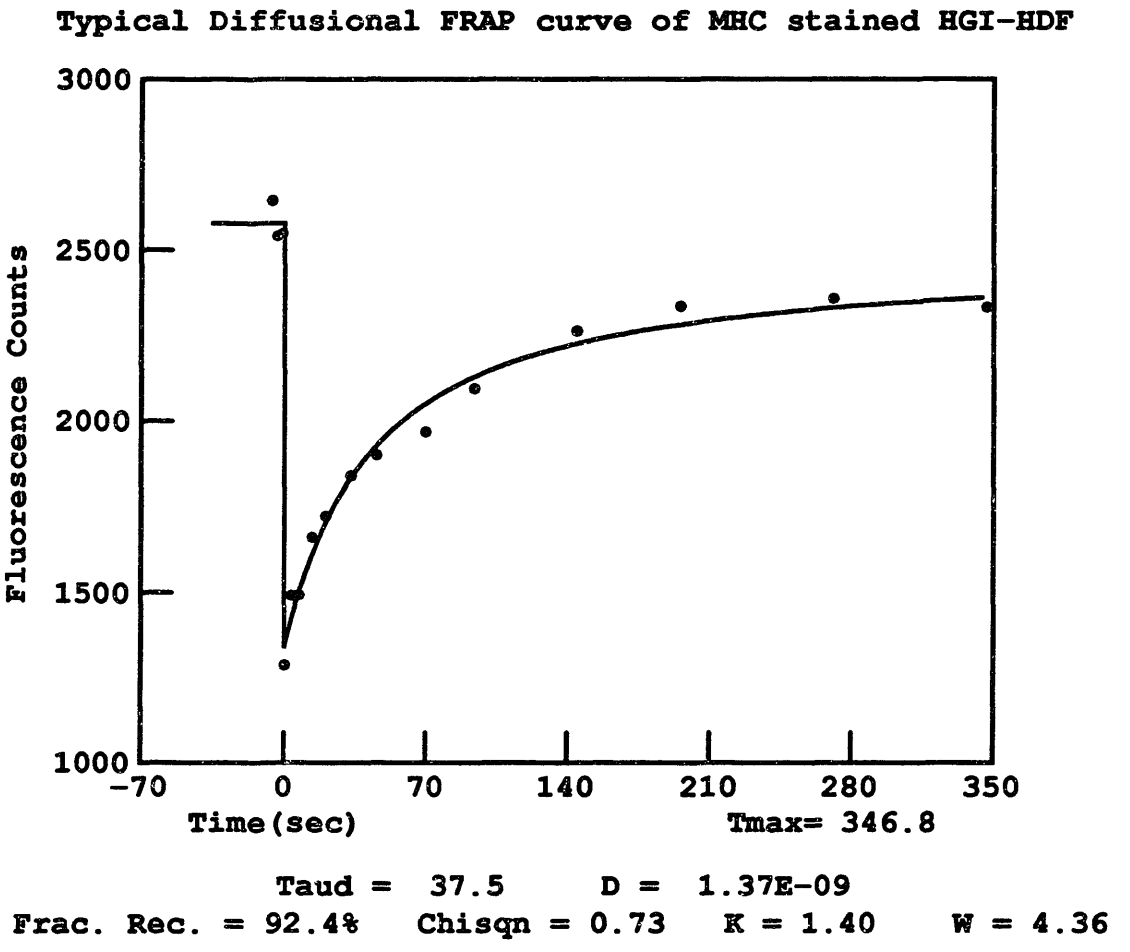

Figure 5.2: Typical data and best fit recovery curve of a FRAP experiment without an electric field are plotted. The values of the best fit parameters are given above.

	Diffusion coefficient D $\times 10^{-9}$ (cm^2/sec)	Fractional recovery (%)	Least-squares error χ^2
1	1.50	60	1.53
2	1.13	88	1.90
3	1.16	72	1.44
4	1.01	96	0.66
5	1.35	96	0.67
6	1.10	65	1.69
7	1.08	98	1.86
8	1.03	100	0.66
9	1.37	62	0.85
10	1.12	73	0.76
11	0.93	113	0.97
12	0.88	122	0.85
13	1.26	103	2.50
Average:	1.15	88	1.41
Stand. Dev:	0.18	20	0.69
n	13	13	13

Table 5.1: The best fit parameters of FRAP experiments run without an electric field are listed.

5.2 FRAP Experiments with an Applied Electric Field

The next experiments were performed in the presense of an applied electric field. The data from the FRAP experiments were now fit to the four parameter model given by equation 3.43; the results are shown in table 5.2. As expected, the diffusion coefficient (1.4×10^{-9}cm^2/sec) does not differ significantly from the one found with no applied field, and the "effective" electrophoretic mobility (7.6×10^{-7}cm^2/V·sec) is comparable to the ones found by Poo et al. [1978, 1979], given in section 1.5.

Data from only five experiments are given here, because many of the experiments ($\sim$ 60%) were found to contain a rise or fall in the fluorescence towards the end of the experiment. As discussed in section 3.4, the rise (or fall) is most likely due to the proteins concentrating (or lessening) at the point on the cell that is being monitored. Section 3.4 defined an experiment as having a rise or fall when the last point is greater than a standard deviation from the average of the fractional recoveries found in the no field runs. Table 5.1 shows that the fractional recovery is 88 $\pm$ 20%. In other instances ($\sim$ 25% of the runs), the data points appeared to recover with a reasonable fractional recovery, yet the fitting program could not find a best fit value for the flow time constant, τ_F; therefore, because τ_F is inversely proportional to μ, as given in equation 3.42, values for the "effective" electrophoretic mobility were sometimes not found. One reason that the routine could not find a best fit value for the τ_F is that the curve fitting routine is sensitive to error in the data. This is discussed in appendix B.

Three typical runs are given in figures 5.3, 5.4, and 5.5. Figure 5.3 shows the data points and the best fit curve of a run that the data fit the criteria of not having a rise or fall, so the curve fitting routine could find the best fit parameters. The best fit diffusion coefficient was $0.66 \pm 0.7 \times 10^{-9}$cm^2/sec, and the best fit "effective" electrophoretic mobility was $3.6 \pm 2.9 \times 10^{-7}$cm^2/V · sec. Figure 5.4 shows typical data points of a run where the final few points increased. Using equation 4.4, the

last point would indicate a fractional recovery of 114%. Figure 5.5 shows typical data points of a run in which the data points dropped. The last point, in this case, would indicate a fractional recovery of 43%. In runs similar to the ones shown in figures 5.4 and 5.5, the data was not included in the totals given in table 5.2, because the theoretical model did not account for these changes.

5.3 Neuraminidase Studies

As discussed in section 2.3, MHC proteins should move within the membrane due to the forces created on them by electroosmotic flow. In an attempt to show this, the membrane charge was altered by pretreating the cells in neuraminidase which cleaves the sialic acid residues, removing some of the fixed negative charge on the membrane. This should dissipate the electroosmotic flow of the counter ions, reducing the Stoke's drag on the protein. By reducing the flow, it was hoped that the accumulation (or decrease) in fluorescence toward the end of the runs would lessen.

Table 5.3 reveals the results of the experiments. The diffusion coefficient was, again, not significantly changed. The "effective" electrophoretic mobility, however, dropped significantly ($p < 0.02$) compared to the runs on the cells not treated with neuraminidase (see appendix A for statistical significance explanations). Showing that the "effective" electrophoretic mobility decreased by removing some of the cell surface charge demonstrates that the movement of MHC receptors is due to viscous forces set up by electroosmotic flow.

5.4 Perturbation Experiments

The theoretical model did not account for the frequent rise or drop in fluorescence in the FRAP experiments, so a directional dependence of the "effective" electrophoretic mobility could not be found. A new approach was, therefore, taken that took advantage of the fact that the glycoproteins can be concentrated by the

	Diffusion coefficient D $\times 10^{-9}$ (cm^2/sec)	"Effec." electro. mobil. $\mu \times 10^{-7}$ (cm^2/V·sec)	% recovery	χ^2 error
1	2.3	11.9	70	0.70
2	1.3	7.7	79	2.2
3	1.8	7.5	93	0.88
4	0.75	7.2	83	1.2
5	0.66	3.6	107	0.93
$\bar{x}$:	1.4	7.5	86	1.2
σ:	0.7	2.9	14	0.6
n	5	5	5	5

Table 5.2: The best fit parameters of FRAP experiments run with an electric field are listed.

	Diffusion coefficient D $\times 10^{-9}$ (cm^2/sec)	"Effec." electro. mobil. $\mu \times 10^{-7}$ (cm^2/V·sec)	% recovery	χ^2 error
1	0.72	3.1	91	0.15
2	0.93	2.9	98	0.80
3	0.85	3.4	91	1.0
4	2.5	2.8	83	0.81
$\bar{x}$:	1.3	3.1	91	.69
σ:	0.84	0.26	6	0.37
n	4	4	4	4

Table 5.3: The best fit values of the parameters from FRAP experiments run with an electric field with the cells pretreated in neuraminidase are listed. The cells were incubated at 37°C in 0.1 unit/ml neuraminidase at pH 6.6 for one hour before staining with the antibody.

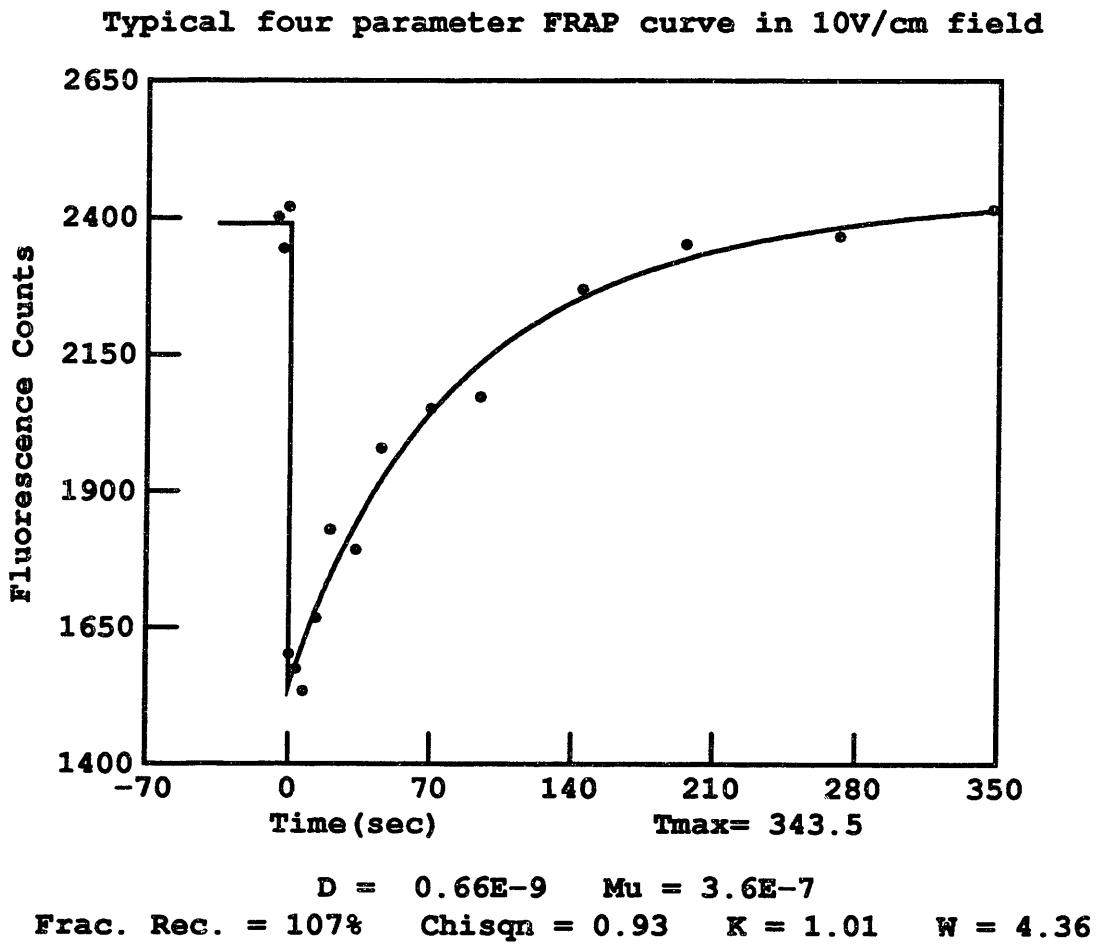

Figure 5.3: FRAP data acquired in a field and best fit four parameter recovery curve. Values for the diffusion coefficient and "effective" electrophoretic mobility are given above.

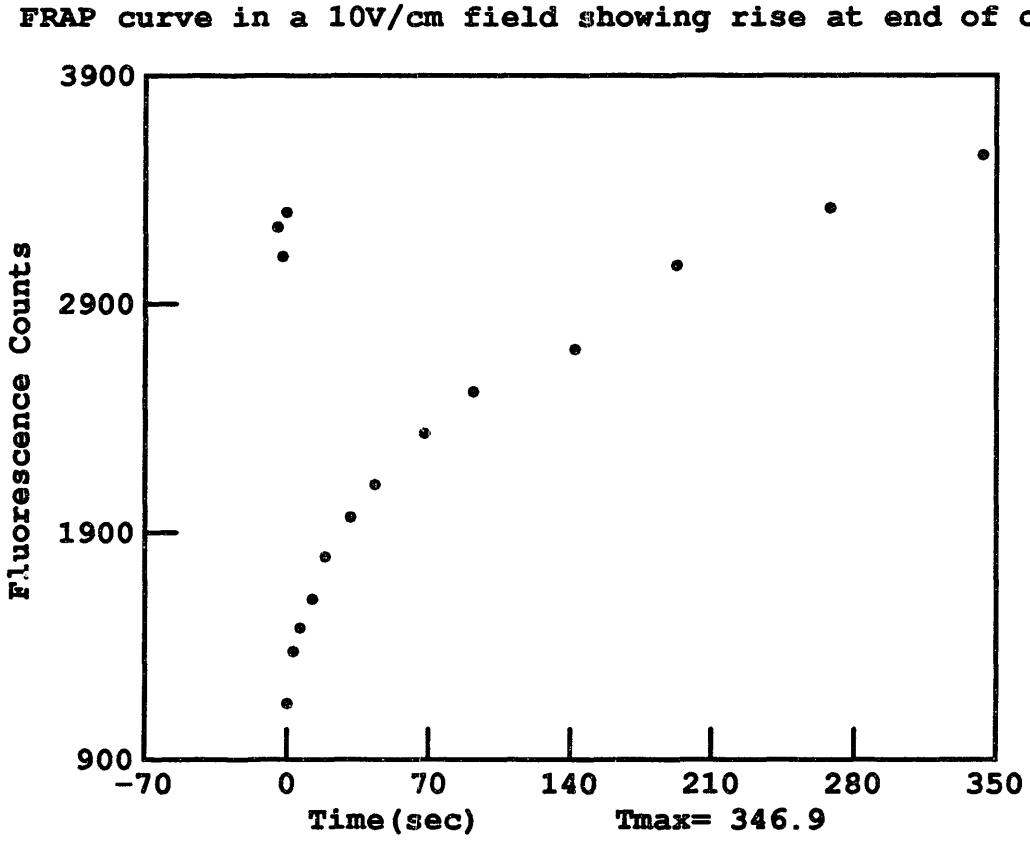

Figure 5.4: A FRAP recovery curve of an experiment with a field showing a rise in fluorescence in the final few points is shown. The last point would indicate a fractional recovery of 114%. This run is modeled incorrectly due to this rise in fluorescence, and thus, was not fit.

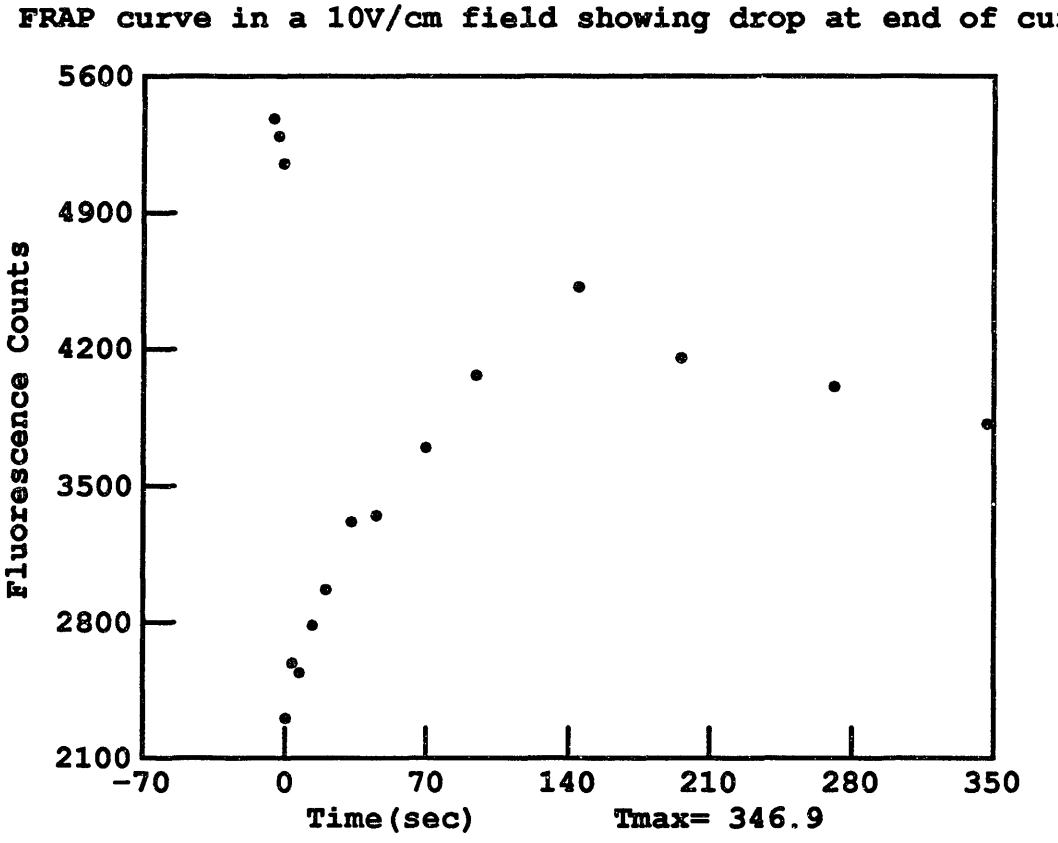

Figure 5.5: A FRAP recovery curve of an experiment with a field showing a drop in fluorescence in the final few points is illustrated. The last point would indicate a fractional recovery of 43%. This run could not be fit to our model due to the drop in fluorescence.

electric field. In these studies, the concentration of the glycoproteins was perturbed slightly by an electric field. Removal of the field allowed the fluorophores to diffuse back to uniform fluorescence. From the recovery data, the back diffusion can be modeled using the theoretical curves derived in section 3.3.6.

A control experiment was run first, similar to the one shown in figure 5.1, except, this time, a 10 V/cm field was applied. Figure 5.6 shows a 25% increase in the fluorescence in the 350 seconds that the field was applied. This data was collected at a monitoring point placed near the edge of the cell along the major axis. When the field polarity was reversed, a decrease in fluorescence was observed. The percentage differed as the monitoring spot was moved about the cell, but the maximum differences occurred when the monitoring spot was close to the edge.

With the monitoring beam on the edge of the cell on the leading edge side, as shown in figure 4.7, the fluorescence was recorded. Removal of the field returned the fluorescence to equilibrium. This data was fit to the exponential function given by equation 3.91. An example run using this procedure is given in figure 5.7. Curve A shows the fluorescence prior to the application of the field. Curve B shows the fluorescence change in a -10 V/cm field; the fluorescence is fit to a straight line as shown in the figure. The triangles indicate the field is negative. A negative field is defined as having its positive pole at the leading edge of the cell and the negative pole at the trailing edge. The fact that the fluorescence decreases indicates that the MHC proteins move toward the negative pole of the field. Our assumption, therefore, that the MHC protein movement is controlled by the flow of the counter ions is substantiated. The slope of curve B is represented as m_-. Curve C shows the recovery back to uniform fluorescence. The points are fit as best as possible to an exponential with time constant τ_+. The field is made positive in curve D, and the slope is represented by m_+. Curve E again shows the back diffusion curve, but this time the exponential is fit to the time constant, τ_-.

Table 5.4 gives a compilation of the back diffusion time constants, their ratios,

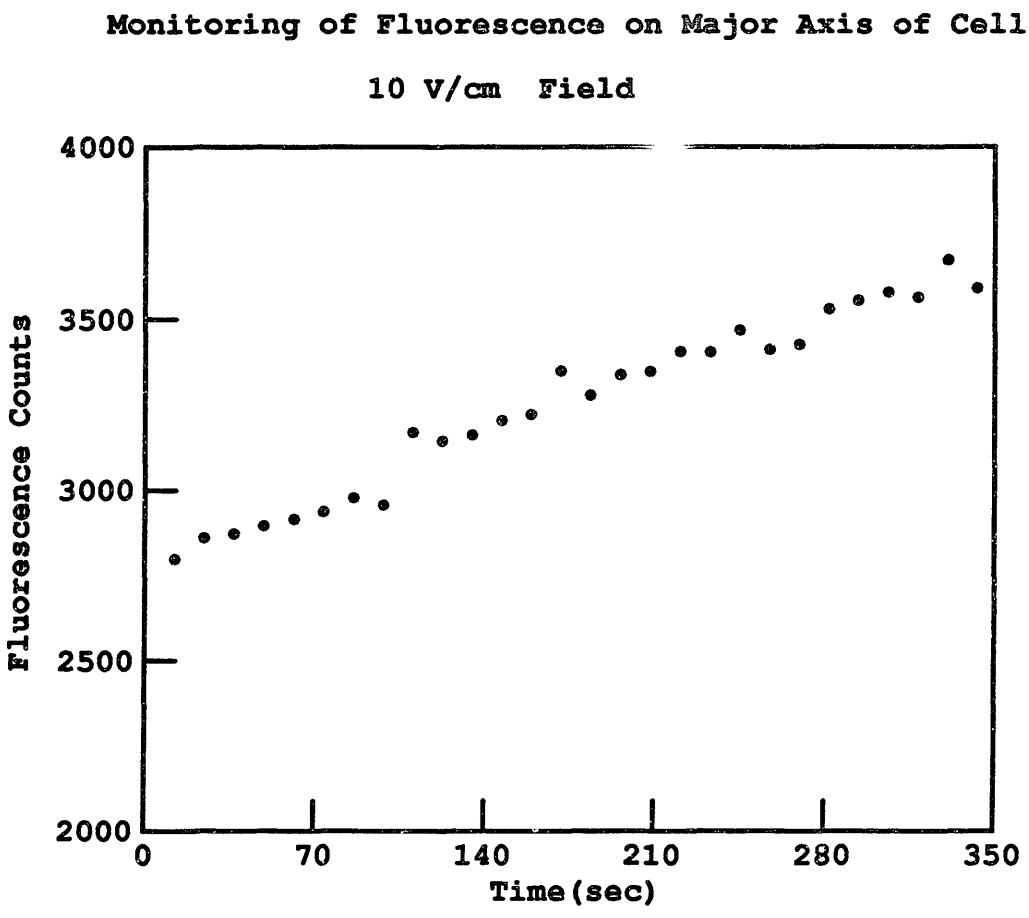

Figure 5.6: The fluorescence is monitored in the presence of a 10 V/cm field without a bleach. A 25% change in fluorescence is observed in 350 seconds. This figure clearly shows that the assumption that the fluorescence does not change in the time frame of a FRAP experiment was invalid.

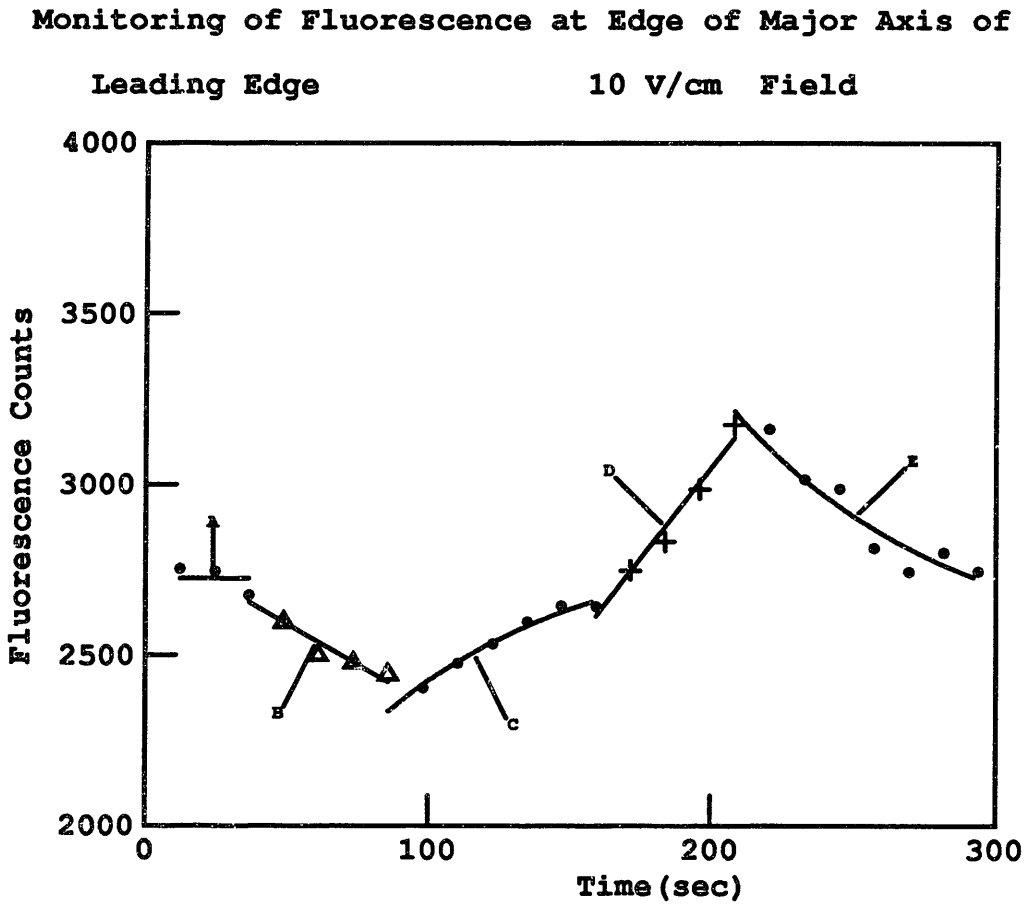

Figure 5.7: This figure shows the flourescence change with a small perturbation in the concentration due to an applied electric field. Curve A is the fluorescence before the field was applied. Curve B has a slope of -4.8 in a negative field. Curve C shows the diffusion back to equilibrium with a time constant $\tau_+ = 62.8$. The field is now positive in curve D and the slope is 10.7. Finally the proteins back diffuse again, as shown in curve E, this time with a time constant $\tau_- = 72.6$.

and the least-squares error of the fit to the exponential. The average of the ratios is given. When compared to unity, the p value of the significance (see appendix A) is $p < 0.10$. This p value indicates that there is a greater that 90% chance that the positive diffusion coefficient, D_+, is greater than the negative diffusion coefficient, D_-. As an indication that this is not an artifact of which direction the field was applied first, the runs in which the negative field was applied first (given by an asterisk in the table) do not show the opposite dependence: that D_- is greater than D_+.

	Back diffusion from high concentration to equilibrium		Back diffusion from low concentration to equilibrium		Ratio
	τ_-	χ^2	τ_+	χ^2	τ_- / τ_+
1	54.4	0.03	36.5	0.05	1.49
2	75.0	0.40	97.9	0.16	0.77
3	26.3	0.11	11.7	0.07	2.24
4 *	72.6	0.46	62.8	0.18	1.16
5	92.4	0.10	67.4	0.20	1.37
6	124.9	0.14	87.4	0.19	1.42
7 *	11.1	0.47	13.6	0.31	0.82
8 *	77.6	0.22	50.3	0.11	1.54
$\overline{x}$:					1.35
σ:					0.46
n:					8

Table 5.4: The above table gives the diffusion time constants, τ_- and τ_+, and their ratios. The average and standard deviation are given. The average is shown to have a p value of $p < 0.10$ when compared with one. An asterisk in the left hand column indicates that the negative field was applied first (τ_+ is found first). Because the cell lengths varied, the τ's varied from cell to cell; therefore, the averages of the τ's were not found. Only the ratios were compared.

Chapter VI

Discussion

6.1 Several Firsts

To our knowledge, this study contains several first in the search for uniaxial anisotropy of cell surface proteins. This work is the first to use FRAP techniques in the presence of an electric field. Even though the model presented here does not account for protein accumulation, the model is accurate when the proteins do not aggregate at the monitoring spot.

This work is the first to investigate the possibility of uniaxial anisotropy at only one point on the cell. Studies have considered anisotropy on the different axes of the cell [Stolpen et al, 1987], and studies have investigated uniaxial anisotropy but only on the entire cell [Smith et al., 1979, Kapitza et al., 1978]. This work has advantage over the above studies. As was stated in section refsec:plasmam, microdomains exist in the bilayer membrane and have characteristic dimensions in the range of one to two microns. Concentrating this investigation at a monitoring spot in the space frame of the microdomains should better characterize the membrane. Searching for anisotropy along the same axis of the cell has more relevance to the search for a mechanism for the established ac electric field effects than the studies investigating biaxial anisotropic properties. A directional dependence along the same axis would lead to a net displacement of the membrane receptors even in a pure sinusoidal field, and may activate a cellular response.

The study also had an advantage over others in the past, for it allowed for the real time monitoring of the protein movement. The studies by Poo et al. [1978, 1979, 1981] and Rabinowitz [1982] required the proteins to be labeled after the application of the field, because the aggregated proteins patched or capped. These studies, however, only perturbed the concentrations, so the proteins did not redistribute to the extent they did in the past work. Also, because MHC proteins

are basically uncharged, they move in an electric field due to the electroosmotic flow of the counter ions external to the cell membrane. Removing the few charged sites on the protein; therefore, by binding the fluorescent antibody to the protein should not effect the "effective" electrophoretic mobility.

6.2 Future Work

This work is a stepping stone for what is proving to be a very exciting field of research. The techniques used in this thesis were based on solid foundations, but as any good research will do, this work demands continuation.

The concentration profile of the proteins as a function of time and space needs to be developed. Real time video imaging of the fluorescence redistribution in an electric field would be invaluable to future FRAP work. it would point out nonlinearities and possible points on the membrane where the concentration is not a function of time. If a point on the cell exists where the concentration does change as the proteins flow through it, as the theory says there should, and it can be consistently determined, the problems of accumulation (or decrease), experienced here, during a FRAP experiment can be avoided.

Of course, video imaging the cell is only one of many paths that will be followed in the quantification of the mechanical properties of the membrane over the next years. Hopefully, after more is understood and published, it will be said that this work had its place in the never ending advancement of science.

Appendix A

Statistical Analysis Tests

This appendix describes the statistical analysis that was used in chapter V to test for significance between different groups of data. The tests were taken from Snedecor and Cochran's [1980] book of statistical methods. Two different statistical tests were used in this thesis. One involved the comparison of two groups of samples of unequal sizes, and the other involved the comparison of an average and standard deviation of a group of points to a known value.

The first test considers two groups of samples that may or may not be the same size. By considering the averages, $\overline{x}_1$ and $\overline{x}_2$, standard deviations, s_1 and s_2, and number of samples, n, a t statistic can be found which. The t statistic is a measure of the likeliness that the two groups of samples fall within the same Gaussian distribution. The t statistic is defined in this case as

$$t = \frac{\overline{x}_1 - \overline{x}_2}{S_{\overline{x}_1 - \overline{x}_2}} \tag{A.1}$$

where $S_{\overline{x}_1 - \overline{x}_2}$ is the weighted standard deviation of the two samples. If there are n samples in group one and m samples in group two, the weighed standard deviation is

$$S_{\overline{x}_1 - \overline{x}_2} = \sqrt{S^2 \frac{(n+m)}{n \cdot m}} \tag{A.2}$$

where

$$S^2 = \frac{(n-1)s_1^2 + (m-1)s_2^2}{m+n-2}. \tag{A.3}$$

The degrees of freedom is given as

$$\mathrm{df} = n + m - 2. \tag{A.4}$$

With the value for t and the degrees of freedom, a value, p, defined as the probability

that the samples are not different, can be looked up in a table of the distribution of t values for a two-tailed test.

For example, the t value for the two groups of "effective" electrophoretic mobilities with and without neuraminidase treatment can be found by

$$t = \frac{8.77 - 3.22}{S_{\bar{x}_1 - \bar{x}_2}} \tag{A.5}$$

where

$$S_{\bar{x}_1 - \bar{x}_2} = \sqrt{\left(\frac{4(0.44)^2 + 14(3.72)^2}{18}\right)\left(\frac{20}{5 \cdot 15}\right)} = 1.7, \tag{A.6}$$

so $t = 3.26$ and df = 18. The p value can now be obtained. As we stated in chapter V, $p < 0.005$. This indicates that there is less than a 0.5% probability that the two sets are the same.

To test if a group of numbers are significantly different from a single value, a similar approach to the last test is used. This time, the t value is written simply as

$$t = \frac{\bar{x} - \mu}{s/\sqrt{n}} \tag{A.7}$$

where μ is the comparison point. The degrees of freedom in this test are given as

$$\mathrm{df} = n - 1 \tag{A.8}$$

this test was used to determine how different the ratios of the back diffusion time constants are from one. Putting in the values yields:

$$t = \frac{1.35 - 1.00}{0.46/\sqrt{8}} = 2.15, \tag{A.9}$$

so $p < 0.10$.

A test was considered not significant if the p value was greater than 0.10.

Appendix B

Inconsistencies of Theoretical Curve Fitting Routines

This appendix presents a possible justification for the inconsistency of the FRAP curve fitting program of finding the best fit parameters of what appears to be reasonable output data.

The problems encountered with the FRAP curve fitting program stemmed from not being able to fit the data to the four parameter model given by equation 3.43. In ~25% of the FRAP runs with an electric field, a best fit value for τ_F could not be found. Several reasons could explain this. First, the best fit parameters are sensitive to noise in the data. τ_F is particularly sensitive because it is squared and is part of the exponential term in equation 3.43. The smaller that τ_F is, compared to the time point, t, the less effect it has on the fluorescence curve. Therefore, the last few points of each run are particularly important in finding the correct convective time constant. Small amounts of error in the final few points have dramatic effects on the estimate of τ_F. Figure B.1 demonstrates that by altering the last point of a typical FRAP run with an electric field by 5%, τ_F increases by 90% while τ_D increases by only 10%. Altering the last point by 10% (still within experimental error), the curve fitting routine changes τ_D by 20%, but cannot find a value for τ_F. The routine made $\tau_F \rightarrow \infty$, which says that $\mu \rightarrow 0$. Another possible explanation for not being able to find a best fit parameter for τ_F is that for large τ_F, migration becomes insignificant and the value of τ_F then has a very small effect on the fluorescence recovery curve. Conversely, small error in the FRAP data can make the estimate of τ_F become very large or infinite.

The program also found the three parameter model much easier to fit to than the four parameter model, for it is not restricted to fitting a highly volatile decaying exponential term. Figure B.2 plots the fractional recovery of diffusion dominated recovery as a function of the bleach parameter, K. This figure shows the

versatility of the three parameter model just by varying K. It was discovered that If τ_F was greater than about five times τ_D, the program made $\tau_F \rightarrow \infty$, so the fit of the data becomes essentially a diffusion dominated recovery curve as described in section 3.2.4.

A better understanding can be had by reading Bevington's [1969] book on data analysis techniques.

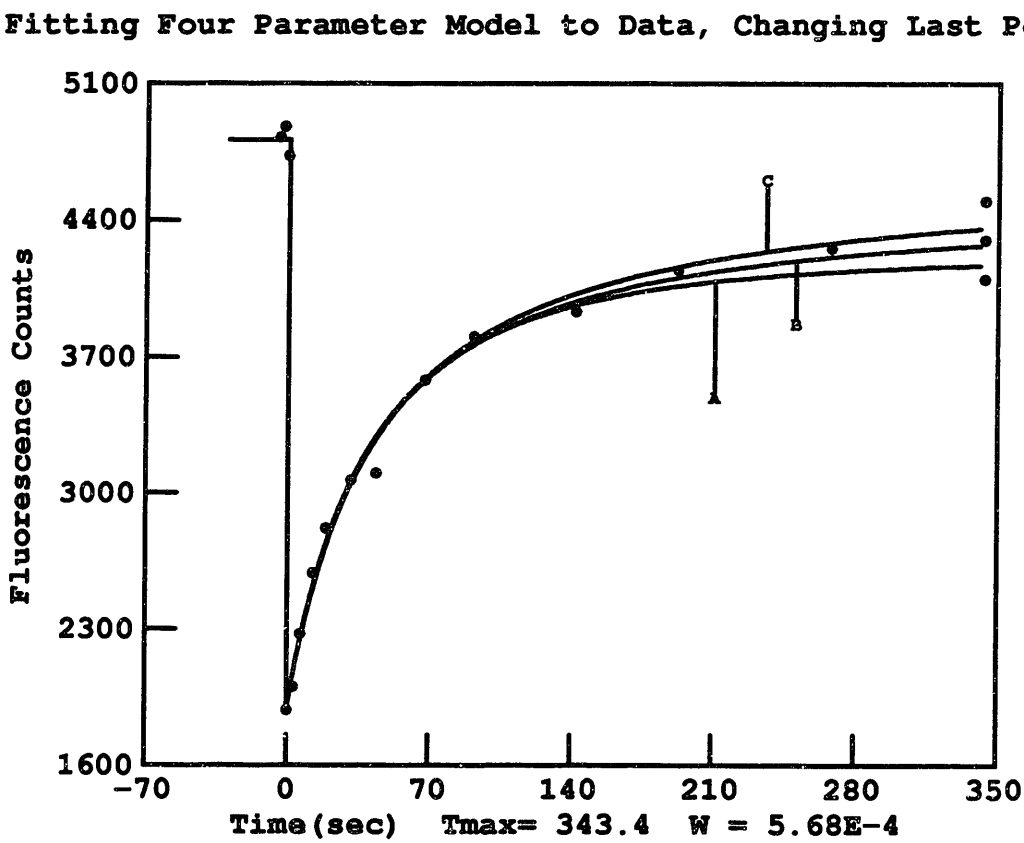

Figure B.1: The curves correspond to the three best fits of the data with the different last points shown. The values for the best fit parameters are an illustration of how sensitive the curve fitting routine is to small amounts of error. The bottom point of the group of three is the actual point measured during the experiment. Curve A is the best four parameter fit to this data. The curve fitting routine found τ_D = 29.1 sec. (D $\sim 2.6 \times 10^{-9}$ cm^2/sec) and τ_F = 73.5 sec. ($\mu \sim 7.7 \times 10^{-7}$ cm^2/V·sec). Curve B is the best fit with the last point increased by 5%. Now, τ_D = 32.1sec. and τ_F = 138.3sec. And curve C corresponds to the last point increased by 10% changing the best fit parameters to: τ_D = 35.3sec. and $\tau_F \rightarrow \infty$

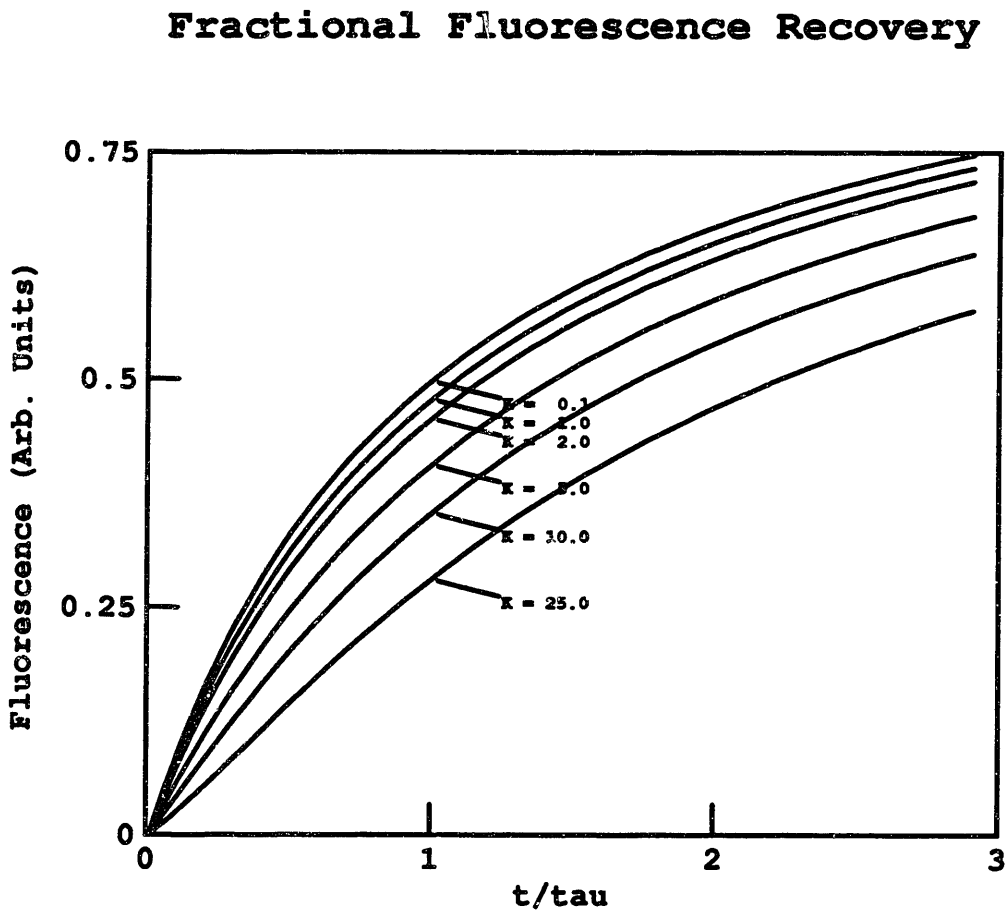

Figure B.2: The fractional fluorescence recovery of diffusion dominated recovery as a function of the bleaching parameter K is shown. This figure is an illustration of the versatility of the three parameter curve fitting function.

Appendix C

Computer Code for Theoretical Curve Fits

This appendix gives the FORTRAN code for the curve fitting routines used in this thesis. The routines are adaptations of those given in Bevington's [1969] book. The first section contains the programs to fit the data acquired during a fluorescence recovery after photobleaching experiment. The program gives the user the option to fit the data to the diffusion dominated recovery curve (equation 3.45), the flow dominated recovery curve (equation 3.46 or the four parameter convection-diffusion equation (equation 3.43). The program also allows the user to supply a diffusion time constant to equation 3.43 so the program finds only the flow time constant, K, and F(∞). The second section gives the code for the least-squares fit to a straight line. This curve fitting routine was used to get th best fit slope of the data taken during the monitoring of the fluorescence accumulation in the presence of an electric field. An exponential fit routine that fits equation 3.91 is given in the third section. The program finds the best fit parameters for F_i, F_0 and τ. The ratio of the τ's of the back diffusion in each direction is used to determine if the diffusion coefficients are dependent on direction. Only the subroutines of the exponential fitting program which are different from the ones fitting the FRAP data are given. Each section also describes the expected form of the input and the output of the routine.

C.1 Curve Fitting Code for FRAP experiments

The code in this section was written to fit an arbitrary curve. Nussbaum [1979], who wrote much of the code written here, took many of the subroutines directly from Bevington's book. The code was adapted to read the data from the FRAP experiment's output files, set initial guesses for the fitting parameters, and fit the data to the functions found in section 3.2.

This program expects an input file that is the same as the one produced by the FRAP routines. Subroutine fin4 opens the data file. It then reads a blank line followed by a sixty character title and a twenty character description of the microscope objective. It then reads the all the FRAP parameters in the following order: the number of measurement points, the number of F(-) points, the number of segments in the measurement schedule, the measurement schedule, the total time of the run, the number of fast measurements (always zero for these experiments), the measurement duration, the bleach duration, the delay for the shutters, the delay between the bleach and the first measuring point of the recovery, the number of measurements per time point (always one in these runs), the value for background fluorescence for a 100ms measurement, the density normalizing factor, the measuring optical density, the bleaching optical density, the laser power, the laser wavelength, the beam radius, and the delay before the first F(-) point. The time and fluorescence coordinates were then read in for the F(-) points and the experimental points respectively.

The subroutine dfunctn calculates the value of the function given the values for the parameters.

The output routine dataout calculates the diffusion coefficient and/or the "effective" electrophoretic mobility from the best fit parameters. It also calculates the F(0) point and the fractional recovery. It then produces a file in 'plop' format, so the data points and the best fit curve can be sent directly to the printer. The other routines are commented appropriately. Further descriptions of the additional routines can, again, be found in Bevington or Nussbaum.

The subroutines are organized in a way so the routines that differ from the ones in section C.3 are at the beginning. The common subroutines then follow in alphabetical order.

PROGRAM FPRFIT

```
      program fprfit

c  User program outline for fitting

c     points to fit
      parameter (maxpts=100)
      integer npts
      real x(maxpts), y(maxpts), sigmay(maxpts)

c  Declare Fit parameters
      parameter (maxtrm=5)
      character ascget
      character mode
      character * 6 finame
      integer nterms
      real terms(maxtrm), deltrm(maxtrm),w
      real fmin(20), tfmin(20)
      integer nfmin,nofunc
      logical cndget
      logical first

      data mode/'s'/

c  Initialize
      print *, 'FRAP Fit Program Version RB3.0'
      first = .true.
10    if (first) then
            first = .false.
      else
              print *
              if (.not. cndget ('another try', .true.)) then
                      stop 'End of Test Fit 3.0'
                      end if
              end if

C  Select which routine you would like to fit to:

      print *, 'Which fit routine would you like:'
      print *, '     (1) diffusion'
      print *, '     (2) convection'
      print *, '     (3) 4 parameter diffusion/convection'
      print *, '     (4) 3 parameter diffusion/convection',
     &                        ' supplying taud'
      print *
      read (5,*) nofunc

c  Read filename, input data, set initial guesses
c   for parameters and deltas.

      call fin4(npts,x,y,nterms,terms,finame,deltrm,w,
```

```
     &  nfmin,fmin,tfmin,nofunc)

c       start
c   User can select different weighting modes. Always set here to 's'
C**      mode = ascget ('Select weighting (e, s, v)', mode)

C  Call the main fitting routine.

        call fit (mode, -1, -1,
     &        npts, x, y, sigmay, nterms, terms, deltrm,
     &        finame,w,nfmin,fmin,tfmin,nofunc)
        goto 10
        end
```

SUBROUTINE DFNCTN

```
        double precision function dfnctn (i, nx, xxx, narg, arg,nofunc)
c  Fitting function for FRAP curve fits

        include 'fit.g'

        integer i, nx, narg, nofunc
        real xxx(*)
        double precision arg(*)
        REAL        MINK
        DOUBLE PRECISION      SUM,TEMP,TERM,sump

        IF (arg(3).NE.0.)       GOTO 5
        dfnctn = arg(2)
        GOTO 300

5       dfnctn = 0.0
        sump = 0.0
        SUM=1D0
        TERM = 1D0
        MINK=-1.*arg(1)

        DO 10 j=1,100
        F = FLOAT(j)
        if (nofunc.ne.2) then
                TERM = TERM*MINK/F
        else
                term = term*mink/(F+1.)
        endif

        if ((nofunc.eq.1).or.(nofunc.eq.3))
     &          TEMP = 1.+ F+ 2.*F*xxx(i)/arg(3)
        if (nofunc.eq.4)        TEMP = 1.+ F+ 2.*F*xxx(i)/taud4
        if (nofunc.eq.1)        SUM = SUM + TERM/temp
        if (nofunc.eq.2)        SUM = SUM + TERM*exp((-2.*F/(F + 1.)) *
     &          (xxx(i)/arg(3))**2)
        if (nofunc.eq.3)        SUM = SUM + TERM *
```

```
     &          (exp((-2.*f*(xxx(i)/arg(4))**2)/temp))/temp
        if (nofunc.eq.4)        SUM = SUM + TERM *
     &          (exp((-2.*f*(xxx(i)/arg(3))**2)/temp))/temp
        if (dabs(sump - sum).lt.0.00001) goto 299
        sump = sum
10      CONTINUE
        print *,'Summation in dfnctn never converged'
299     dfnctn = SNGL(SUM*arg(2))
300     RETURN
        END
```

SUBROUTINE FIN4

```
        SUBROUTINE FIN4(nm,x,y,nterms,terms,fname,deltrm,w,
     &  nfmin,fmin,tfmin,nofunc)

        character * 1        TITLE(60),OBJ(20)
        character * 6 fname
        real x(*),y(*),terms(*),deltrm(*),FMIN(*),TFMIN(*)
        real RMEAS,BKG,EXT,RMOD,BOD,FL1
        real POW,w,DELAY,ttot,c1,c2
        real f0,finf,r,fhlf
        integer NM,NFMIN,NSCHD(20,2),NSEG,NFAST,ndeg,NBLCH,LAG,NPRE,NMPT
        integer lamda,nofunc

c   Read input file name

11      write(6,100)
100     FORMAT ('0ENTER A SIX CHARACTER FILE NAME --> ')
        READ (5,102) FNAME

102     FORMAT(1A6)

c   READ RAW FPR DATA AND PARAMETERS FROM file:

10      OPEN(UNIT=3,file=fname//'.dat',status='OLD')
        read(3,*)
        READ(3,110) (TITLE(I),I=1,60),(OBJ(I),I=1,20)
110     FORMAT(60A1,1X,20A1)
        READ(3,*) NM,NFMIN,NSEG,((NSCHD(J,K),K=1,2),J=1,NSEG),TTOT,NFAST
        READ(3,*) RMEAS,NBLCH,LAG,NPRE,NMPT,BKG,EXT,RMOD,BOD,FL1,
     &                pow,LAMDA,W,DELAY
        READ(3,*) (FMIN(I),TFMIN(I),I=1,NFMIN)
        READ(3,*) (y(I),x(I),I=1,NM)
        CLOSE (UNIT=3)

C  SUBTRACT BACKGROUND

        BK = BKG*RMEAS*0.01
        DO 13 JK=1,NFMIN
13      FMIN(JK) = FMIN(JK) - BK
```

```
        DO 14 JK=1,NM
14      y(JK) = y(JK) - BK

C   Initialize parameters: 1=K, 2=finf, 3=taud, (4=tauf)

        nterms=3
        if (nofunc.eq.3)        nterms=4

c   Arbitrarily set k=2

                terms(1) = 2.
        call avesd(y,nm-5,nm,finf,r)
                terms(2) = finf
        f0 = y(1)
        fhlf = (f0 + finf) * 0.5
        call serch2(y,fhlf,-1.)
                terms(3) = x(int(fhlf))
                if(nofunc.eq.3)                 terms(4) = terms(3)

c  Delta set to 1% at corresponding paramter

        deltrm(1) = 0.01 * terms(1)
        deltrm(2) = 0.01 * terms(2)
        deltrm(3) = 0.01 * terms(3)
        if(nofunc.eq.3)         deltrm(4) = 0.01 * terms(4)
        goto 20

20      RETURN
        END
```

SUBROUTINE FIT

```
        subroutine fit (mode, outf, dbgf,
     &            npxy, xx, yy, sigyy, nparms, parms, delprm,
     &            fname,w,nfmin,fmin,tfmin,nofunc)
        include 'fit.g'
c
        character mode
        integer outf, dbgf
        integer npxy, nparms
        real xx(*), yy(*), sigyy(*), parms(*), delprm(*)
        character fname
        real w
        integer nfmin,nofunc
        real fmin(*), tfmin(*)

c       coordinates curve fitting flow of control

c       *** initialize ***
```

```
C  Debugging tools:

        if (outf .gt. 0) then
                out = outf
                output = .true.
        else
                output = .false.
        endif
        if (dbgf .gt. 0) then
                dbg = dbgf
                debug = .true.
        else
                debug = .false.
        endif

c    Again, the fit routine used here, used mode 's'

        equwtf = .false.
        stawtf = .false.
        varwtf = .false.
        if (mode .eq. 'e') equwtf = .true.
        if (mode .eq. 's') stawtf = .true.
        if (mode .eq. 'v') varwtf = .true.

C Supply taud here if necessary.

        if (nofunc.eq.4) then
                print *,' Input taud:'
                print *
                read (5,*) taud4
        endif
c
        flamda = 0.001
        fuzz = 1.0E-7
        maxitr = 50
c
        print *, 'Curve Fitting Subsystem Version 1.3'
        nfunc = nofunc
        points = npxy

C   Reread input data

        do 10 i = 1, npxy
                x(i) = xx(i)
                y(i) = yy(i)
                sigmay(i) = sigyy(i)
10      continue
c
        terms = nparms
        do 20 i = 1, nparms
                a(i) = parms(i)
```

```
                deltaa(i) = delprm(i)
20      continue

c *** starting fit,  Print out initial parameters***
        print *, '*** starting fit ***'
        print 30, mode, nparms, npxy
        if (output) write (out, 30) mode, nparms, npxy
30      format (1x, 'Mode=', a1, '  Terms=', i4, '  Points=', i4)

C 'Work' does the main iterations of the fitting

        call work
c
        do 40 i = 1, nparms
                parms(i) = a(i)
40      continue
c

c    'Comp' is a debugging tool.  Did not use.
C*          call comp

c    'Dataout' set up an appropriate output file.

        call dataout (fname,w,nfmin,fmin,tfmin)
c
        print *, '*** fit done ***'

        return
        end
```

SUBROUTINE WORK

```
        subroutine work
        include 'fit.g'

c    Calls curfit until no significant change in chi squared

        integer i
        real chisqq

c   Main body of work routine
c   Find chi squared of initial fitting attempt

        nfree = points - terms
        if (nfree .le. 0) then
                print 10, nfree
                return
        end if
10      format (' No degrees of freedom! nfree = ', i5)
```

```
c       evaluate weights
        do 20 i = 1, points
                weight(i) = 1.0
                if (stawtf .and. (y(i) .ne. 0.0)) weight(i) = 1.0/abs(y(i))
                if (varwtf) weight(i) = 1.0/(sigmay(i)*sigmay(i))
20      continue

        if(nfunc.eq.1)  print *, 'chisq,     K,      FINF,     TauD'
        if(nfunc.eq.2)  print *, 'chisq,     K,      FINF,     TauF'
        if(nfunc.eq.3)  print *, 'chisq,     K,  FINF,  TauD,  TauF'
        if(nfunc.eq.4)  print *, 'chisq,     K,      FINF,     TauF'
        call dsplay
        call curfit
        call dsplay
c     Call curfit until no significant change in chi squared
        do 30 i = 1, maxitr
                chisqq = chisqr
                call curfit
                call dsplay
                if (abs((chisqr-chisqq)/chisqr) .lt. fuzz) goto 40
30      continue
        print 50, maxitr
40      print 60, i
        return

50      format (' Warning: iterations exceed maximum. [', i4, ']  Change
     &  fuzz in fit.f')
60      format (' Done after ', i4, ' iterations. ')
        end
```

SUBROUTINE AVESD

```
      SUBROUTINE AVEsd(DATA,n1,N,AVE,sd)
      DIMENSION DATA(N)

c   Given an array of numbers, returns the average
c    and standard deviation
      AVE=0.0
      sd=0.0
      DO 11 J=n1,N
      AVE=AVE+DATA(J)
11    CONTINUE
      AVE=AVE/(N-n1+1)
      DO 12 J=n1,N
      S=DATA(J)-AVE
      sd=sd+S*S
12    CONTINUE
```

```
      sd=sd/(N-n1)
      RETURN
      END
```

SUBROUTINE COMP

```
        subroutine comp
        include 'fit.g'

c     prints a comparison table of
c     the predicted and actual values of y.

        real perc
c
        if (output) then
                write (out, 20)
                write (out, 30)
                do 10 i = 1, points
                        if (yfit(i) .eq. 0.0) then
                                perc = 0.0
                        else
                                perc = 100.0 * (y(i)-yfit(i))/yfit(i)
                        endif
                        write (out, 40) x(i), yfit(i),
     &                                  y(i),y(i)-yfit(i),perc
 10             continue
                write (out, 50) chisqr
                end if

 20      format (/, 'Comparison of Predicted and Actual Values for Y')
 30      format (1x, 7x,'X',7x, 5x,'Y Fit',5x, 3x,'Y Observed',2x,
     &              3x,'Deviation',3x, 2x,'% Deviation',2x)
 40      format (1x, 4(1x, 1pg14.4), 1x, 0pf14.3)
 50      format (/, 'Chi squared was ',1pg20.10)
c
        return
c
        end
```

SUBROUTINE CURFIT

```
        subroutine curfit
        include 'fit.g'

c    Performs curve fitting while you wait

        real chisqq, det, diff, fchisq
```

```
      double precision array(10,10), b(10)
      double precision alpha(10,10), beta(10), dfnctn

c   Evaluate alpha and beta matraces

      do 20 j = 1, terms
              beta(j) = 0.0
              do 10 k = 1, j
                      alpha(j,k) = 0.0
10            continue
20    continue
c
      do 50 i = 1, points
              ij = i
              call fderiv (ij)
      diff = weight(i) * (y(i)-dfnctn(ij,points,x,terms,a,nfunc))
              do 40 j = 1, terms

                      beta(j) = beta(j) + diff*deriv(j)
                      do 30 k= 1, j
                              alpha(j,k) = alpha(j,k)
     &                             + weight(i)*deriv(j)*deriv(k)
30                    continue
40            continue
50    continue

c    duplicate upper triangle in lower triangle

      do 70 j = 1, terms-1
              do 60 k = j+1, terms
                      alpha(j,k) = alpha(k,j)
60            continue
70    continue

c    Evaluate chi squared at starting point
       do 80 i = 1, points
              ij = i
              yfit(i) = dfnctn (ij, points, x, terms, a,nfunc)
80     continue
c
      chisqq = fchisq (chisqq)

c    Invert modified curvature matrix to find new parameters

90    continue
      do 110 j = 1, terms
             do 100 k = 1, terms
                     if (k .ne. j) then
                        array(j,k) = alpha(j,k)
     &                     / dsqrt(dabs(alpha(j,j)*alpha(k,k)))
                     endif
```

```
100             continue
                array(j,j) = 1. + flamda
110     continue
c
        call matinv (array, terms, det)

        do 130 j = 1, terms
                b(j) = a(j)
                do 120 k = 1, terms
                        b(j)=b(j)+beta(k)*array(j,k)
     &                          / dsqrt(dabs(alpha(j,j)*alpha(k,k)))
120             continue
130     continue

c   If chi squared increased increase flamda and try again

      do 140 i = 1, points
                ij = i
                yfit(i) = dfnctn (ij, points, x, terms, b,nfunc)
140   continue

        chisqr = fchisq (chisqr)
        if (chisqr .gt. chisqq) then
                flamda = 10.0*flamda
                goto 90
        end if

c   Evaluate parameters and uncertainties

        do 150 j = 1, terms
                a(j) = b(j)
                sigmaa(j) = dsqrt (dabs(array(j,j)/alpha(j,j)))
150     continue
c
        flamda = flamda/10.0
c
        return
        end
```

SUBROUTINE DSPLAY

```
        subroutine dsplay
c***
        include 'fit.g'
        real t
c
        double precision dfnctn
c***
        sum=0.0
```

```
        do 200 i=1,points
200     sum = sum + dfnctn(i,points,x,terms,a,nfunc)
        chisqn = (chisqr * 1000.)/(sum/float(points))
        write(8,*) chisqn
        print 10, chisqn, (a(n), n=1,terms)
        if (output) write (out, 10) chisqr, (a(n), n=1,terms)
10      format (1x, 1pg12.5, 1p10g15.8)
        return
        end
```

SUBROUTINE FCHISQ

```
        real function fchisq (chisqq)
        include 'fit.g'
        real chisqq

c   Computes chi squared

        real*8 chisq, weigh

        chisq = 0.0
        if (nfree .le. 0) then
                fchisq = 0.0
                goto 40
        endif

c   Accumulate chi squared

        do 10 i = 1, points
                weigh = 1.0
                if (varwtf) weigh = 1.0 / (sigmay(i)*sigmay(i))
                if (stawtf .and. (y(i) .ne. 0.0)) weigh = 1.0/abs(y(i))
                chisq = chisq + weigh*(y(i)-yfit(i))**2
10      continue

        if (debug) then
                write (dbg, '(1x, ''Chi Squared = '', 1pg15.6)') chisq
                end if

        if (chisq .gt. 1.3E31) then
                print '('' error: chi squared overflowed'')'
                end if

c   Divide by number of degrees of freedom

        free = nfree
        fchisq = chisq/free
40      return
        end
```

SUBROUTINE FDERIV

```
        subroutine fderiv (i)
        include 'fit.g'

c   This subroutine numerically calculates partial derivatives

        double precision aj, yf, delta, dfnctn

        do 10 j = 1, terms
           aj = a(j)

c  'delta' set tc 1% of value of parameter

           delta = 0.01 * aj
           a(j) = aj + delta
           yf = dfnctn (i, points, x, terms, a,nfunc)
           a(j) = aj - delta
           deriv(j) = (yf-dfnctn(i,points,x,terms,a,nfunc))/(2.0*delta)
           a(j) = aj
10      continue

        if (debug) then
                write (dbg, 9920) i, yf
                do 9910 j = 1, terms
                        write (out, 9930) j, a(j), deriv(j)
9910            continue
                end if
c
9920    format ('  derivatives at i=', i5, 1pg20.10)
9930    format (1x, i5, 1p2g20.10)
c
        return
        end
```

SUBROUTINE FIT.G

```
c        *** global fit parameters ***

c   Weighting flags
        logical equwtf, stawtf, varwtf
c   Output flags
        logical output, debug
        integer out, dbg
c    Fit limits
        integer maxitr, nfree
        real flamda, fuzz, chisqr
```

```
c     Input data
        integer points
        real x(100), y(100), sigmay(100), weight(100)
c     Fit data
        integer terms, nfunc
        double precision a(10), yfit(100),taud4
        real sigmaa(10), deltaa(10), deriv(10)

        common /fitio/ output, out, debug, dbg
        common /fitin/ points, x, y, sigmay, weight
        common /fitaux/ equwtf, stawtf, varwtf,
     &           maxitr, nfree, flamda, fuzz, chisqr
        common /fitout/ terms, nfunc, a, sigmaa, deltaa,
     &           deriv, yfit, taud4
```

SUBROUTINE MATINV

```
        subroutine matinv (array, norder, det)
        double precision array(10,10)
        double precision amax, save
        integer ik(10), jk(10)
        det = 1.0

c     Matrix inversion Routine:  Described in Bevington.
c     Find largest element array(i,j) in rest of matrix

        do 80 k = 1, norder
                amax = 0.0
 10             continue
                do 20 i = k, norder
                do 20 j = k, norder
                        if (dabs(amax) .le. dabs(array(i,j))) then
                                amax = array(i,j)
                                ik(k) = i
                                jk(k) = j
                                end if
 20             continue

c      Interchange rows and columns to put amax in array (k,k)

                if (amax .eq. 0.0) then
                        det = 0.
                        goto 120
                        end if
                i = ik(k)
                if (i .lt. k) goto 10
                if (i .gt. k) then
                        do 30 j = 1, norder
                                save = array(k,j)
```

```
                        array(k,j) = array(i,j)
                        array(i,j) = -save
 30                 continue
                    end if
                j = jk(k)
                if (j .lt. k) goto 10
                if (j .gt. k) then
                        do 40 i = 1, norder
                                save = array(i,k)
                                array(i,k) = array(i,j)
                                array(i,j) = -save
 40                     continue
                end if

c     Accumulate elements of inverse matrix

                do 50 i = 1, norder
                        if (i .ne. k) array(i,k) = -array(i,k)/amax
 50             continue

                do 60 i = 1, norder
                do 60 j = 1, norder
                        if ((i .ne. k) .and. (j .ne. k)) then
                                array(i,j)=array(i,j)+array(i,k)*array(k,j)
                        end if
 60             continue

                do 70 j=1,norder
                        if (j .ne. k) array(k,j)=array(k,j)/amax
 70             continue
                array(k,k) = 1.0/amax
                det = det*amax
 80     continue

c    Restore ordering of matrix

        do 110 l = 1, norder
                k = norder-l+1
                j = ik(k)
                if (j .gt. k) then
                        do 90 i = 1, norder
                                save = array(i,k)
                                array(i,k) = -array(i,j)
                                array(i,j) = save
90                      continue
                end if
                i = jk(k)
                if (i .gt. k) then
                        do 100 j = 1, norder
                                save = array(k,j)
                                array(k,j) = -array(i,j)
```

```
                                array(i,j) = save
100                         continue
                    end if
110         continue
120         return
            end
```

SUBROUTINE SERCH2

```
            SUBROUTINE SERCH2(y,F1,F2)

            real y(*)
            real f1,f2

C  A rough search for the indices which corespond to F1 and F2

            j = 1
            ft = f1
10          if (ft.le.y(j))          goto 50
            j = j +1
            goto 10
50          if (ft.eq.f2)            goto 60
            f1 = j
            ft = f2
            goto 10
60          return
            end
```

C.2 Line Fitting Program

This section gives the routine used to fit the data acquired during the perturbation experiments with an applied field to the best fit line: $y = a + bx$. The least-squares concepts are taken directly from Bevington's book.

The following program reads the number of pairs of points followed by the (x,y) pairs to be fit. The slope, b, y intercept, a, and the correlation function (a measure of how well the line fit the data) are sent to the standard output.

SUBROUTINE LINFIT

```
      program linfit

      double precision sum, sumx, sumy, sumx2, sumxy, sumy2
      double precision x1, y1, delta, varnce
      character * 6 fname
      real x(40), y(40)

10    write(6,20)
20    FORMAT ('OENTER A SIX CHARACTER FILE NAME --> ')
      READ (5,30) FNAME

30    FORMAT(1A6)

c     Read in data points
40    OPEN(UNIT=3,file=fname,status='OLD')

      read(3,*) n1

      do 50 n=1,n1
        read(3,*) x(n),y(n)
50    continue

C  Accumulate sums

60    if (n.lt.2) print *,' number of points < 2'
      sum = 0
      sumx =0
      sumy =0
      sumx2 =0
      sumxy =0
      sumy2 =0

70    do 80 i=1,n-1
      x1 = x(i)
      y1 = y(i)
      sum = sum + 1
      sumx = sumx + x1
      sumy = sumy + y1
      sumx2 = sumx2 + x1*x1
      sumxy = sumxy + x1*y1
      sumy2 = sumy2 + y1*y1
80    continue

c    calculate coefficients and standard deviation

      delta = sum*sumx2 - sumx*sumx
      a = (sumx2*sumy - sumx*sumxy) / delta
      b = (sumxy*sum - sumx*sumy) / delta
      c = n-2

      varnce=(sumy2+a*a*sum+b*b*sumx2-2.*
```

```
     &           (a*sumy + b*sumxy -a*b*sumx))/c
         sigmaa = dsqrt(varnce * sumx2 /delta)
         sigmab = dsqrt(varnce * sum /delta)
         r = (sum * sumxy - sumx*sumy) /
     &         dsqrt(delta * (sum*sumy2 - sumy*sumy))
         print * ,'       a + bx'
         print * ,' a = ',a
         print * ,' b = ',b
         print * ,' r = ',r

100      end
```

C.3 Exponential Fitting Routines

This fitting routine uses the concepts of section C.1, but fits the data to the exponential

$$(F_i - F_\infty)e^{-t/\tau} + F_\infty. \tag{C.1}$$

The program allows the user to supply F_i, F_∞, both F_i and F_∞, or none of the parameters, in which case the program fits all three parameters to the data as best it can. The option to subtract the first x data point from the others is also available. This was used to normalize time to zero.

The input file is read in subroutine fin4. The routine expects the same format for the input data file as in the line fitting program. The output routine, dataout, produces a 'plop' file for hard copy output. Only the routines which differ from the first section are given here.

PROGRAM EXPONFIT

```
c  program  exponfit

c  Exponential program for fitting
c  Points to fit
        parameter (maxpts=100)
        integer npts
```

```
      real x(maxpts), y(maxpts), sigmay(maxpts)
c
c  Fit parameters
      parameter (maxtrm=5)
      character ascget
      character mode
      character * 6 finame
      integer nterms
      real terms(maxtrm), deltrm(maxtrm),w
      real fmin(20), tfmin(20)
      integer nfmin,nofunc
c
      logical cndget
      logical first
c
      data mode/'s'/
c
c   Initialize
      print *, 'Exponential Fit Program Version RB1.0'
      first = .true.
10    if (first) then
            first = .false.
      else
            print *
            if (.not. cndget ('another try', .true.)) then
                  stop 'End of Test Fit 4.0'
            end if
      end if

      print *,' Which parameters would you like to supply?'
      print *,'        (1) none'
      print *,'        (2) F0'
      print *,'        (3) Finf'
      print *,'        (4) F0 and Finf'
      print *
      read(5,*) nofunc

c    Call input routine
c
      call fin4(npts,x,y,nterms,terms,finame,deltrm,w,
     &    nfmin,fmin,tfmin,nofunc)

c     start
C****   mode = ascget ('Select weighting (e, s, v)', mode)
      call fit (mode, -1, -1,
     &         npts, x, y, sigmay, nterms, terms, deltrm,
     &         finame,w,nfmin,fmin,tfmin,nofunc)
      goto 10
      end
```

PROGRAM DFNCTN

```
        double precision function dfnctn (i, nx, xxx, narg, arg,nofunc)

c     Fitting function

        include 'fit.g'
c
        integer i, nx, narg, nofunc
        double precision arg(*)
        real xxx(*)

        if (nofunc.eq.1) then
          dfnctn = (arg(2)-arg(3))*dexp(-1.*xxx(i)/arg(1)) + arg(3)
        endif
        if (nofunc.eq.2) then
         dfnctn = (f0-arg(2))*dexp(-1.*xxx(i)/arg(1)) + arg(2)
        endif
        if (nofunc.eq.3) then
          dfnctn = (arg(1)-finf)*dexp(-1.*xxx(i)/arg(1)) + finf
        endif
        if (nofunc.eq.4) then
          dfnctn = (f0-finf)*dexp(-1.*xxx(i)/arg(1)) + finf
        endif
        RETURN
         END
```

PROGRAM FIN4

```
        SUBROUTINE FIN4(nm,x,y,nterms,terms,fname,deltrm,w,
     &      nfmin,fmin,tfmin,nofunc)
c
        character * 1         TITLE(60),OBJ(20)
        character * 6 fname
        real x(*),y(*),terms(*),deltrm(*),FMIN(*),TFMIN(*)
        real f0,finf,r,fhlf
        integer NM,NFMIN
        integer lamda,nofunc,i5

11      write(6,100)
100     FORMAT ('OENTER A SIX CHARACTER FILE NAME --> ')
        READ (5,102) FNAME

102     FORMAT(1A6)


        print * ,'Do you want to normalize time to t=0?(0=no,1=yes)'
        read (5,103) i5
```

```
103     format(1I1)

C ***  READ x(),y() arrays from file:

10      OPEN(UNIT=3,file=fname,status='OLD')
        read(3,*) nm
45      do 50 n=1,nm
        read(3,*) x(n),y(n)
        if(i5.eq.1) then
                if(n.eq.1)    t1 = x(1)
                x(n) = x(n) - t1
        endif
50      continue
        CLOSE (UNIT=3)

        do 233 n=1,nm
233     continue

C ****     Initialize parameters:
C
        if (nofunc.eq.1) then
c    1=tau, 2=f0, 3=finf
                nterms=3
                terms(1) = x(nm)/2
                terms(2) = y(1)
                terms(3) = y(nm)
        endif

        if (nofunc.eq.2) then
c    1=tau, 2=Finf
                nterms=2
                terms(1) = x(nm)/2
                terms(2) = y(nm)
        endif
        if (nofunc.eq.3) then
c    1=tau, 2=F0
                nterms=2
                terms(1) = x(nm)/2
                terms(2) = y(1)
        endif
        if (nofunc.eq.4) then
c    1=tau
                nterms=1
                terms(1) = x(nm)/2
        endif
        deltrm(1) = .05 * terms(1)
        deltrm(2) = .05 * terms(2)
        deltrm(3) = .05 * terms(3)

20      RETURN
        END
```

PROGRAM FIT

```
      subroutine fit (mode, outf, dbgf,
     &           npxy, xx, yy, sigyy, nparms, parms, delprm,
     &           fname,w,nfmin,fmin,tfmin,nofunc)
      include 'fit.g'
c
      character mode
      integer outf, dbgf
      integer npxy, nparms
      real xx(*), yy(*), sigyy(*), parms(*), delprm(*)
      character fname
      real w
      integer nfmin,nofunc
      real fmin(*), tfmin(*)
c
c  coordinates curve fitting flow of control
c
c  *** initialize ***
c
      if (outf .gt. 0) then
              out = outf
              output = .true.
      else
              output = .false.
      endif
      if (dbgf .gt. 0) then
              dbg = dbgf
              debug = .true.
      else
              debug = .false.
      endif
c
      equwtf = .false.
      stawtf = .false.
      varwtf = .false.
      if (mode .eq. 'e') equwtf = .true.
      if (mode .eq. 's') stawtf = .true.
      if (mode .eq. 'v') varwtf = .true.
c
      if (nofunc.eq.2) then
              print *,' Input F0:'
              print *
              read (5,*) f0
      endif
      if (nofunc.eq.3) then
              print *,' Input Finf:'
              print *
```

```
                read (5,*) finf
        endif
        if (nofunc.eq.4) then
                print *,' Input F0, Finf:'
                print *
                read (5,*) f0,finf
        endif
c
        flamda = 0.001
        fuzz = 1.0E-7
        maxitr = 100
c
        print *, 'Curve Fitting Subsystem Version 1.3'
        nfunc = nofunc
        points = npxy
        do 10 i = 1, npxy
                x(i) = xx(i)
                y(i) = yy(i)
                sigmay(i) = sigyy(i)
10      continue
c
        terms = nparms
        do 20 i = 1, nparms
                a(i) = parms(i)
                deltaa(i) = delprm(i)
20      continue
c
c *** starting fit ***
        print *, '*** starting fit ***'
        print 30, mode, nparms, npxy
        if (output) write (out, 30) mode, nparms, npxy
30      format (1x, 'Mode=', a1, '  Terms=', i4, '  Points=', i4)
c
        call work
c
        do 40 i = 1, nparms
                parms(i) = a(i)
40      continue
c
c   Did not use subroutint comp
C**        call comp
c
        call dataout (fname,w,nfmin,fmin,tfmin)
c
        print *, '*** fit done ***'

        return
        end
```

PROGRAM WORK

```
        subroutine work
        include 'fit.g'
c
c  calls curfit until no significant change in chi squared
c
        integer i
        real chisqq
c
c  main body of work routine
c  find chi squared of initial fitting attempt
c
        nfree = points - terms
        if (nfree .le. 0) then
                print 10, nfree
                return
        end if
10      format (' No degrees of freedom! nfree = ', i5)
c
c  evaluate weights
        do 20 i = 1, points
          weight(i) = 1.0
          if (stawtf .and. (y(i) .ne. 0.0)) weight(i) = 1.0/abs(y(i))
          if (varwtf) weight(i) = 1.0/(sigmay(i)*sigmay(i))
20      continue
C***
c
        if (nofunc.eq.1)   print *, ' Chisqn,    Tau     F0,     Finf'
        if (nofunc.eq.2)   print *, ' Chisqn,    Tau     F0'
        if (nofunc.eq.3)   print *, ' Chisqn,    Tau     Finf'
        if (nofunc.eq.4)   print *, ' Chisqn,    Tau'
        call dsplay
        call curfit
        call dsplay
        do 30 i = 1, maxitr
                chisqq = chisqr
                call curfit
c**                call dsplay (output, out, chisqr, terms, a)
                call dsplay
                if (abs((chisqr-chisqq)/chisqr) .lt. fuzz) goto 40
30      continue
        print 50, maxitr
40      print 60, i
        return
c
50      format (' Warning: iterations exceed maximum. [', i4, ']
     &      Change maxitr in fit3exp.f')
60      format (' Done after ', i4, ' iterations. ')
        end
```

PROGRAM DATAOUT

```
      subroutine dataout(fname,w,nfmin,fmin,tfmin)

      include 'fit.g'
c
      real fmin(*),tfmin(*)
      character * 6 fname
      real w,fmn,z(1)
      integer nfmin
      DOUBLE PRECISION        SUM,TEMP,TERM
      DOUBLE PRECISION        dfnctn
c
      sum = 0.0
      do 10 i=1, points
10    sum = sum + dfnctn(i,points,x,terms,a,nfunc)
      if (points.ne.0)        gave = sum/float(points)
      if (gave.ne.0)          chisqn = (chisqr * 1000.)/gave

      open(unit=9,file=fname//'.plp',status='new')

      write(9,110)
110   format(' title top "Exponential Fit to Back Diffusion"')

      write(9,120)
120   format(' label left "fluorescence counts"')
      write(9,130) x(points)
130   format(' label bottom "Time(sec)        Tmax= ',F5.1,'"')
      write(9,135) fname,sngl(a(1))
135   format(' label bottom 0.75 "',1A6,'  Tau = ',F10.4,'"')

      if (nfunc.eq.1) then
      write(9,138) sngl(a(2)),sngl(a(3))
138   format(' label bottom 1.00"F0 = ',F10.4,'Finf = ',F10.4,'"')
      f0 = a(2)
      finf = a(3)
      endif

      if (nfunc.eq.2) then
      write(9,148) sngl(a(2)),finf
148   format(' label bottom 1.00 "F0 =',F10.4,'Finf =',F10.4,'"')
      f0 = a(2)
      endif

      if (nfunc.eq.3) then
      write(9,158) f0, sngl(a(2))
158   format(' label bottom 1.00"F0 =',F10.4,'Finf = ',F10.4,'"')
      finf = a(2)
      endif
```

```
      if (nfunc.eq.4) then
      write(9,168) f0, finf
168   format(' label bottom 1.00 "F0 = ',F10.4,'Finf = ',F10.4,'"')
      endif

      write(9,139) (int(f0/100)-4)*100,(int(finf)/100+4)*100
139   format(' y axis scale ',I4,1X,I4)
      write(9,140)
140   format(' plot dots')
      do 160 i=1,points
      write(9,*) x(i),y(i)
160   continue
      write(9,*)
      write(9,170)
170   format(' plot line')

      z(1) = x(1)
      do 190 i=1,99
      write(9,*) z(1),dfnctn(1,points,z,terms,a,nfunc)
      z(1) = z(1) + (x(points)-x(1))*0.01
190   continue
c
      close (unit=9)
      return
```

Appendix D

References

Aidley, D.J. (1978): The Physiology of Excitable Cells, Cambridge University Press, NY.

Alberts B., Bray D., Lewis J., Raff M., Roberts K., and Watson J.D. (1983): *Molecular Biology of the Cell* Garland Publishing, NY & London.

Assailly B., Monet J.D., Goureau Y., Christel, P. and Pilla A.A. (1981): Effect of Weak Inductively Coupled Pulsaing Currents on Calcium Uptake in Embryonic Chick Tibia Explants. *Bioelectrochemistry and Bioenergenics.* 8:515-521.

Axelrod D., Koppel D.E., Schlessinger J., Elson E. and Webb W.W. (1976): Mobility Measurement by Analysis of Fluorescence Photobleaching Recovery Kinetics. *Biophys. J.* 16:1055-1069.

Barnstable C.J., Bodmer W.F., Brown G., Galfre G., Milstein C., Williams A.F., and Ziegler A. (1978): Production of Monoclonal Antibodies to Group A Erythrocytes, HLA and Other Human Cell Surface Antigens-New Tools for Genetic Analysis. *Cell* 14:9-20.

Bevington P.R. (1969): Data Reduction and Error Analysis for the Physical Sciences. McGraw-Hill, Inc., New York. 336 pp.

Bierer B.E., Herrmann S.H., Brown C.S., Burakoff S.J., and Golan D.E. (1987): Lateral Mobility of Class I Histocompatibility Antigens in B Lymphoblastoid Cell Membranes: Modulation by Cross-linking and Effect of Cell Density. *J. of Cell Biol.* 105:1147-1152.

Bjorkman P.J., Saper M.A., Samraoui B., Bennett W.S., Strominger J.L., and Wiley D.C. (1987): Structure of the Class I Histocompatibility Antigen, HLA-A2. *Nature* 329:506-512.

Borgens, R.B., (1984): Endogeneous Ionic Currents Traverse Intact and Damaged Bone. *Science* 225:478-482.

Brevet A., Pinto E., Peacock J., and Stockdale F.E. (1976): Myosin Synthesis Increased by Electrical Stimulation of Skeletal Muscle Cell Cultures. *Science* 193:1152-1154.

Brighton C.T., Unger A.S. and Stambough J.L. (1977): In Vitro Capacitively Coupled Electrical Stimulation of Articular Chondrocyte Pellets in Varying Serum Concentrations. *Trans. of the Biol. Repair and Growth Soc.* 2:8.

Chao N.M., Young S.H., Poo M.M. (1981): Localization of Cell Membrane Components by Surface Diffusion into a "Trap". *Biophys. J.* 36:139-153.

Chiabrera A., Grattarola M., and Viviani, R. (1984): Interaction Between Electromagnetic Fields and Cells: Microelectric Effect on Ligands and Surface Receptors. *Bioelectromagnetics* 5:173-191.

Carpenter G. and Cohen S. (1979): Epidermal Growth Factor *Ann. Rev. Biochem.* 48:193-216.

Darnell J., Lodish H., and Baltimore D. (1986): *Molecular Cell Biology* Scientific American Books, NY.

Edidin M., and Wei T. (1982): Lateral Diffusion of H-2 Antigens on Mouse Fibroblasts. *J. of Cell Biol.* 95:458-462.

Edidin M., Zagyansky Y, and Lardner T.J. (1976): Measurement of Membrane Protein Lateral Diffusion in Single Cells *Science.* 196:466-468.

Eldridge C.A., Elson E.L. and Webb W.W. (1980): Fluorescence Photobleaching Recovery Measurements of the Surface Lateral Mobilities on the Normal and SV40-transformed Mouse Fibroblasts. *Biochemistry.* 19:2075-2079.

Eylar E.H., Morton M.A., Brody O.V., Oncley J.L. (1962): The Contribution of Sialic Acid to the Surface Charge of the Erythrocyte. *J. of Biological Chem.* 237(6):1992-2000.

Findl E. (1984): Field/Cell Interaction Model. *IEEE Frontiers of Engineering and Computing in Health Care.* 196-201.

Frank, E.H. and Grodzinsky, A.J. (1987): Cartilage Electromechanics II: A Continuum Model of Cartilage Electrokinetics. *J. Biomech.* 20:629-639.

Geddes L.A. and Baker L.E. (1969): Hazards in the Use of Low Frequencies for the Measurement of Physiological Events by Impedence. *Med. Bio. Eng.* 7(3):289-296.

Giugni T.D., Braslau D.L. and Haigler H.T. (1987): Electric Field-induced Redistribution and Postfield Relaxation of Epidermal Growth Factor Receptors on A431 Cells. *The J. Cell Biology.* 104:1291-1297.

Golan D.E., Brown C.S., Cianci C.M.L., Furlong S.T. and Caulfield J.P. (1986): Schistosomula of *Schistosoma mansoni* Use Lysophospatidylcholine to Lyse Adherent Human Red Blood Cells and Immobilize Red Cell Membrane Components. *The J. Cell Biology.* 103:819-828.

Goodman R., Bassett C.A.L. and Henderson A.S. (1983): Pulsing Electromagnetic Fields Induce Cellular transscription. *Science.* 220:1283-1285.

Gross D., Loew L.M. and Webb W.W. (1986): Optical Imaging of Cell Membrane Potential Changes Induced by Applied Electric Fields. *Biophys. J.* 50:339-348.

Hille B. (1984): *Ionic Channels of Excitable Membranes.* Sinauer Associates Inc., Sunderland, MA.

Jacobson K., Elson E., Koppel D. and Webb W. (1982): Fluorscence Photobleaching in Cell Biology. *Nature.* 28:283-284.

Jacobson K., Wu E. and Poste G. (1976): Measurement of the Translational Mobility of Concanavalin A in Glycerol-saline Solutions and on the Cell Surface br Fluorescence Recovery After Photobleaching. *Biochimica et Biophys. Acta.* 433:215-222.

Jaffe L.F. (1977): Electrophoresis Along Cell Membranes. *Nature.* 265:600-602.

Kapitza H.A., McGregor G. and Jacobson K.A. (1985): Direct Measurement of Lateral Transport in Membranes by Using Time-resolved Spatial Photometry *Proc. Natl. Acad. Sci. USA. Biophysics.* 82:4122-4126.

Kloss D.A. and Cartensen D.L. (1983): Effects of ELF Electric Fields on the Isolated Frog Heart. *IEEE Trans. Biomed. Eng.* 30(6):347-348.

Krangel M.S., Orr H.T. and Strominger J.L. (1980): Structure, Function, and Biosynthesis of the Major Histocompatibility Antigens (HLA-A and HLA-B). *Scand. J. Immunology* 11:561-571.

Koppel D.E. (1979): Fluorescence Redistribution After Photobleaching–a New Multipoint Analysis of Membrane Translational Dynamics. *Biophsys. J.* 28:281-292.

Koppel D.E., Axelrod D., Schlessinger J., Elson E.L. and Webb W.W. (1976): Dynamics of Fluorescence Marker Concentration as a Probe of Mobility. *Biophsys. J.* 16:1315-1329.

Lee R.C., Rich J.B., Kelley K.M., Weiman D.S. and MAthews M.B. (1982): A Comparison of in Vitro Cellular Response to Mechanical and Electrical Stimulation.

Am. Surgeon. 48(11):567-572.

Levitt D.G. (1985): Strong Electrolyte Continuum Theory Solution for Equilibrium Profiles, Diffision Limitation, and Conductance in Charged Ion ¡Channels. *Biophys. J.* 48:19-31.

Liebmann P.A. and Entine G. (1974): Lateral Diffusion of Visual Pigment in Photoreceptor Disk Membranes. *Science.* 185:457-459.

Levich V.G. (1962): *Physicochemical Hydrodynamics.* Prentice-Hall, Inc. Englewood Cliffs, NJ.

Liveh E., Benveniste M., Prywes R., Felder S., Kam Z. and Schlessinger J. (1986): Large Deletions in the Cytoplasmic Kinase Domain of the Epidermal Growth Factor Receptor Do Not Affect Its Lateral Mobility. *The J. Cell Biology.* 103:327-331.

Lloyd C.W. (1975): Sialic Acid and the Social Behaviour of Cells. *Biol. Rev.* 50:325-350.

MacGinitie L.A. (1988): Electrical and Thermal Modulation of Protein Synthesis in Cartilage: A Model for Field Effects on Biological Tissues. *Ph.D. Thesis-MIT* Cambridge, MA.

Malissen M., Malissen B., and Jordan B.R. (1982): Exon/intron Organization and Complete Nucleotide Sequence od an HLA Gene. *Proc. Nat. Adac. Sci.* 79:893-897.

McLaughlin S. and Poo M. (1981): The Role of Electro-osmosis in the Electric-field-induced Movement of Charged Macromolecules on the Surfaces of Cells. *Biophys. J.* 34:85-93.

McLeod K.J. (1986): Modulation of Biosynthesis by Physiologically Relevant Electric Fields. *Ph.D. Thesis-MIT* Cambridge, MA.

McLeod K.J., Lee R.C., and Ehrlich H.P. (1987): Frequency Dependence of Electric Field Modulation of Fibroblast Protein Synthesis. *Science.* 236:1465-1469.

Melcher J.R. (1981): *Contiuum Electromechanics.* M.I.T. Press, Cambridge, MA.

Nathenson S.G., Geliebter J., Pfaffenbach G.M., and Zeff R.A. (1986): Murine Major Histocompatibility Complex Class-I Mutants: Molecular Analysis and Structure-Function Implications. *Ann. Rev. Immunology* 4:471-502.

Nussbaum J.H. (1979): Some Techniques of Data Analysis. *B.S. Thesis-MIT* Cam-

bridge, MA.

Petty H.R., Smith L.M., Fearon D.T., and McConnell H.M. (1980): Lateral Distribution and Diffusion of the Cb receptor of Complement, HLA antigens, and Lipid Probes in Periperal Blood Leukocytes. *Proc. Natl. Acad. Sci.* 77(11):6587-6591.

Poo M. (1981): In Situ Electrophoresis of Membrane Components. *Ann. Rev. Biophys. Bioeng.* 10:245-276.

Poo M. and Cone (1974): Lateral Diffusion of Rhodopsin in the Photoreceptor Membrane. *Nature.* 247:438-441.

Poo M., Lam J.W., Orida N. and Chao A.W. (1979): Electrophoresis and Diffusion in the Plane of the Cell Membrane. *Biophy. J.* 26:1-22.

Poo M., Poo W.H. and Lam J.W. (1978): Lateral Electrophoresis and Diffusion of Concanavalin A Receptors in the Membrane of Embryonic Muscle Cell. *J. Cell Biology.* 76:483-501.

Poo M. and Robinson K.R. (1977): Electrophoresis of Concanavalin A Receptors Along Embryonic Muscle Cell Membrane. *Nature.* 265:602-605.

Rabinowitz J.R. (1982): The Effect of Electric Field Induced Perturbation of the Distribution of Ions Near the Cell Surface on the Migration of Charged Membrane Components. *J. Theor. Biol.* 99:377-389.

Rodan G.A., Bourett L.A. and Norton L.A. (1978): DNA Synthesis in Cartilage Cells is Stimulated by Oscillating Electric Fields. *Science.* 199:690-692.

Schlesinger, M.J., Kelley, K.M., Aliperti and Malfer, C. (1982): in *Heat Shock from Bacteria to Man*, Schlesinger, M.J., Ashburner, M. and Tissieres, A., eds. Cold Spring Harbor Laboratory, pp.243-250.

Schlessinger J., Axelrod D., Koppel D.E., Webb W.W., Elson E.L. (1977): Lateral Transport of a Lipid Probe and Labeled Proteins on a Cell Membranes, *Science.* 195:305-308.

Schlessinger J. and Elson E.L. (1982): Fluorescence Methods for Studying Membrane Dynamics. *Methods od Exp. Physics* 20:197-227.

Schlessinger J., Koppel D.E., Axelrod D., Jacobson K., Webb W.W., Elson E.L. (1976): Lateral Transport on Cell Membranes: Mobility of Concanavalin A Receptors on Myoblasts. *Proc. Natl. Acad. Sci. USA. Cell Biology.* 73:2409-2413.

Schlessinger J., Schreiber A.B., Levi A., Lax I., Libermann T. and Yarden Y. (1983): Regulation of Cell Proliferation by Epidermal Growth Factor. *CRC Critical Reviews in Biochemistry.* 14(2):93-111.

Schlessinger J., Schlechter Y. Cuatrecasas P. Willingham M.C. and Pastan I. (1978): Quantitative Determination of the Lateral Diffusion Coefficients of the Hormone-receptor Complexes of Insulin and Epidermal Growth Factor on the Plasma Membrane of Cultured Fibroblasts. *Proc. Natl. Acad. Sci. USA. Biochemistry.* 75:5353-5357.

Smith B.A., Clark W.R. and McConnell (1978): Determination of Molecular Motion in Membranes Using Periodic Pattern Photobleaching. *Proc. Natl. Acad. Sci. USA.* 75(6):2759-2763.

Smith B.A. and McConnell (1979): Anisotropic Molecular Motion on Cell Surfaces. *Proc. Natl. Acad. Sci. USA.* 76(11):5641-5644.

Snedecor G.W. and Cochran W.G. (1980): Statistical Methods Iowa State Univ. Press, 7^{th} ed., Ames, Iowa.

Soumpasis D.M. (1983): Theoretical Analysis of Fluorescence Photobleaching Recovery Experiments. *Biophsys. J.* 41:95-97.

Speigal S., Schlessinger J., and Fishman P.H. (1984): Incorporation of Fluorescent Gangliosides into Human Fibroblasts: Mobility, Fate, and Interaction with Fibronectin. *J. of Cell Biology* 99:699-704.

Stolpen A.H., Brown C.S., Golan D.E. (1987): Characterization of Microscopic Laser Beams by Two-Dimensional Scanning of Fluorescence Emission. submitted: *Biophys. J.*

Stolpen A.H., Pober J.S., Brown C.A., Golan D.E. (1987): Class I MHC Proteins Diffuse Isotropically on Immune Interferon-activated Endothelial Cells Despite Anisotropic Cell Shape and Cytoskeletal Organization: Application of Fluorescense Photobleaching Recovery with an Elliptical Beam. submitted: *Proc. Natl. Acad. Sci. USA.*

Tragardh L., Rask L., Wiman K., Fohlman J., Peterson P.A. (1979): Amino Acid Sequence of an Immunoglobulin-like HLA Antigen Heavy Chain Domain. *Proc. Natl. Acad. Sci. USA.* 76:5839-5842.

Ullrich A., Coussens L., Hayflick J.S., Dull T.J., Gray A., Tam A.W., Lee J., Yarden Y., Libermann T.A., Schlessinger J., Downward J., Whittle N., Waterfield M.D. and Seeburg P.H. (1984): Structure of Human Epidermal Growth Factor Receptor and

Expression of Normal and Variant mRNAs in Epidermoid Carcinoma Cells. *Cancer Cells 3/Growth Factors and Transformations* Cold Harbor Springs Laboratory pp: 1-9.

Wier M.L. and Edidin M. (1986): Effects of Cell Density and Extracellular Matrix on the Lateral Diffusion of Major Histocompatibility Antigens in Cultured Fibroblasts. *J. Cell Biology* 103:215-222.

Yguerabide J., Schmidt J.A. and Yguerabide E.E. (1982): Lateral Mobility in Membranes as Detected by Fluorescence Recovery After Photobleaching. *Biophys. J.* 39:69-75.

Zagyansky Y.A., and Jard S., (1979): Does Lectin-receptor complex formation produce zones of restricted mobility within the membrane? *Nature* 280:591

Zagyansky Y.A., and Edidin M. (1976): Lateral Diffusion of Concanavalin Receptors in the Plasma Membrane of Mouse Fibroblasts. *Biochimica et Biophysica Acta* 433:209-214.